



Submitted to: Phys. Rev. D



CERN-PH-EP-2015-111
6th November 2015

Search for new light gauge bosons in Higgs boson decays to four-lepton final states in pp collisions at $\sqrt{s} = 8$ TeV with the ATLAS detector at the LHC

The ATLAS Collaboration

Abstract

This paper presents a search for Higgs bosons decaying to four leptons, either electrons or muons, via one or two light exotic gauge bosons Z_d , $H \rightarrow ZZ_d \rightarrow 4\ell$ or $H \rightarrow Z_d Z_d \rightarrow 4\ell$. The search was performed using pp collision data corresponding to an integrated luminosity of about 20 fb^{-1} at the center-of-mass energy of $\sqrt{s} = 8$ TeV recorded with the ATLAS detector at the Large Hadron Collider. The observed data are well described by the Standard Model prediction. Upper bounds on the branching ratio of $H \rightarrow ZZ_d \rightarrow 4\ell$ and on the kinetic mixing parameter between the Z_d and the Standard Model hypercharge gauge boson are set in the range $(1-9) \times 10^{-5}$ and $(4-17) \times 10^{-2}$ respectively, at 95% confidence level assuming the Standard Model branching ratio of $H \rightarrow ZZ^* \rightarrow 4\ell$, for Z_d masses between 15 and 55 GeV. Upper bounds on the effective mass mixing parameter between the Z and the Z_d are also set using the branching ratio limits in the $H \rightarrow ZZ_d \rightarrow 4\ell$ search, and are in the range $(1.5-8.7) \times 10^{-4}$ for $15 < m_{Z_d} < 35$ GeV. Upper bounds on the branching ratio of $H \rightarrow Z_d Z_d \rightarrow 4\ell$ and on Higgs portal coupling parameter, controlling the strength of the coupling of the Higgs boson to dark vector bosons, are set in the range $(2-3) \times 10^{-5}$ and $(1-10) \times 10^{-4}$ respectively, at 95% confidence level assuming the Standard Model Higgs boson production cross sections, for Z_d masses between 15 and 60 GeV.

1 Introduction

Hidden sector or dark sector states appear in many extensions to the Standard Model (SM) [1–10], to provide a candidate for the dark matter in the universe [11] or to explain astrophysical observations of positron excesses [12–14]. A hidden or dark sector can be introduced with an additional $U(1)_d$ dark gauge symmetry [5–10].

In this paper, we present model-independent searches for dark sector states. We then interpret the results in benchmark models where the dark gauge symmetry is mediated by a dark vector boson Z_d . The dark sector could couple to the SM through kinetic mixing with the hypercharge gauge boson [15–17]. In this hypercharge portal scenario, the kinetic mixing parameter ϵ controls the coupling strength of the dark vector boson and SM particles. If, in addition, the $U(1)_d$ symmetry is broken by the introduction of a dark Higgs boson, then there could also be a mixing between the SM Higgs boson and the dark sector Higgs boson [5–10]. In this scenario, the Higgs portal coupling κ controls the strength of the Higgs coupling to dark vector bosons. The observed Higgs boson would then be the lighter partner of the new Higgs doublet, and could also decay via the dark sector. There is an additional Higgs portal scenario where there could be a mass-mixing between the SM Z boson and Z_d [7, 8]. In this scenario, the dark vector boson Z_d may couple to the SM Z boson with a coupling proportional to the mass mixing parameter δ .

The presence of the dark sector could be inferred either from deviations from the SM-predicted rates of Drell-Yan (DY) events or from Higgs boson decays through exotic intermediate states. Model-independent upper bounds, from electroweak constraints, on the kinetic mixing parameter of $\epsilon \leq 0.03$ are reported in Refs. [5, 18, 19] for dark vector boson masses between 1 GeV and 200 GeV. Upper bounds on the kinetic mixing parameter based on searches for dilepton resonances, $pp \rightarrow Z_d \rightarrow \ell\ell$, below the Z -boson mass are found to be in range of 0.005–0.020 for dark vector boson masses between 20 and 80 GeV [20]. The discovery of the Higgs boson [21–23] during Run 1 of the Large Hadron Collider (LHC) [24, 25] opens a new and rich experimental program that includes the search for exotic decays $H \rightarrow ZZ_d \rightarrow 4\ell$ and $H \rightarrow Z_d Z_d \rightarrow 4\ell$. This scenario is not entirely excluded by electroweak constraints [5–10, 18, 20]. The $H \rightarrow ZZ_d$ process probes the parameter space of ϵ and m_{Z_d} , or δ and m_{Z_d} , where m_{Z_d} is the mass of the dark vector boson, and the $H \rightarrow Z_d Z_d$ process covers the parameter space of κ and m_{Z_d} [5, 6]. DY production, $pp \rightarrow Z_d \rightarrow \ell\ell$, offers the most promising discovery potential for dark vector bosons in the event of no mixing between the dark Higgs boson and the SM Higgs boson. The $H \rightarrow ZZ_d \rightarrow 4\ell$ process offers a discovery potential complementary to the DY process for $m_{Z_d} < m_Z$ [5, 20]. Both of these would be needed to understand the properties of the dark vector boson [5]. If the dark Higgs boson mixes with the SM Higgs boson, the $H \rightarrow Z_d Z_d \rightarrow 4\ell$ process would be important, probing the dark sector through the Higgs portal coupling [5, 6].

This paper presents a search for Higgs bosons decaying to four leptons via one or two Z_d bosons using pp collision data at $\sqrt{s} = 8$ TeV collected at the CERN LHC with the ATLAS experiment. The search uses a dataset corresponding to an integrated luminosity of 20.7 fb⁻¹ with an uncertainty of 3.6% for $H \rightarrow ZZ_d \rightarrow 4\ell$ based on the luminosity calibration used in Refs. [26, 27], and 20.3 fb⁻¹ with an uncertainty of 2.8% for $H \rightarrow Z_d Z_d \rightarrow 4\ell$ based on a more recent calibration [28]. Same-flavor decays of the Z and Z_d bosons to electron and muon pairs are considered, giving the $4e$, $2e2\mu$, and 4μ final states. Final states including τ leptons are not considered in the $H \rightarrow ZZ_d \rightarrow 4\ell$ and $H \rightarrow Z_d Z_d \rightarrow 4\ell$ decays. In the absence of a significant signal, upper bounds are set on the relative branching ratios $\text{BR}(H \rightarrow ZZ_d \rightarrow 4\ell)/\text{BR}(H \rightarrow 4\ell)$ and $\text{BR}(H \rightarrow Z_d Z_d \rightarrow 4\ell)/\text{BR}(H \rightarrow ZZ^* \rightarrow 4\ell)$ as functions of the mass of the dark vector boson m_{Z_d} . The branching ratio limits are used to set upper bounds on the kinetic mixing, mass mixing, and Higgs boson mixing parameters [5, 6]. The search is restricted to the

mass range where the Z_d from the decay of the Higgs boson is on-shell, i.e. $15 \text{ GeV} < m_{Z_d} < m_H/2$, where $m_H = 125 \text{ GeV}$. Dark vector boson masses below 15 GeV are not considered in the present search. Although the low-mass region is theoretically well motivated [7, 8], the high p_T of the Z_d boson relative to its mass leads to signatures that are better studied in dedicated searches [29].

The paper is organized as follows. The ATLAS detector is briefly described in Sec. 2. The signal and background modeling is summarized in Sec. 3. The dataset, triggers, and event reconstruction are presented in Sec. 4. Detailed descriptions of the searches are given in Sec. 5 and Sec. 6 for $H \rightarrow ZZ_d \rightarrow 4\ell$ and $H \rightarrow Z_d Z_d \rightarrow 4\ell$ processes respectively. Finally, the concluding remarks are presented in Sec. 7.

2 Experimental Setup

The ATLAS detector [30] covers almost the whole solid angle around the collision point with layers of tracking detectors, calorimeters and muon chambers. The ATLAS inner detector (ID) has full coverage¹ in the azimuthal angle ϕ and covers the pseudorapidity range $|\eta| < 2.5$. It consists of a silicon pixel detector, a silicon microstrip detector, and a straw-tube tracker that also measures transition radiation for particle identification, all immersed in a 2 T axial magnetic field produced by a superconducting solenoid.

High-granularity liquid-argon (LAr) electromagnetic sampling calorimeters, with excellent energy and position resolution, cover the pseudorapidity range $|\eta| < 3.2$. The hadronic calorimetry in the range $|\eta| < 1.7$ is provided by a scintillator-tile calorimeter, consisting of a large barrel and two smaller extended barrel cylinders, one on either side of the central barrel. The LAr endcap ($1.5 < |\eta| < 3.2$) and forward sampling calorimeters ($3.1 < |\eta| < 4.9$) provide electromagnetic and hadronic energy measurements.

The muon spectrometer (MS) measures the deflection of muon trajectories with $|\eta| < 2.7$ in a toroidal magnetic field. Over most of the η -range, precision measurement of the track coordinates in the principal bending direction of the magnetic field is provided by monitored drift tubes. Cathode strip chambers are used in the innermost layer for $2.0 < |\eta| < 2.7$. The muon spectrometer is also instrumented with dedicated trigger chambers, resistive-plate chambers in the barrel and thin-gap chambers in the end-cap, covering $|\eta| < 2.4$.

The data are collected using an online three-level trigger system [31] that selects events of interest and reduces the event rate from several MHz to about 400 Hz for recording and offline processing.

3 Monte Carlo Simulation

Samples of Higgs boson production in the gluon fusion (ggF) mode, with $H \rightarrow ZZ_d \rightarrow 4\ell$ and $H \rightarrow Z_d Z_d \rightarrow 4\ell$, are generated for $m_H = 125 \text{ GeV}$ and $15 < m_{Z_d} < 60 \text{ GeV}$ (in 5 GeV steps) in MADGRAPH5 [32] with CTEQ6L1 [33] parton distribution functions (PDF) using the Hidden Abelian Higgs Model (HAHM) as a benchmark signal model [5, 9, 10]. PYTHIA8 [34, 35] and PHOTOS [36–38] are used to take into account parton showering, hadronization, and initial- and final-state radiation.

¹ ATLAS uses a right-handed coordinate system with its origin at the nominal interaction point (IP) in the center of the detector and the z -axis along the beam pipe. The x -axis points from the IP to the center of the LHC ring, and the y -axis points upward. The azimuthal angle ϕ is measured around the beam axis, and the polar angle θ is measured with respect to the z -axis. ATLAS defines transverse energy $E_T = E \sin\theta$, transverse momentum $p_T = p \sin\theta$, and pseudorapidity $\eta = -\ln(\tan[\theta/2])$.

The background processes considered in the $H \rightarrow ZZ_d \rightarrow 4\ell$ and $H \rightarrow Z_d Z_d \rightarrow 4\ell$ searches follow those used in the $H \rightarrow ZZ^* \rightarrow 4\ell$ measurements [39], and consist of:

- Higgs boson production via the SM ggF, VBF (vector boson fusion), WH , ZH , and $t\bar{t}H$ processes with $H \rightarrow ZZ^* \rightarrow 4\ell$ final states. In the $H \rightarrow Z_d Z_d \rightarrow 4\ell$ search, these background processes are normalized with the theoretical cross sections, where the Higgs boson production cross sections and decay branching ratios, as well as their uncertainties, are taken from Refs. [40, 41]. In the $H \rightarrow ZZ_d \rightarrow 4\ell$ search, the normalization of $H \rightarrow 4\ell$ is determined from data. The cross section for the ggF process has been calculated to next-to-leading-order (NLO) [42–44] and next-to-next-to-leading-order (NNLO) [45–47] in QCD. In addition, QCD soft-gluon resummations calculated in the next-to-next-to-leading-logarithmic (NNLL) approximation are applied for the ggF process [48]. NLO electroweak (EW) radiative corrections are also applied [49, 50]. These results are compiled in Refs. [51–53] assuming factorization between QCD and EW corrections. For the VBF process, full QCD and EW corrections up to NLO [54–56] and approximate NNLO QCD [57] corrections are used to calculate the cross section. The cross sections for the associated WH and ZH production processes are calculated at NLO [58] and at NNLO [59] in QCD, and NLO EW radiative corrections are applied [60]. The cross section for associated Higgs boson production with a $t\bar{t}$ pair is calculated at NLO in QCD [61–64]. The SM ggF and VBF processes producing $H \rightarrow ZZ^* \rightarrow 4\ell$ backgrounds are modeled with POWHEG, PYTHIA8 and CT10 PDFs [33]. The SM WH , ZH , and $t\bar{t}H$ processes producing $H \rightarrow ZZ^* \rightarrow 4\ell$ backgrounds are modeled with PYTHIA8 with CTEQ6L1 PDFs.
- SM ZZ^* production. The rate of this background is estimated using simulation normalized to the SM cross section at NLO. The $ZZ^* \rightarrow 4\ell$ background is modeled using simulated samples generated with POWHEG [65] and PYTHIA8 [35] for $q\bar{q} \rightarrow ZZ^*$, and gg2ZZ [66] and JIMMY [67] for $gg \rightarrow ZZ^*$, and CT10 PDFs for both.
- Z +jets and $t\bar{t}$. The rates of these background processes are estimated using data-driven methods. However Monte Carlo (MC) simulation is used to understand the systematic uncertainty on the data-driven techniques. The Z +jets production is modeled with up to five partons using ALPGEN [68] and is divided into two sources: Z +light-jets, which includes $Zc\bar{c}$ in the massless c -quark approximation and $Zb\bar{b}$ with $b\bar{b}$ from parton showers; and $Zb\bar{b}$ using matrix-element calculations that take into account the b -quark mass. The matching scheme of matrix elements and parton shower evolution (see Ref. [69] and the references therein) is used to remove any double counting of identical jets produced via the matrix-element calculation and the parton shower, but this scheme is not implemented for b -jets. Therefore, $b\bar{b}$ pairs with separation $\Delta R \equiv \sqrt{(\Delta\phi)^2 + (\Delta\eta)^2} > 0.4$ between the b -quarks are taken from the matrix-element calculation, whereas for $\Delta R < 0.4$ the parton-shower $b\bar{b}$ pairs are used. For comparison between data and simulation, the NNLO QCD FEWZ [70, 71] and NLO QCD MCFM [72, 73] cross-section calculations are used to normalize the simulations for inclusive Z boson and $Zb\bar{b}$ production, respectively. The $t\bar{t}$ background is simulated with MC@NLO-4.06 [74] with parton showers and underlying-event modeling as implemented in HERWIG 6.5.20 [75] and JIMMY. The AUET2C [76] tune for the underlying events is used for $t\bar{t}$ with CT10 PDFs.
- SM WZ and WW production. The rates of these backgrounds are normalized to theoretical calculations at NLO in perturbative QCD [77]. The simulated event samples are produced with SHERPA [78] and CT10 PDFs.
- Backgrounds containing J/ψ and Υ , namely ZJ/ψ and $Z\Upsilon$. These backgrounds are normalized using the ATLAS measurements described in Ref. [79]. These processes are modeled with PYTHIA8 [35] and CTEQ6L1 PDFs.

Differing pileup conditions (multiple proton-proton interactions in the same or neighboring bunch-crossings)

as a function of the instantaneous luminosity are taken into account by overlaying simulated minimum-bias events generated with PYTHIA8 onto the hard-scattering process and reweighting them according to the distribution of the mean number of interactions observed in data. The MC generated samples are processed either with a full ATLAS detector simulation [80] based on the GEANT4 program [81] or a fast simulation based on the parameterization of the response to the electromagnetic and hadronic showers in the ATLAS calorimeters [82] and a detailed simulation of other parts of the detector and the trigger system. The results based on the fast simulation are validated against fully simulated samples and the difference is found to be negligible. The simulated events are reconstructed and analyzed with the same procedure as the data, using the same trigger and event selection criteria.

4 Event Reconstruction

A combination of single-lepton and dilepton triggers is used to select the data samples. The single-electron trigger has a transverse energy (E_T) threshold of 25 GeV while the single-muon trigger has a transverse momentum (p_T) threshold of 24 GeV. The dielectron trigger has a threshold of $E_T = 12$ GeV for both electrons. In the case of muons, triggers with symmetric thresholds at $p_T = 13$ GeV and asymmetric thresholds at 18 GeV and 8 GeV are used. Finally, electron-muon triggers are used with electron E_T thresholds of 12 GeV or 24 GeV depending on the electron identification requirement, and a muon p_T threshold of 8 GeV. The trigger efficiency for events passing the final selection is above 97% [39] in each of the final states considered.

Data events recorded during periods when significant portions of the relevant detector subsystems were not fully functional are rejected. These requirements are applied independently of the lepton final state. Events in a time window around a noise burst in the calorimeter are removed [83]. Further, all triggered events are required to contain a reconstructed primary vertex formed from at least 3 tracks, each with $p_T > 0.4$ GeV.

Electron candidates consist of clusters of energy deposited in the electromagnetic calorimeter and associated with ID tracks [84]. The clusters matched to tracks are required to satisfy a set of identification criteria such that the longitudinal and transverse shower profiles are consistent with those expected from electromagnetic showers. The electron transverse momentum is computed from the cluster energy and the track direction at the interaction point. Selected electrons must satisfy $E_T > 7$ GeV and $|\eta| < 2.47$. Each electron must have a longitudinal impact parameter (z_0) of less than 10 mm with respect to the reconstructed primary vertex, defined as the vertex with at least three associated tracks for which the $\sum p_T^2$ of the associated tracks is the highest. Muon candidates are formed by matching reconstructed ID tracks with either complete or partial tracks reconstructed in the muon spectrometer [85]. If a complete track is present, the two independent momentum measurements are combined; otherwise the momentum is measured using the ID. The muon reconstruction and identification coverage is extended by using tracks reconstructed in the forward region ($2.5 < |\eta| < 2.7$) of the MS, which is outside the ID coverage. In the center of the barrel region ($|\eta| < 0.1$), where there is no coverage from muon chambers, ID tracks with $p_T > 15$ GeV are identified as muons if their calorimetric energy deposits are consistent with a minimum ionizing particle. Only one muon per event is allowed to be reconstructed in the MS only or identified with the calorimeter. Selected muons must satisfy $p_T > 6$ GeV and $|\eta| < 2.7$. The requirement on the longitudinal impact parameter is the same as for electrons except for the muons reconstructed in the forward region without an ID track. To reject cosmic-ray muons, the impact parameter in the bending plane (d_0) is required to be within 1 mm of the primary vertex.

In order to avoid double-counting of leptons, an overlap removal procedure is applied. If two reconstructed electron candidates share the same ID track or are too close to each other in η and ϕ ($\Delta R < 0.1$), the one with the highest transverse energy deposit in the calorimeter is kept. An electron within $\Delta R = 0.2$ of a muon candidate is removed, and a calorimeter-based reconstructed muon within $\Delta R = 0.2$ of an electron is removed.

Once the leptons have been selected with the aforementioned basic identification and kinematic requirements, events with at least four selected leptons are kept. All possible combinations of four leptons (quadruplets) containing two same-flavor, opposite-charge sign (SFOS) leptons, are made. The selected leptons are ordered by decreasing transverse momentum and the three highest- p_T leptons should have respectively $p_T > 20$ GeV, $p_T > 15$ GeV and $p_T > 10$ GeV. It is then required that one (two) leptons match the single-lepton (dilepton) trigger objects. The leptons within each quadruplet are then ordered in SFOS pairs, and denoted 1 to 4, indices 1 and 2 being for the first pair, 3 and 4 for the second pair.

5 $H \rightarrow ZZ_d \rightarrow 4\ell$

5.1 Search strategy

The $H \rightarrow ZZ_d \rightarrow 4\ell$ search is conducted with the same sample of selected 4ℓ events as used in Refs. [26, 27] with the four-lepton invariant mass requirement of $115 < m_{4\ell} < 130$ GeV. This collection of events is referred to as the 4ℓ sample. The invariant mass of the opposite-sign, same-flavor pair closest to the Z -boson pole mass of 91.2 GeV [86] is denoted m_{12} . The invariant mass of the remaining dilepton pair is defined as m_{34} . The $H \rightarrow 4\ell$ yield, denoted $n(H \rightarrow 4\ell)$, is determined by subtracting the relevant backgrounds from the 4ℓ sample as shown in Eq. (1):

$$n(H \rightarrow 4\ell) = n(4\ell) - n(ZZ^*) - n(t\bar{t}) - n(Z + \text{jets}). \quad (1)$$

The other backgrounds from WW , WZ , ZJ/ψ and $Z\Upsilon$ are negligible and not considered.

The search is performed by inspecting the m_{34} mass spectrum and testing for a local excess consistent with the decay of a narrow Z_d resonance. This is accomplished through a template fit of the m_{34} distribution, using histogram-based templates of the $H \rightarrow ZZ_d \rightarrow 4\ell$ signal and backgrounds. The signal template is obtained from simulation and is described in Sec. 5.2. The m_{34} distributions and the expected normalizations of the $t\bar{t}$ and Z +jets backgrounds, along with the m_{34} distributions of the $H \rightarrow ZZ^* \rightarrow 4\ell$ background, as shown in Fig. 1, are determined as described in Sec. 5.4. The pre-fit signal and $H \rightarrow ZZ^* \rightarrow 4\ell$ background event yields are set equal to the $H \rightarrow 4\ell$ observed yield given by Eq. (1). The expected yields for the 4ℓ sample are shown in Table 1.

In the absence of any significant local excess, the search can be used to constrain a relative branching ratio R_B , defined as:

$$\begin{aligned} R_B &= \frac{\text{BR}(H \rightarrow ZZ_d \rightarrow 4\ell)}{\text{BR}(H \rightarrow 4\ell)} \\ &= \frac{\text{BR}(H \rightarrow ZZ_d \rightarrow 4\ell)}{\text{BR}(H \rightarrow ZZ_d \rightarrow 4\ell) + \text{BR}(H \rightarrow ZZ^* \rightarrow 4\ell)}, \end{aligned} \quad (2)$$

Channel	ZZ^*	$t\bar{t} + Z$ +jets	Sum	Observed	$H \rightarrow 4\ell$
4μ	$3.1 \pm 0.02 \pm 0.4$	$0.6 \pm 0.04 \pm 0.2$	$3.7 \pm 0.04 \pm 0.6$	12	$8.3 \pm 0.04 \pm 0.6$
$4e$	$1.3 \pm 0.02 \pm 0.5$	$0.8 \pm 0.07 \pm 0.4$	$2.1 \pm 0.07 \pm 0.9$	9	$6.9 \pm 0.07 \pm 0.9$
$2\mu 2e$	$1.4 \pm 0.01 \pm 0.3$	$1.2 \pm 0.10 \pm 0.4$	$2.6 \pm 0.10 \pm 0.6$	7	$4.4 \pm 0.10 \pm 0.6$
$2e 2\mu$	$2.1 \pm 0.02 \pm 0.3$	$0.6 \pm 0.04 \pm 0.2$	$2.7 \pm 0.10 \pm 0.5$	8	$5.3 \pm 0.04 \pm 0.5$
all	$7.8 \pm 0.04 \pm 1.2$	$3.2 \pm 0.1 \pm 1.0$	$11.1 \pm 0.1 \pm 1.8$	36	$24.9 \pm 0.1 \pm 1.8$

Table 1: The estimated pre-fit background yields of (MC) ZZ^* , (data-driven) $t\bar{t} + Z$ +jets, their sum, the observed 4ℓ event yield and the estimated pre-fit $H \rightarrow 4\ell$ contribution in the 4ℓ sample. The $H \rightarrow 4\ell$ estimate in the last column is obtained as the difference between the observed event yield and the sum of the ZZ^* and $t\bar{t} + Z$ +jets backgrounds. The pre-fit $H \rightarrow ZZ^* \rightarrow 4\ell$ background and $H \rightarrow ZZ_d \rightarrow 4\ell$ signal events are normalized to the $H \rightarrow 4\ell$ observed events. The uncertainties are statistical and systematic respectively. The systematic uncertainties are discussed in Section 5.5. Uncertainties on the $H \rightarrow 4\ell$ rates do not include the statistical uncertainty from the observed number.

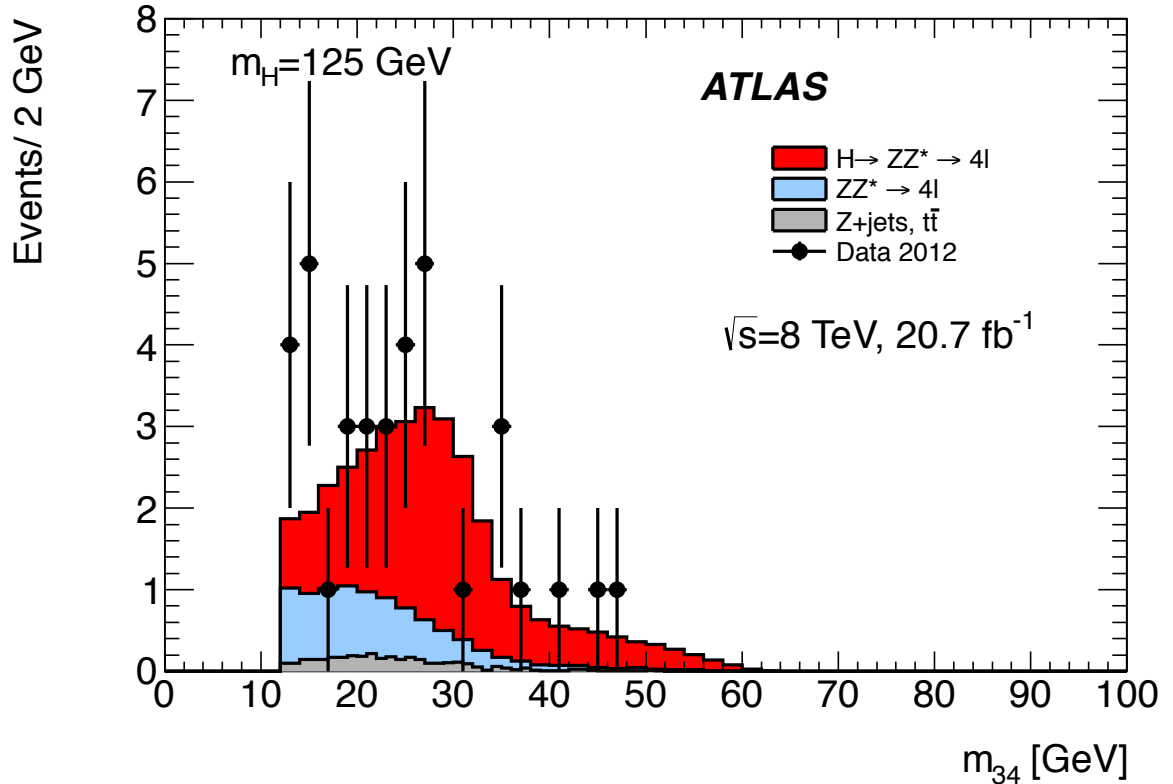


Figure 1: The distribution of the mass of the second lepton pair, m_{34} , of the $\sqrt{s}=8$ TeV data (filled circles with error bars) and the expected (pre-fit) backgrounds. The $H \rightarrow ZZ^* \rightarrow 4\ell$ expected (pre-fit) normalization, for a mass hypothesis of $m_H=125$ GeV, is set by subtracting the expected contributions of the ZZ^* , Z +jets and $t\bar{t}$ backgrounds from the total number of observed 4ℓ events in the data.

where R_B is zero in the Standard Model. A likelihood function (\mathcal{L}) is defined as a product of Poisson probability densities (\mathcal{P}) in each bin (i) of the m_{34} distribution, and is used to obtain a measurement of R_B :

$$\begin{aligned}
\mathcal{L}(\rho, \mu_H, \nu) &= \prod_{i=1}^{N_{\text{bins}}} \mathcal{P}(n_i^{\text{obs}} | n_i^{\text{exp}}) \\
&= \prod_{i=1}^{N_{\text{bins}}} \mathcal{P}(n_i^{\text{obs}} | \mu_H \times (n_i^{Z^*} + \rho \times n_i^{Z_d}) + b_i(\nu)),
\end{aligned} \tag{3}$$

where μ_H is the normalization of the $H \rightarrow ZZ^* \rightarrow 4\ell$ background (and allowed to float in the fit), ρ the parameter of interest related to the $H \rightarrow ZZ_d \rightarrow 4\ell$ normalization and $\rho \times \mu_H$ the normalization of the $H \rightarrow ZZ_d \rightarrow 4\ell$ signal. The symbol ν represents the systematic uncertainties on the background estimates that are treated as nuisance parameters, and N_{bins} the total number of bins of the m_{34} distribution. The likelihood to observe the yield in some bin, n_i^{obs} , given the expected yield n_i^{exp} is then a function of the expected yields $n(H \rightarrow 4\ell)$ of $H \rightarrow ZZ_d \rightarrow 4\ell$ ($\mu_H \times \rho \times n_i^{Z_d}$) and $H \rightarrow ZZ^* \rightarrow 4\ell$ ($\mu_H \times n_i^{Z^*}$), and the contribution of backgrounds $b_i(\nu)$.

An upper bound on ρ is obtained from the binned likelihood fit to the data, and used in Eq. (2) to obtain a measurement of R_B , taking into account the detector acceptance (\mathcal{A}) and reconstruction efficiency (ε):

$$\begin{aligned}
R_B &= \frac{\rho \times \mu_H \times n(H \rightarrow 4\ell)}{\rho \times \mu_H \times n(H \rightarrow 4\ell) + C \times \mu_H \times n(H \rightarrow 4\ell)} \\
&= \frac{\rho}{\rho + C},
\end{aligned} \tag{4}$$

where C is the ratio of the products of the acceptances and reconstruction efficiencies in $H \rightarrow ZZ_d \rightarrow 4\ell$ and $H \rightarrow ZZ^* \rightarrow 4\ell$ events:

$$C = \frac{\mathcal{A}_{ZZ_d} \times \varepsilon_{ZZ_d}}{\mathcal{A}_{ZZ^*} \times \varepsilon_{ZZ^*}}. \tag{5}$$

The acceptance is defined as the fraction of generated events that are within a fiducial region. The reconstruction efficiency is defined as the fraction of events within the fiducial region that are reconstructed and selected as part of the 4ℓ signal sample.

5.2 Signal modeling

A signal would produce a narrow peak in the m_{34} mass spectrum. The width of the m_{34} peak for the Z_d signal is dominated by detector resolution for all Z_d masses considered. For the individual decay channels and their combination, the resolutions of the m_{34} distributions are determined from Gaussian fits. The m_{34} resolutions show a linear trend between $m_{Z_d} = 15$ GeV and $m_{Z_d} = 55$ GeV and vary from 0.3 GeV to 1.5 GeV respectively, for the combination of all the final states. The resolutions of the m_{34} distributions are smaller than the mass spacing between the generated signal samples (5 GeV), requiring an interpolation to probe intermediate values of m_{Z_d} . Histogram-based templates are used to model the Z_d signal where no simulation is available; these templates are obtained from morphed signals produced with the procedure defined in Ref. [87]. The morphed signal templates are generated with a mass spacing of 1 GeV.

The acceptances and reconstruction efficiencies of the $H \rightarrow ZZ_d \rightarrow 4\ell$ signal and $H \rightarrow ZZ^* \rightarrow 4\ell$ background are used in Eqs. (4) and (5) to obtain the measurement of the relative branching ratio R_B . The

Method	Estimated background
	4μ
m_{12} fit: Z +jets contribution	$2.4 \pm 0.5 \pm 0.6$
m_{12} fit: $t\bar{t}$ contribution	$0.14 \pm 0.03 \pm 0.03$
	$2e2\mu$
m_{12} fit: Z +jets contribution	$2.5 \pm 0.5 \pm 0.6$
m_{12} fit: $t\bar{t}$ contribution	$0.10 \pm 0.02 \pm 0.02$
	$2\mu 2e$
$\ell\ell + e^\pm e^\mp$ relaxed requirements: sum of Z + jets and $t\bar{t}$ contributions	$5.2 \pm 0.4 \pm 0.5$
	$4e$
$\ell\ell + e^\pm e^\mp$ relaxed requirements: sum of Z + jets and $t\bar{t}$ contributions	$3.2 \pm 0.5 \pm 0.4$

Table 2: Summary of the estimated expected numbers of Z +jets and $t\bar{t}$ background events for the 20.7 fb^{-1} of data at $\sqrt{s} = 8 \text{ TeV}$ for the full mass range after kinematic selections, for the $H \rightarrow ZZ_d \rightarrow 4\ell$ search. The first uncertainty is statistical while the second is systematic. The uncertainties are given on the event yields. Approximately 80% of the $t\bar{t}$ and Z +jets backgrounds have $m_{4\ell} < 160 \text{ GeV}$.

acceptances and efficiencies are derived with $H \rightarrow ZZ_d \rightarrow 4\ell$ and $H \rightarrow ZZ^* \rightarrow 4\ell$ MC samples where the Higgs boson is produced via ggF. The product of acceptance and reconstruction efficiency for VBF differs from ggF by only 1.2% and the contribution of VH and $t\bar{t}H$ production modes is negligible: the products of acceptance and reconstruction efficiency obtained using the ggF production mode are used also for VBF, VH and $t\bar{t}H$.

5.3 Event selection

The Higgs boson candidate is formed by selecting two pairs of SFOS leptons. The value of m_{12} is required to be between 50 GeV and 106 GeV. The value of m_{34} is required to be in the range $12 \text{ GeV} \leq m_{34} \leq 115 \text{ GeV}$. The four-lepton invariant mass $m_{4\ell}$ is required to be in the range $115 < m_{4\ell} < 130 \text{ GeV}$. After applying the selection to the 8 TeV data sample, 36 events are left as shown in Table 1. The events are grouped into four channels based on the flavor of the reconstructed leptons. Events with four electrons are in the $4e$ channel. Events in which the Z boson is reconstructed with electrons, and m_{34} is formed from muons, are in the $2e2\mu$ channel. Similarly, events in which the Z is reconstructed from muons and m_{34} is formed from electrons are in the $2\mu 2e$ channel. Events with four muons are in the 4μ channel.

5.4 Background estimation

The search is performed using the same background estimation strategy as the $H \rightarrow ZZ^* \rightarrow 4\ell$ measurements. The expected rates of the $t\bar{t}$ and Z +jets backgrounds are estimated using data-driven methods as described in detail in Refs. [26, 27]. The results of the expected $t\bar{t}$ and Z +jets background estimations from data control regions are summarized in Table 2. In the “ m_{12} fit method”, the m_{12} distribution of $t\bar{t}$ is fitted with a second-order Chebychev polynomial, and the Z +jets component is fitted with a Breit-Wigner lineshape convolved with a Crystal Ball resolution function [26]. In the “ $\ell\ell + e^\pm e^\mp$ relaxed requirements” method, a background control region is formed by relaxing the electron selection criteria for electrons of the subleading pairs [26]. Since a fit to the data using m_{34} background templates is carried out in the

Systematic Uncertainties (%)				
Source	4μ	$4e$	$2\mu 2e$	$2e 2\mu$
Electron Identification	–	9.4	8.7	2.4
Electron Energy Scale	–	0.4	–	0.2
Muon Identification	0.8	–	0.4	0.7
Muon Momentum Scale	0.2	–	0.1	–
Luminosity	3.6	3.6	3.6	3.6
$t\bar{t}$ and Z +jets Normalization	25.0	25.0	25.0	25.0
ZZ^* (QCD scale)	5.0	5.0	5.0	5.0
ZZ^* ($q\bar{q}$ /PDF and α_s)	4.0	4.0	4.0	4.0
ZZ^* (gg /PDF and α_s)	8.0	8.0	8.0	8.0

Table 3: The relative systematic uncertainties on the event yields in the $H \rightarrow ZZ_d \rightarrow 4\ell$ search.

search, both the distribution in m_{34} and normalization of the backgrounds are relevant. For all relevant backgrounds ($H \rightarrow ZZ^* \rightarrow 4\ell$, ZZ^* , $t\bar{t}$ and Z +jets) the m_{34} distribution is obtained from simulation.

5.5 Systematic uncertainties

The sources of the systematic uncertainties in the $H \rightarrow ZZ_d \rightarrow 4\ell$ search are the same as in the $H \rightarrow ZZ^* \rightarrow 4\ell$ measurements. Uncertainties on the lepton reconstruction and identification efficiencies, as well as on the energy and momentum reconstruction and scale are described in detail in Refs. [26, 27], and shown in Table 3. The lepton identification is the dominant contribution to the systematic uncertainties on the ZZ^* background. The largest uncertainty in the $H \rightarrow ZZ_d \rightarrow 4\ell$ search is the normalization of the $t\bar{t}$ and Z +jets backgrounds. Systematic uncertainties related to the determination of selection efficiencies of isolation and impact parameters requirements are shown to be negligible in comparison with other systematic uncertainties. The uncertainty in luminosity [28] is applied to the ZZ^* background normalization. The electron energy scale uncertainty is determined from $Z \rightarrow ee$ samples and for energies below 15 GeV from $J/\psi \rightarrow ee$ decays [26, 27]. Final-state QED radiation modeling and background contamination affect the mass scale uncertainty negligibly. The muon momentum scale systematic uncertainty is determined from $Z \rightarrow \mu\mu$ samples and from $J/\psi \rightarrow \mu\mu$ as well as $\Upsilon \rightarrow \mu\mu$ decays [26, 27]. Theory related systematic uncertainties on the Higgs production cross section and branching ratios are discussed in Refs. [39–41], but do not apply in this search since the $H \rightarrow 4\ell$ normalization is obtained from data. Uncertainties on the m_{34} shapes arising from theory uncertainties on the PDFs and renormalization and factorization scales are found to be negligible. Theory cross-section uncertainties are applied to the ZZ^* background. Normalization uncertainties are taken into account for the Z +jets and $t\bar{t}$ backgrounds based on the data-driven determination of these backgrounds.

5.6 Results and interpretation

A profile-likelihood test statistic is used with the CL_s modified frequentist formalism [88–91] implemented in the RooStats framework [92] to test whether the data are compatible with the signal-plus-background and background-only hypotheses. Separate fits are performed for different m_{Z_d} hypotheses

from 15 GeV to 55 GeV, with 1 GeV spacing. After scanning the m_{34} mass spectrum for an excess consistent with the presence of a $H \rightarrow ZZ_d \rightarrow 4\ell$ signal, no significant deviation from SM expectations is observed.

The asymptotic approximation [90] is used to estimate the expected and observed exclusion limits on ρ for the combination of all the final states, and the result is shown in Fig. 2. The relative branching ratio

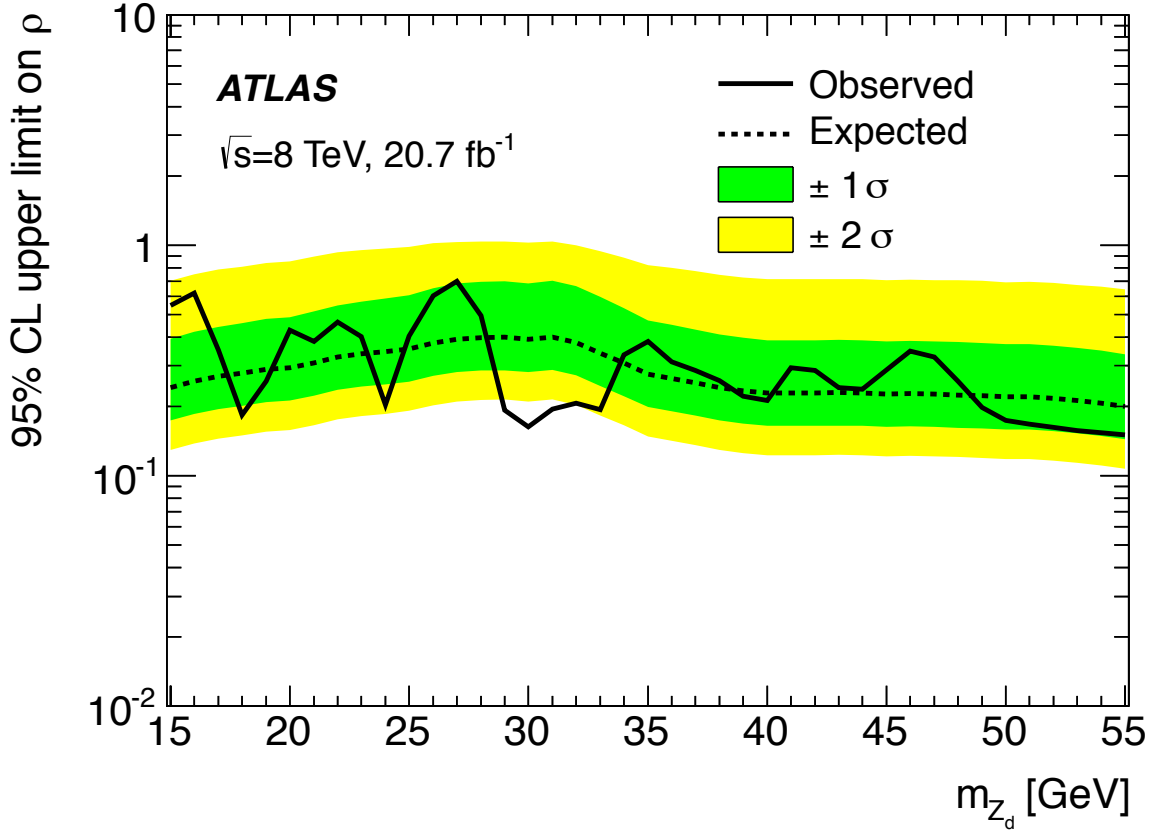


Figure 2: The observed (solid line) and median expected (dashed line) 95% confidence level (CL) upper limits on the parameter ρ related to the $H \rightarrow ZZ_d \rightarrow 4\ell$ normalization as a function of m_{Z_d} , for the combination of all four channels (4μ , $4e$, $2\mu 2e$, $2e2\mu$). The $\pm 1\sigma$ and $\pm 2\sigma$ expected exclusion regions are indicated in green and yellow, respectively.

R_B as a function of m_{Z_d} is extracted using Eqs. (2) and (4) where the value of C as a function of m_{34} is shown in Fig. 3, for the combination of all four final states. This is then used with ρ to constrain the value of R_B , and the result is shown in Fig. 4 for the combination of all four final states.

The simplest benchmark model adds to the SM Lagrangian [6–8, 10] a $U(1)_d$ gauge symmetry that introduces the dark vector boson Z_d . The dark vector boson may mix kinetically with the SM hypercharge gauge boson with kinetic mixing parameter ϵ [6, 10]. This enables the decay $H \rightarrow ZZ_d$ through the Hypercharge Portal. The Z_d is assumed to be narrow and on-shell. Furthermore, the present search assumes prompt Z_d decays consistent with current bounds on ϵ from electroweak constraints [18, 19]. The coupling of the Z_d to SM fermions is given in Eq. (47) of Ref. [6] to be linear in ϵ , so that $\text{BR}(Z_d \rightarrow \ell\ell)$ is independent of ϵ due to cancellations [6]. In this model, the $H \rightarrow ZZ_d \rightarrow 4\ell$ search can be used to constrain the

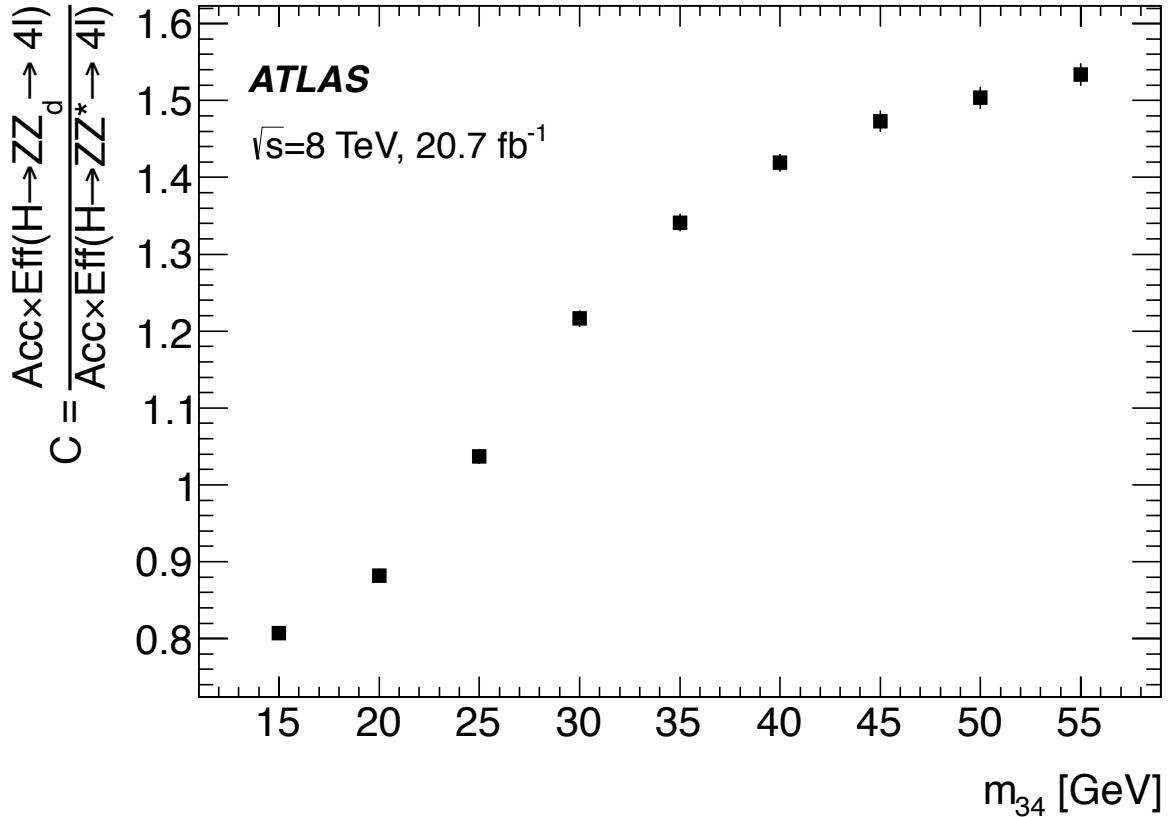


Figure 3: The ratio C of the products of the acceptances and reconstruction efficiencies in $H \rightarrow ZZ_d \rightarrow 4\ell$ and $H \rightarrow ZZ^* \rightarrow 4\ell$ events as a function of m_{34} .

hypercharge kinetic mixing parameter ϵ as follows: the upper limit on R_B shown in Fig. 4 leads to an upper limit on $\text{BR}(H \rightarrow ZZ_d \rightarrow 4\ell)$ assuming the SM branching ratio of $H \rightarrow ZZ^* \rightarrow 4\ell$ of 1.25×10^{-4} [40, 41] as shown in Fig. 5. The limit on ϵ can be obtained directly from the $\text{BR}(H \rightarrow ZZ_d \rightarrow 4\ell)$ upper bounds and by using Table 2 of Ref. [5]. The 95% CL upper bounds on ϵ are shown in Fig. 6 as a function of m_{Z_d} in the case $\epsilon \gg \kappa$ where κ is the Higgs portal coupling.

The measurement of the relative branching ratio R_B as shown in Fig. 4 can also be used to constrain the mass-mixing parameter of the model described in Refs. [7, 8] where the SM is extended with a dark vector boson and another Higgs doublet, and a mass mixing between the dark vector boson and the SM Z boson is introduced. This model explores how a $U(1)_d$ gauge interaction in the hidden sector may manifest itself in the decays of the Higgs boson. The model also assumes that the Z_d , being in the hidden sector, does not couple directly to any SM particles including the Higgs boson (i.e. the SM particles do not carry dark charges). However, particles in the extensions to the SM, such as a second Higgs doublet, may carry dark charges allowing for indirect couplings via the Z - Z_d mass mixing. The possibility of mixing between the SM Higgs boson with other scalars such the dark sector Higgs boson is not considered for simplicity. The Z - Z_d mass-mixing scenario also leads to potentially observable $H \rightarrow ZZ_d \rightarrow 4\ell$ decays at the LHC even with the total integrated luminosity collected in Run 1. The partial widths of $H \rightarrow ZZ_d \rightarrow 4\ell$ and $H \rightarrow ZZ_d$ are given in terms of the Z - Z_d mass-mixing parameter δ and m_{Z_d} in Eq. (34) of Ref. [8] and Eq. (A.4) of Ref. [7] respectively. As a result, using the measurement of the relative branching ratio R_B

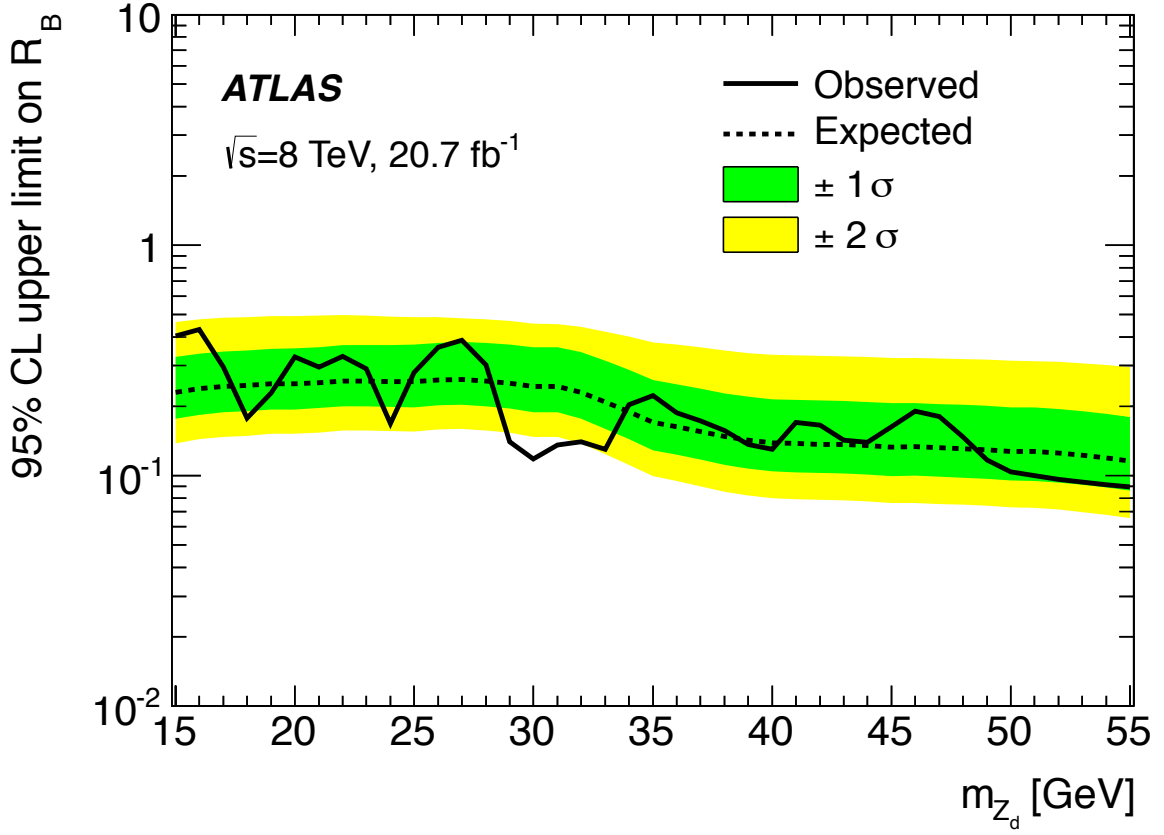


Figure 4: The 95% CL upper limits on the relative branching ratio, $R_B = \frac{\text{BR}(H \rightarrow ZZ_d \rightarrow 4\ell)}{\text{BR}(H \rightarrow 4\ell)}$ as a function of m_{Z_d} . The $\pm 1\sigma$ and $\pm 2\sigma$ expected exclusion regions are indicated in green and yellow, respectively.

described in this paper, one may set upper bounds on the product $\delta^2 \times \text{BR}(Z_d \rightarrow 2\ell)$ as function of m_{Z_d} as follows. From Eq. (2) and for $m_{Z_d} < (m_H - m_Z)$

$$\begin{aligned}
 \frac{\text{BR}(H \rightarrow ZZ_d \rightarrow 4\ell)}{\text{BR}(H \rightarrow ZZ^* \rightarrow 4\ell)} &= \frac{R_B}{(1 - R_B)}, \\
 &\simeq \frac{\Gamma(H \rightarrow ZZ_d)}{\Gamma_{\text{SM}}} \times \\
 &\frac{\text{BR}(Z^* \rightarrow 2\ell) \times \text{BR}(Z_d \rightarrow 2\ell)}{\text{BR}(H \rightarrow ZZ^* \rightarrow 4\ell)},
 \end{aligned} \tag{6}$$

where Γ_{SM} is the total width of the SM Higgs boson and $\Gamma(H \rightarrow ZZ_d) \ll \Gamma_{\text{SM}}$. From Eqs. (4), (A.3) and (A.4) of Ref. [7], $\Gamma(H \rightarrow ZZ_d) \sim \delta^2$. It therefore follows from Eq. (6), with the further assumption

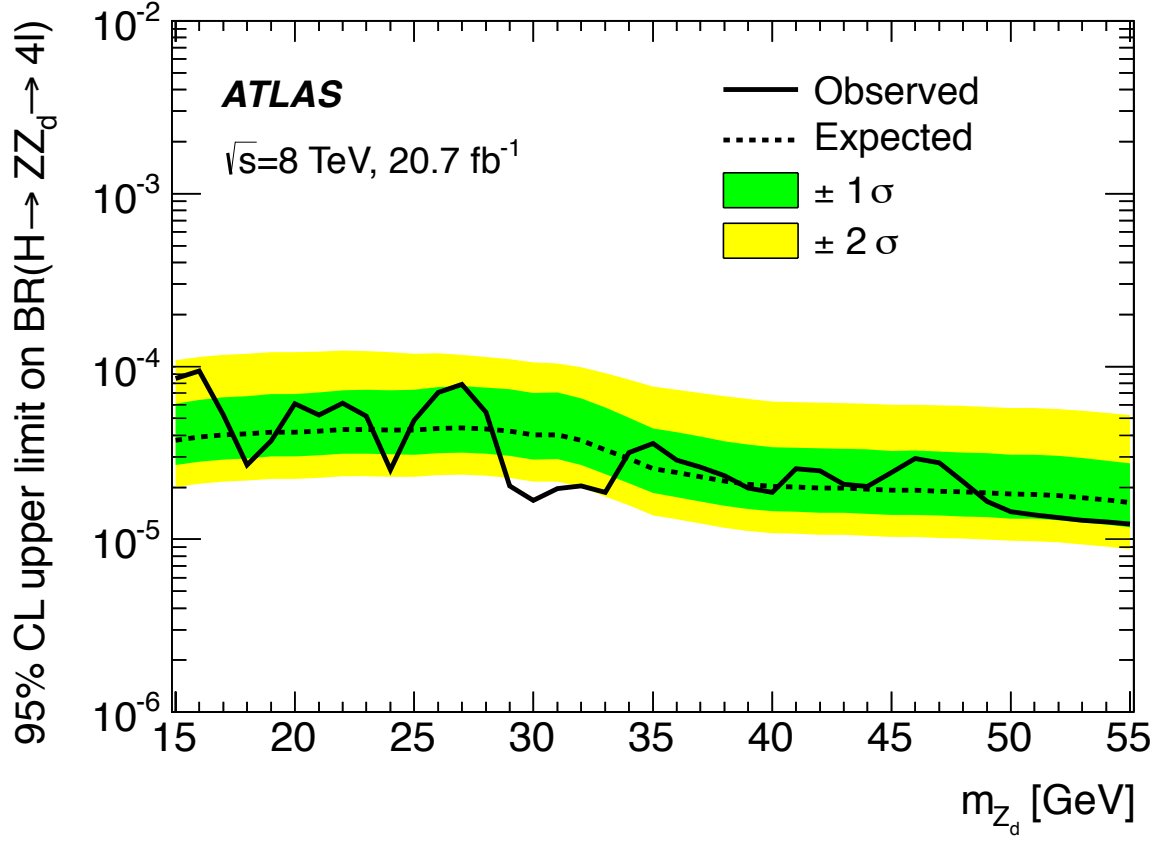


Figure 5: The 95% CL upper limits on the branching ratio of $H \rightarrow ZZ_d \rightarrow 4\ell$ as a function of m_{Z_d} using the combined upper limit on R_B and the SM branching ratio of $H \rightarrow ZZ^* \rightarrow 4\ell$.

$m_{Z_d}^2 \ll (m_H^2 - m_Z^2)$ that:

$$\begin{aligned} \frac{R_B}{(1 - R_B)} &\simeq \delta^2 \times \text{BR}(Z_d \rightarrow 2\ell) \times \\ &\frac{\text{BR}(Z^* \rightarrow 2\ell)}{\text{BR}(H \rightarrow ZZ^* \rightarrow 4\ell)} \times \frac{f(m_{Z_d})}{\Gamma_{\text{SM}}}, \\ f(m_{Z_d}) &= \frac{1}{16\pi} \frac{(m_H^2 - m_Z^2)^3}{v^2 m_H^3}. \end{aligned} \quad (7)$$

where v is the vacuum expectation value of the SM Higgs field. The limit is set on the product $\delta^2 \times \text{BR}(Z_d \rightarrow 2\ell)$ since both δ and $\text{BR}(Z_d \rightarrow 2\ell)$ are model-dependent: in the case where kinetic mixing dominates, $\text{BR}(Z_d \rightarrow 2\ell) \sim 30\%$ for the model presented in Ref. [6] but it could be smaller when Z - Z_d mass mixing dominates [8]. In the m_{Z_d} mass range of 15 GeV to $(m_H - m_Z)$, the upper bounds on $\delta^2 \times \text{BR}(Z_d \rightarrow 2\ell)$ are in the range $\sim (1.5\text{--}8.7) \times 10^{-5}$ as shown in Fig. 7, assuming the same signal acceptances shown in Fig. 3.

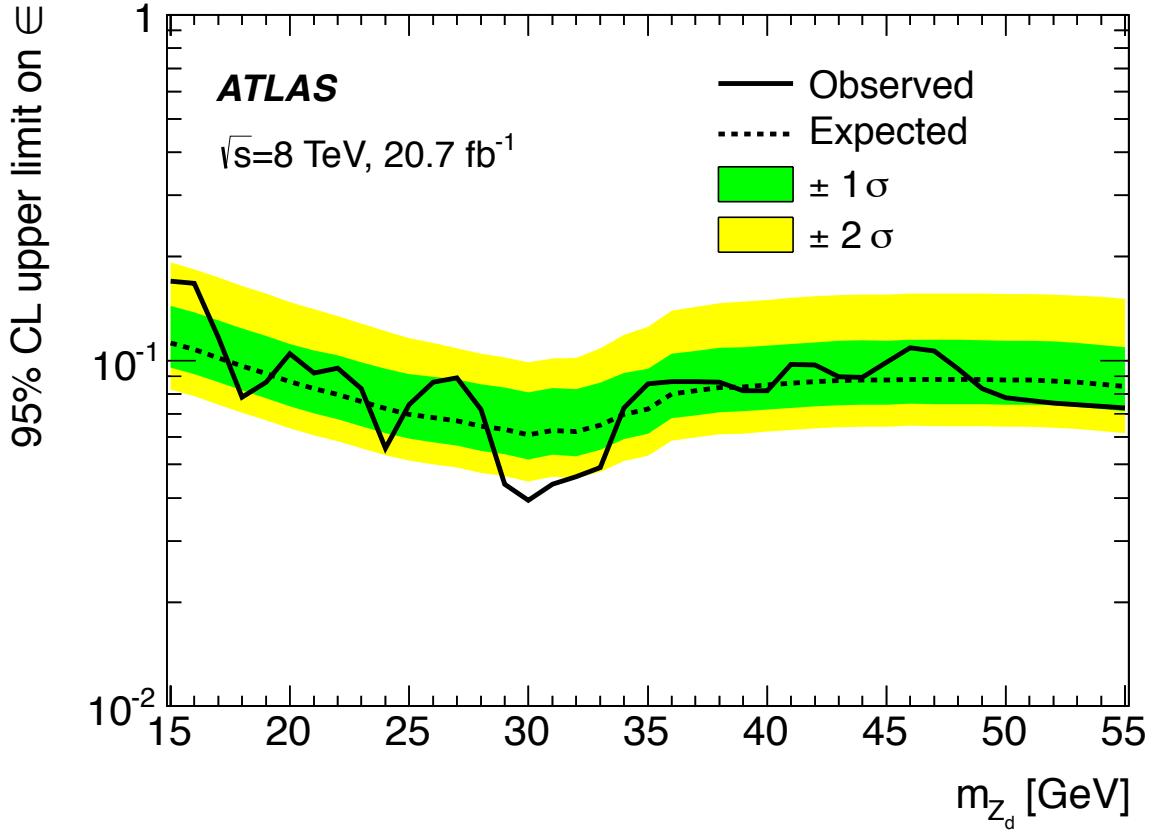


Figure 6: The 95% CL upper limits on the gauge kinetic mixing parameter ϵ as a function of m_{Z_d} using the combined upper limit on the branching ratio of $H \rightarrow ZZ_d \rightarrow 4\ell$ and Table 2 of Ref. [5].

6 $H \rightarrow Z_d Z_d \rightarrow 4\ell$

6.1 Search strategy

$H \rightarrow Z_d Z_d \rightarrow 4\ell$ candidate events are selected as discussed in Sec. 6.2. The Z , J/ψ , Υ vetoes are applied as also discussed in Sec. 6.2. Subsequently, the analysis exploits the small mass difference between the two SFOS lepton pairs of the selected quadruplet to perform a counting experiment. After the small mass difference requirements between the SFOS lepton pairs, the estimated background contributions, coming from $H \rightarrow ZZ^* \rightarrow 4\ell$ and $ZZ^* \rightarrow 4\ell$, are small. These backgrounds are normalized with the theoretical calculations of their cross sections. The other backgrounds are found to be negligible. Since there is no significant excess, upper bounds on the signal strength, defined as the ratio of the $H \rightarrow Z_d Z_d \rightarrow 4\ell$ rate normalized to the SM $H \rightarrow ZZ^* \rightarrow 4\ell$ expectation are set as a function of the hypothesized m_{Z_d} . In a benchmark model where the SM is extended with a dark vector boson and a dark Higgs boson, the measured upper bounds on the signal strength are used to set limits on the branching ratio of $H \rightarrow Z_d Z_d$ and on the Higgs boson mixing parameter as a function of m_{Z_d} [5, 6].

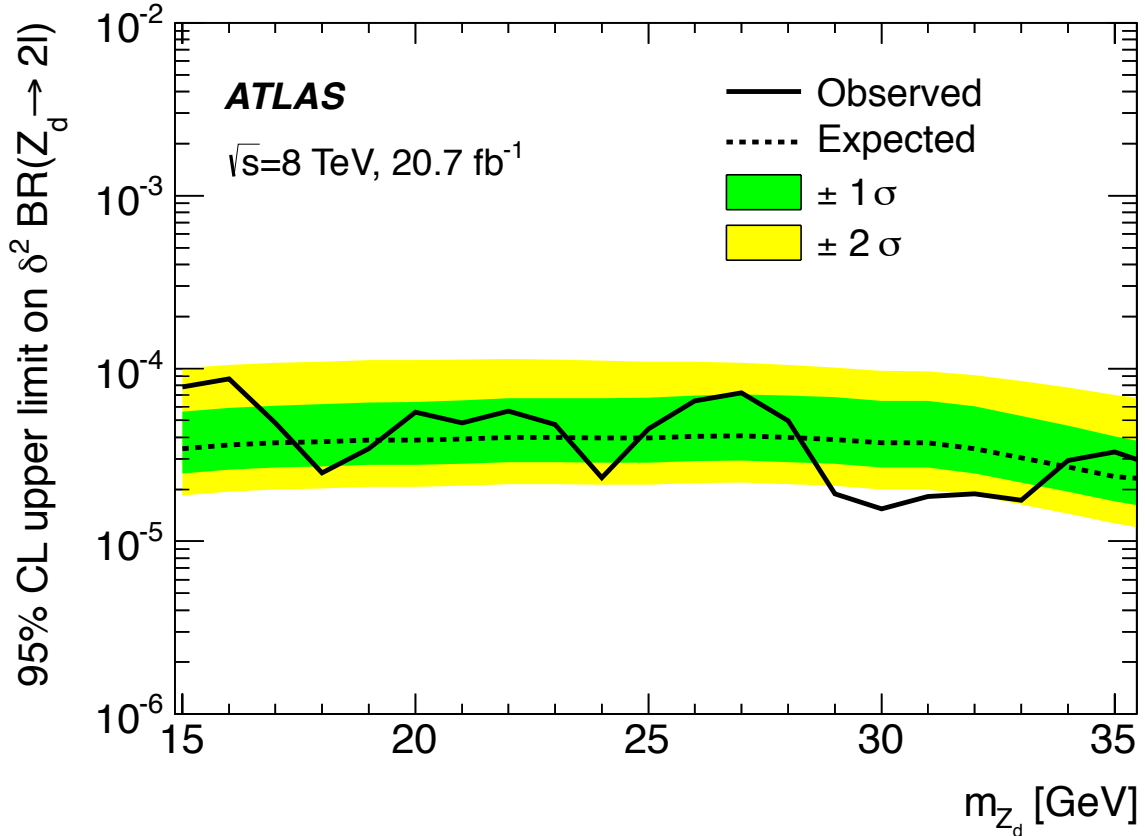


Figure 7: The 95% CL upper limits on the product of the mass-mixing parameter δ and the branching ratio of Z_d decays to two leptons (electrons, or muons), $\delta^2 \times \text{BR}(Z_d \rightarrow 2\ell)$, as a function of m_{Z_d} using the combined upper limit on the relative branching ratio of $H \rightarrow ZZ_d \rightarrow 4\ell$ and the partial width of $H \rightarrow ZZ_d$ computed in Refs. [7, 8].

6.2 Event selection

For the $H \rightarrow Z_d Z_d \rightarrow 4\ell$ search, unlike in the $H \rightarrow ZZ^* \rightarrow 4\ell$ study [93], there is no distinction between a primary pair (on-shell Z) and a secondary pair (off-shell Z), since both Z_d bosons are considered to be on-shell. Among all the different quadruplets, only one is selected by minimizing the mass difference $\Delta m = |m_{12} - m_{34}|$ where m_{12} and m_{34} are the invariant masses of the first and second pairs, respectively. The mass difference Δm is expected to be minimal for the signal since the two dilepton systems should have invariant masses consistent with the same m_{Z_d} . No requirement is made on Δm ; it is used only to select a unique quadruplet with the smallest Δm . Subsequently, isolation and impact parameter significance requirements are imposed on the leptons of the selected quadruplet as described in Ref. [39]. Figure 8 shows the minimal value of Δm for the $2e2\mu$ final state after the impact parameter significance requirements. Similar distributions are found for the $4e$ and 4μ final states. The dilepton and four-lepton invariant mass distributions are shown in Figs. 9 and 10 respectively for m_{12} and m_{34} combined.

For the $H \rightarrow Z_d Z_d \rightarrow 4\ell$ search with hypothesized m_{Z_d} , after the impact parameter significance requirements on the selected leptons, four final requirements are applied:

- (1) $115 < m_{4\ell} < 130$ GeV where $m_{4\ell}$ is the invariant mass of the four leptons in the quadruplet, consistent

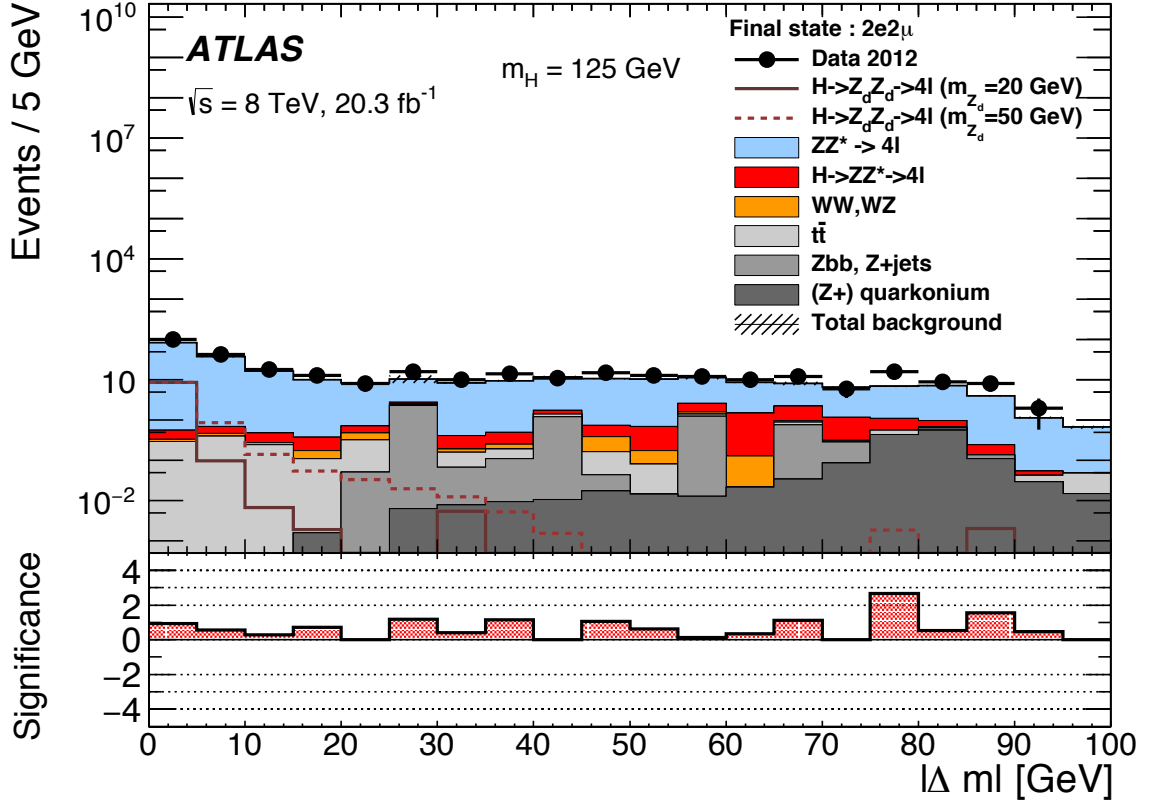


Figure 8: Absolute mass difference between the two dilepton pairs, $\Delta m = |m_{12} - m_{34}|$ in the $2e2\mu$ channel, for $m_H = 125$ GeV. The shaded area shows both the statistical and systematic uncertainties. The bottom plot shows the significance of the observed number of events in the data compared to the expected number of events from the backgrounds. These distributions are obtained after the impact parameter significance requirements.

with the mass of the discovered Higgs boson of about 125 GeV [94].

- (2) Z , J/ψ , and Υ vetoes on all SFOS pairs in the selected quadruplet. The Z veto discards the event if either of the dilepton invariant masses is consistent with the Z -boson pole mass: $|m_{12} - m_Z| < 10$ GeV or $|m_{34} - m_Z| < 10$ GeV. For the J/ψ and Υ veto, the dilepton invariant masses are required to be above 12 GeV. This requirement suppresses backgrounds with Z bosons, J/ψ , and Υ .
- (3) the loose signal region requirement: $m_{12} < m_H/2$ and $m_{34} < m_H/2$, where $m_H = 125$ GeV. In the $H \rightarrow Z_d Z_d \rightarrow 4\ell$ search, the kinematic limit for on-shell Z_d is $m_{Z_d} < m_H/2$.
- (4) the tight signal region requirement: $|m_{Z_d} - m_{12}| < \delta m$ and $|m_{Z_d} - m_{34}| < \delta m$. The optimized values of the δm requirements are 5/3/4.5 GeV for the $4e/4\mu/2e2\mu$ final states respectively (the δm requirement varies with the hypothesized m_{Z_d} but the impact of the variation is negligible). This requirement suppresses the backgrounds further by restricting the search region to within δm of the hypothesized m_{Z_d} .

These requirements (1)–(4) define the signal region (SR) of $H \rightarrow Z_d Z_d \rightarrow 4\ell$ that is dependent on the hypothesized m_{Z_d} , and is essentially background-free, but contains small estimated background contributions from $H \rightarrow ZZ^* \rightarrow 4\ell$ and $ZZ^* \rightarrow 4\ell$ processes as shown in Sec. 6.5.

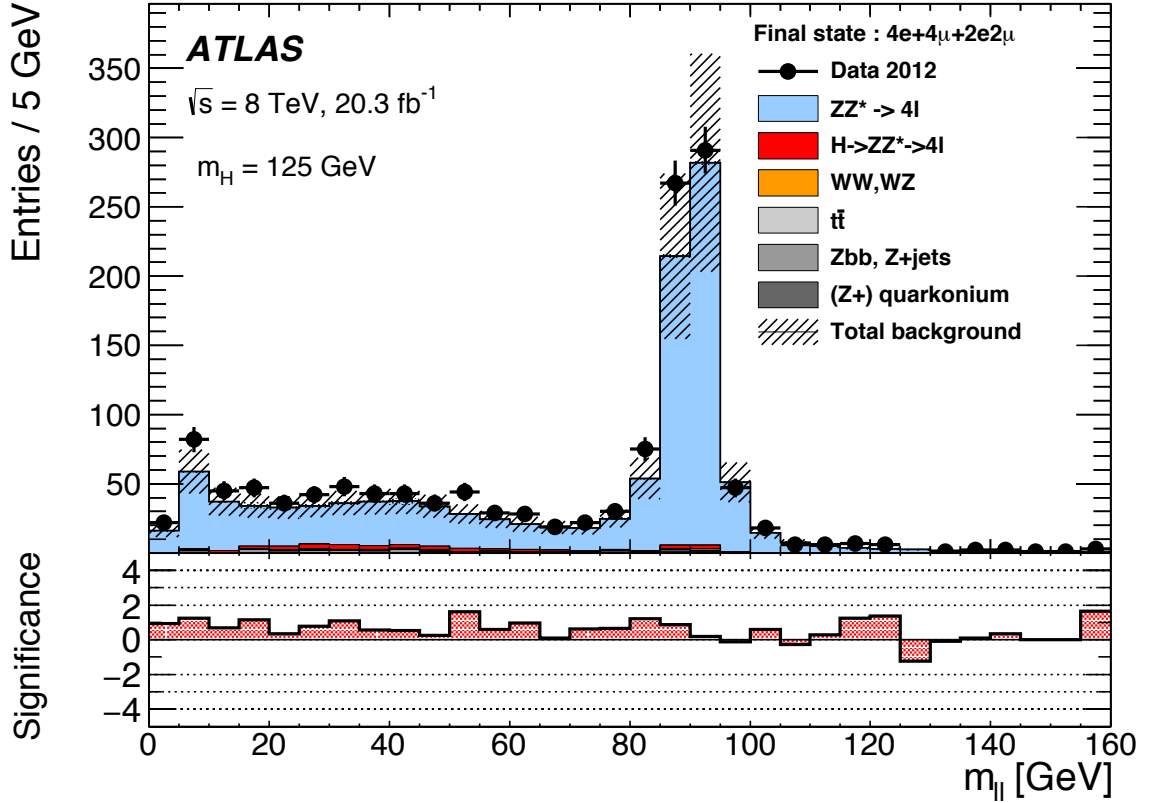


Figure 9: Dilepton invariant mass, $m_{\ell\ell} \equiv m_{12} \text{ or } m_{34}$, in the combined $4e + 2e2\mu + 4\mu$ final state, for $m_H = 125 \text{ GeV}$. The shaded area shows both the statistical and systematic uncertainties. The bottom plots show the significance of the observed number of events in the data compared to the expected number of events from the backgrounds. These distributions are obtained after the impact parameter significance requirement.

6.3 Background estimation

For the $H \rightarrow Z_d Z_d \rightarrow 4\ell$ search, the main background contributions in the signal region come from the $H \rightarrow ZZ^* \rightarrow 4\ell$ and $ZZ^* \rightarrow 4\ell$ processes. These backgrounds are suppressed by the requirements of the tight signal region, as explained in Sec. 6.2. Other backgrounds with smaller contributions come from the Z +jets and $t\bar{t}$, WW and WZ processes as shown in Fig. 11. The $H \rightarrow ZZ^* \rightarrow 4\ell$, $ZZ^* \rightarrow 4\ell$, WW and WZ backgrounds are estimated from simulation and normalized with theoretical calculations of their cross sections. After applying the tight signal region requirements described in Sec. 6.2, the Z +jets, $t\bar{t}$ and diboson backgrounds are negligible. In the case where the Monte Carlo calculation yields zero expected background events in the tight signal region, an upper bound at 68% CL on the expected events is estimated using 1.14 events [86], scaled to the data luminosity and normalized to the background cross section:

$$N_{\text{background}} < L \times \sigma \times \left(\frac{1.14}{N_{\text{tot}}} \right), \quad (8)$$

where L is the total integrated luminosity, σ the cross section of the background process, and N_{tot} the total number of weighted events simulated for the background process.

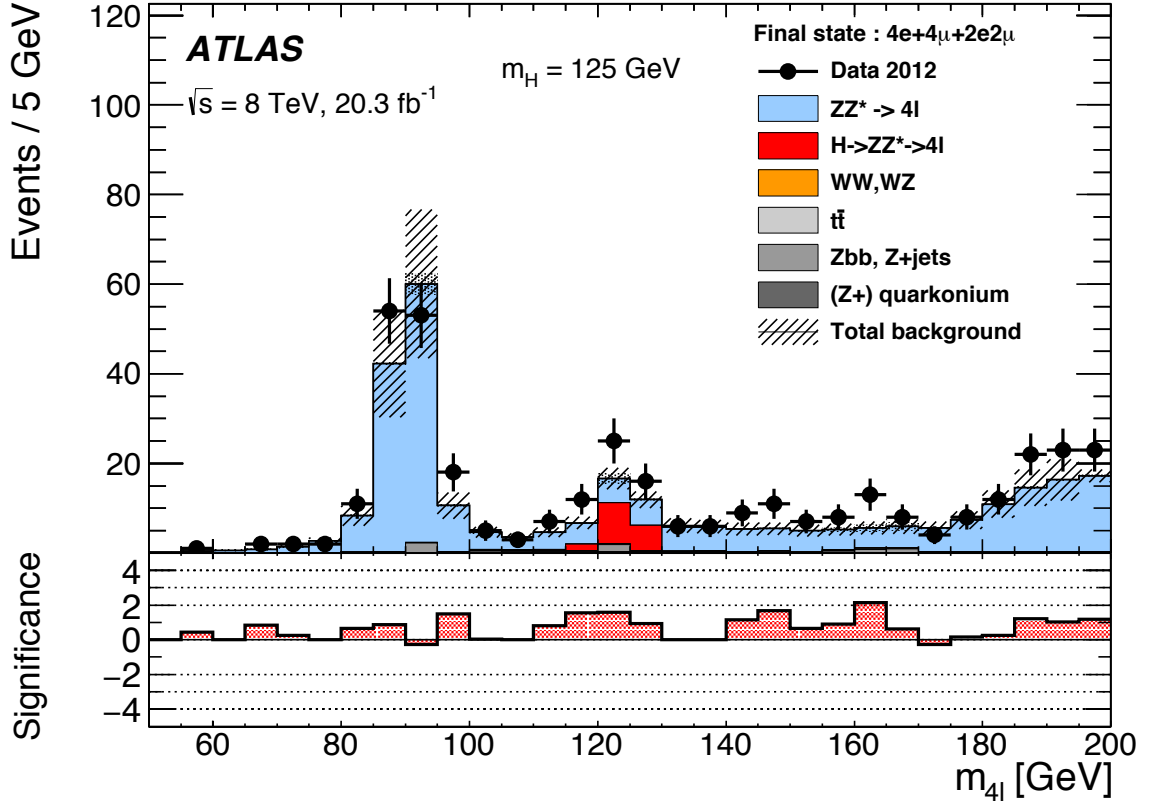


Figure 10: Four-lepton invariant mass, in the combined $4e + 2e2\mu + 4\mu$ final state, for $m_H = 125 \text{ GeV}$. The shaded area shows both the statistical and systematic uncertainties. The bottom plots show the significance of the observed number of events in the data compared to the expected number of events from the backgrounds. These distributions are obtained after the impact parameter significance requirement.

To validate the background estimation, a signal depleted control region is defined by reversing the four-lepton invariant mass requirement with an $m_{4\ell} < 115 \text{ GeV}$ or $m_{4\ell} > 130 \text{ GeV}$ requirement. Good agreement between expectation and observation is found in this validation control region as shown in Fig. 12.

6.4 Systematic uncertainties

The systematic uncertainties on the theoretical calculations of the cross sections used in the event selection and identification efficiencies are taken into account. The effects of PDFs, α_S , and renormalization and factorization scale uncertainties on the total inclusive cross sections for the Higgs production by ggF, VBF, VH and $t\bar{t}H$ are obtained from Refs. [40, 41]. The renormalization, factorization scales and PDFs and α_S uncertainties are applied to the ZZ^* background estimates. The uncertainties due to the limited number of MC events in the $t\bar{t}$, $Z+jets$, ZJ/ψ , $Z\Upsilon$ and WW/WZ background simulations are estimated as described in Sec. 6.3. The luminosity uncertainty [28] is applied to all signal yields, as well as to the background yields that are normalized with their theory cross sections. The detector systematic uncertainties due to uncertainties in the electron and muon identification efficiencies are estimated within the acceptance of the signal region requirements. There are several components to these uncertainties. For the muons,

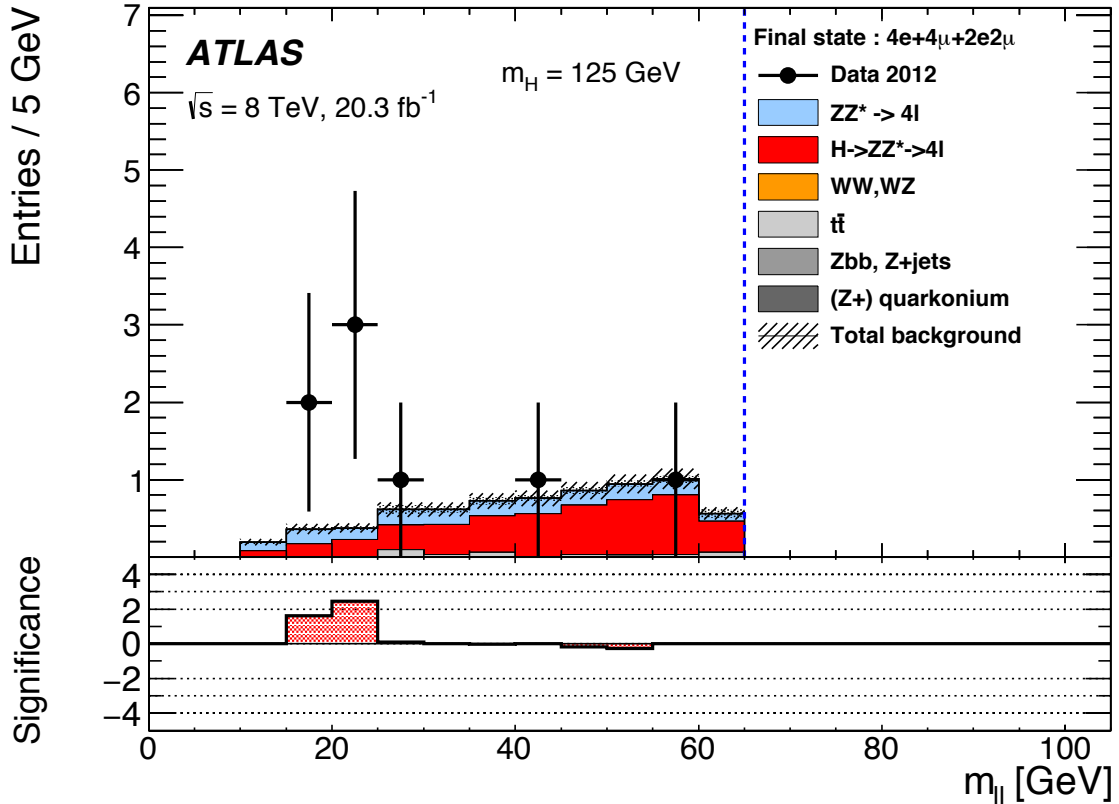


Figure 11: Dilepton invariant mass, $m_{\ell\ell} \equiv m_{12}$ or m_{34} after the loose signal region requirements described in Sec. 6.2 for the $4e$, 4μ and, $2e2\mu$ final states combined, for $m_H = 125$ GeV. The data is represented by the black dots, and the backgrounds are represented by the filled histograms. The shaded area shows both the statistical and systematic uncertainties. The bottom plots show the significance of the observed data events compared to the expected number of events from the backgrounds. The dashed vertical line is the kinematic limit (m_{12} or $m_{34} < 63$ GeV) of the loose signal region requirements as discussed in Sec. 6.2.

uncertainties in the reconstruction and identification efficiency, and in the momentum resolution and scale, are included. For the electrons, uncertainties in the reconstruction and identification efficiency, the isolation and impact parameter significance requirements, the energy scale and energy resolution are considered. The systematic uncertainties are summarized in Table 4.

6.5 Results and interpretation

Figures 11 and 13 show the distributions of the dilepton invariant mass (for m_{12} and m_{34} combined) and the absolute mass difference $\Delta m = |m_{12} - m_{34}|$ after the loose signal region requirements. Four data events pass the loose signal region requirements, one in the $4e$ channel, two in the 4μ channel and one in the $2e2\mu$ channel. Two of these four events pass the tight signal region requirements: the event in the $4e$ channel and one of the events in the 4μ channel. The event in the $4e$ channel has dilepton masses of 21.8 GeV and 28.1 GeV as shown in Fig. 11, and is consistent with a Z_d mass in the range $23.5 \leq m_{Z_d} \leq 26.5$ GeV. For the event in the 4μ channel that passes the tight signal region requirements, the dilepton invariant masses are 23.2 GeV and 18.0 GeV as shown in Fig. 11, and they are consistent with a Z_d mass in the

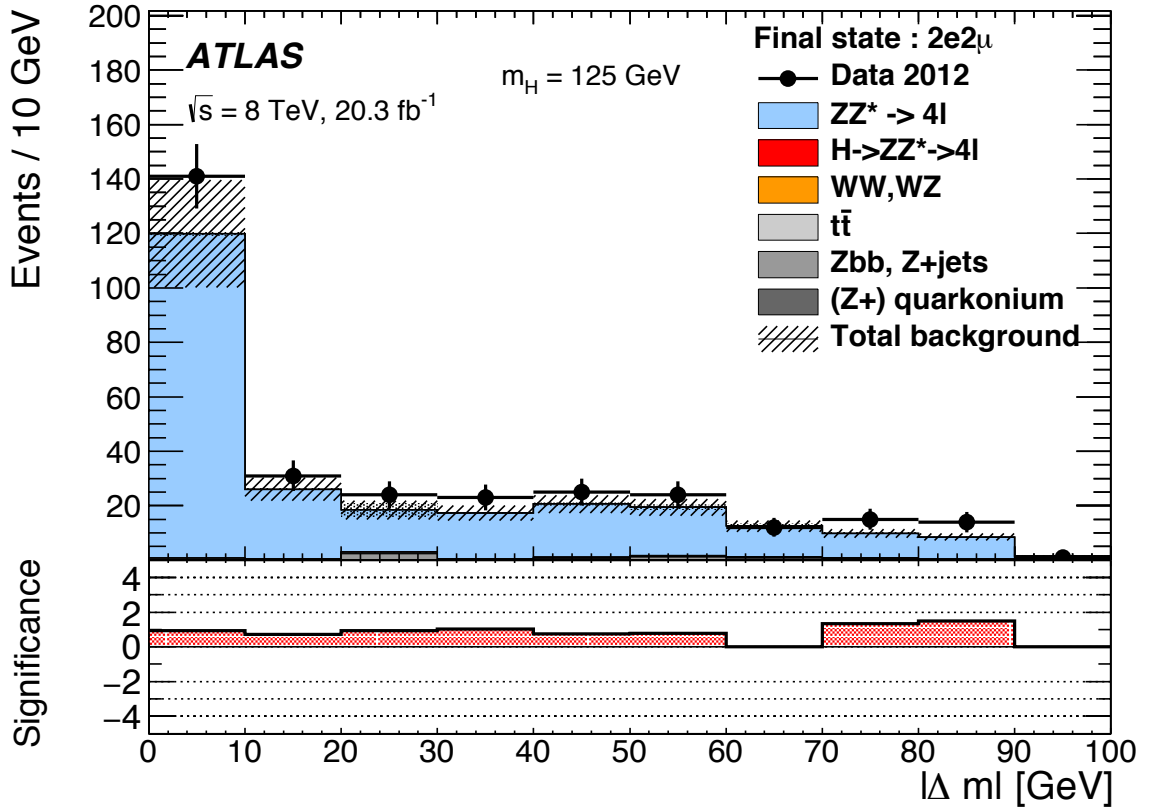


Figure 12: The minimal absolute mass difference for the $2e2\mu$ final state. Events are selected after the impact parameter significance requirement and $m_{4\ell} \notin (115, 130) \text{ GeV}$. The shaded area shows both the statistical and systematic uncertainties. The bottom plots show the significance of the measured number of events in the data compared to the estimated number of events from the backgrounds.

Systematic Uncertainties (%)			
Source	4μ	$4e$	$2e2\mu$
Electron Identification	–	6.7	3.2
Electron Energy Scale	–	0.8	0.3
Muon Identification	2.6	–	1.3
Muon Momentum Scale	0.1	–	0.1
Luminosity	2.8	2.8	2.8
ggF QCD	7.8	7.8	7.8
ggF PDFs and α_S	7.5	7.5	7.5
ZZ^* Normalization	5.0	5.0	5.0

Table 4: The relative systematic uncertainties on the event yields in the $H \rightarrow Z_d Z_d \rightarrow 4\ell$ search.

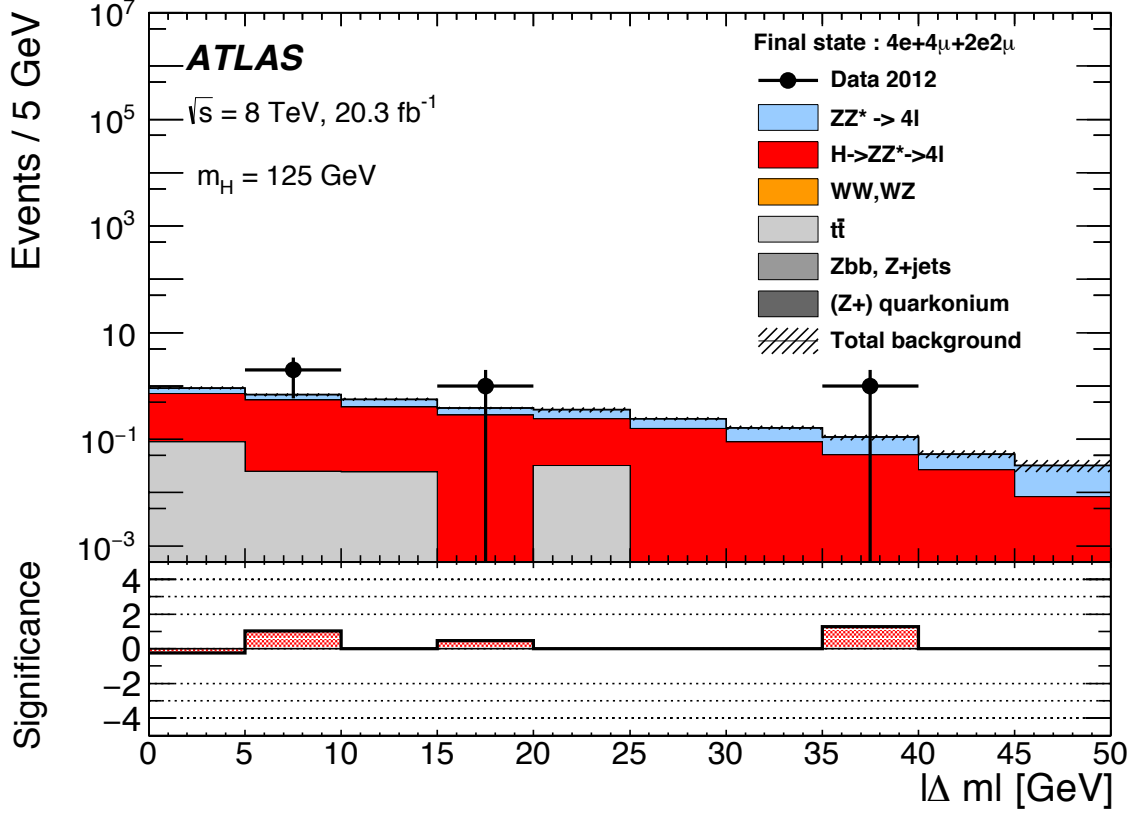


Figure 13: Absolute mass difference, $\Delta m = |m_{12} - m_{34}|$ after the loose signal region requirements described in Sec. 6.2 for the $4e$, 4μ and, $2e2\mu$ final states combined, for $m_H = 125$ GeV. The data is represented by the black dots, and the backgrounds are represented by the filled histograms. The shaded area shows both the statistical and systematic uncertainties. The bottom plots show the significance of the observed data events compared to the expected number of events from the backgrounds.

range $20.5 \leq m_{Z_d} \leq 21.0$ GeV. In the m_{Z_d} range of 15 to 30 GeV where four data events pass the loose signal region requirements, histogram interpolation [87] is used in steps of 0.5 GeV to obtain the signal acceptances and efficiencies at the hypothesized m_{Z_d} . The expected numbers of signal, background and data events, after applying the tight signal region requirements, are shown in Table 5.

For each m_{Z_d} , in the absence of any significant excess of events consistent with the signal hypothesis, the upper limits are computed from a maximum-likelihood fit to the numbers of data and expected signal and background events in the tight signal regions, following the CL_s modified frequentist formalism [88, 89] with the profile-likelihood test statistic [90, 91]. The nuisance parameters associated to the systematic uncertainties described in Sec. 6.4 are profiled. The parameter of interest in the fit is the signal strength μ_d defined as the ratio of the $H \rightarrow Z_d Z_d \rightarrow 4\ell$ rate relative to the SM $H \rightarrow ZZ^* \rightarrow 4\ell$ rate:

$$\mu_d = \frac{\sigma \times \text{BR}(H \rightarrow Z_d Z_d \rightarrow 4\ell)}{[\sigma \times \text{BR}(H \rightarrow ZZ^* \rightarrow 4\ell)]_{\text{SM}}}. \quad (9)$$

The systematic uncertainties in the electron and muon identification efficiencies, renormalization and factorization scales and PDF are 100% correlated between the signal and backgrounds. Pseudoexperiments are used to compute the 95% CL upper bound μ_d in each of the final states and their combination, and

Process	$4e$	4μ	$2e2\mu$
$H \rightarrow ZZ^* \rightarrow 4\ell$	$(1.5 \pm 0.3 \pm 0.2) \times 10^{-2}$	$(1.0 \pm 0.3 \pm 0.3) \times 10^{-2}$	$(2.9 \pm 1.0 \pm 2.0) \times 10^{-3}$
$ZZ^* \rightarrow 4\ell$	$(7.1 \pm 3.6 \pm 0.5) \times 10^{-4}$	$(8.4 \pm 3.8 \pm 0.5) \times 10^{-3}$	$(9.1 \pm 3.6 \pm 0.6) \times 10^{-3}$
WW, WZ	$< 0.7 \times 10^{-2}$	$< 0.7 \times 10^{-2}$	$< 0.7 \times 10^{-2}$
$t\bar{t}$	$< 3.0 \times 10^{-2}$	$< 3.0 \times 10^{-2}$	$< 3.0 \times 10^{-2}$
$Zbb, Z+\text{jets}$	$< 0.2 \times 10^{-2}$	$< 0.2 \times 10^{-2}$	$< 0.2 \times 10^{-2}$
ZJ/ψ and $Z\Upsilon$	$< 2.3 \times 10^{-3}$	$< 2.3 \times 10^{-3}$	$< 2.3 \times 10^{-3}$
Total background	$< 5.6 \times 10^{-2}$	$< 5.9 \times 10^{-2}$	$< 5.3 \times 10^{-2}$
Data	1	0	0
$H \rightarrow ZZ^* \rightarrow 4\ell$	$(1.2 \pm 0.3 \pm 0.2) \times 10^{-2}$	$(5.8 \pm 2.0 \pm 2.0) \times 10^{-3}$	$(2.6 \pm 1.0 \pm 0.2) \times 10^{-3}$
$ZZ^* \rightarrow 4\ell$	$(3.5 \pm 2.0 \pm 0.2) \times 10^{-3}$	$(4.1 \pm 2.7 \pm 0.2) \times 10^{-3}$	$(2.0 \pm 0.6 \pm 0.1) \times 10^{-2}$
WW, WZ	$< 0.7 \times 10^{-2}$	$< 0.7 \times 10^{-2}$	$< 0.7 \times 10^{-2}$
$t\bar{t}$	$< 3.0 \times 10^{-2}$	$< 3.0 \times 10^{-2}$	$< 3.0 \times 10^{-2}$
$Zbb, Z+\text{jets}$	$< 0.2 \times 10^{-2}$	$< 0.2 \times 10^{-2}$	$< 0.2 \times 10^{-2}$
ZJ/ψ and $Z\Upsilon$	$< 2.3 \times 10^{-3}$	$< 2.3 \times 10^{-3}$	$< 2.3 \times 10^{-3}$
Total background	$< 5.3 \times 10^{-2}$	$< 5.1 \times 10^{-2}$	$< 6.4 \times 10^{-2}$
Data	0	1	0

Table 5: The expected and observed numbers of events in the tight signal region of the $H \rightarrow Z_d Z_d \rightarrow 4\ell$ search for each of the three final states, for the hypothesized mass $m_{Z_d} = 25$ GeV and 20.5 GeV. Statistical and systematic uncertainties are given respectively for the signal and the background expectations. One event in data passes all the selections in the $4e$ channel and is consistent with $23.5 \leq m_{Z_d} \leq 26.5$ GeV. One other data event passes all the selections in the 4μ channel and is consistent with $20.5 \leq m_{Z_d} \leq 21.0$ GeV. The $H \rightarrow ZZ^* \rightarrow 4\ell$ numbers are summed over the ggF, VBF, ZH , WH and $t\bar{t}H$ processes.

for each of the hypothesized m_{Z_d} . The 95% confidence-level upper bounds on the $H \rightarrow Z_d Z_d \rightarrow 4\ell$ rates are shown in Fig. 14 relative to the SM Higgs boson process $H \rightarrow ZZ^* \rightarrow 4\ell$ as a function of the hypothesized m_{Z_d} for the combination of the three final states $4e$, $2e2\mu$ and 4μ . Assuming the SM Higgs boson production cross section and using $\text{BR}(H \rightarrow ZZ^* \rightarrow 4\ell)_{\text{SM}} = 1.25 \times 10^{-4}$ [40, 41], upper bounds on the branching ratio of $H \rightarrow Z_d Z_d \rightarrow 4\ell$ can be obtained from Eq. (9), as shown in Fig. 15.

The simplest benchmark model is the SM plus a dark vector boson and a dark Higgs boson as discussed in Refs. [6, 10], where the branching ratio of $Z_d \rightarrow \ell\ell$ is given as a function of m_{Z_d} . This can be used to convert the measurement of the upper bound on the signal strength μ_d into an upper bound on the branching ratio $\text{BR}(H \rightarrow Z_d Z_d)$ assuming the SM Higgs boson production cross section. Figure 16 shows the 95% CL upper limit on the branching ratio of $H \rightarrow Z_d Z_d$ as a function of m_{Z_d} using the combined μ_d of the three final states. The weaker bound at higher m_{Z_d} is due to the fact that the branching ratio $Z_d \rightarrow \ell\ell$ drops slightly at higher m_{Z_d} [6] as other decay channels become accessible. The $H \rightarrow Z_d Z_d$ decay can be used to obtain a m_{Z_d} -dependent limit on an Higgs mixing parameter κ' [6]:

$$\kappa' = \kappa \times \frac{m_H^2}{|m_H^2 - m_S^2|}, \quad (10)$$

where κ is the size of the Higgs portal coupling and m_S is the mass of the dark Higgs boson. The partial width of $H \rightarrow Z_d Z_d$ is given in terms of κ [5]. In the regime where the Higgs mixing parameter dominates

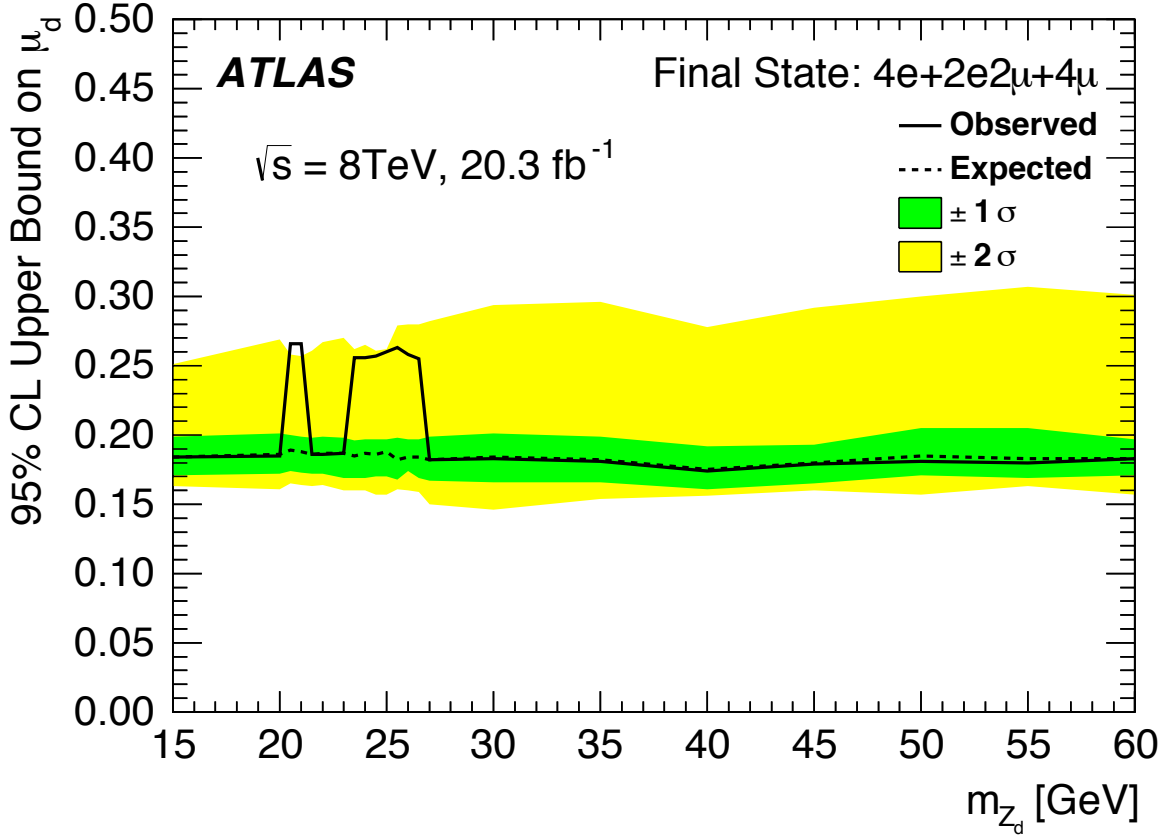


Figure 14: The 95% confidence level upper bound on the signal strength $\mu_d = \frac{\sigma \times \text{BR}(H \rightarrow Z_d Z_d \rightarrow 4\ell)}{[\sigma \times \text{BR}(H \rightarrow ZZ^* \rightarrow 4\ell)]_{\text{SM}}}$ of $H \rightarrow Z_d Z_d \rightarrow 4\ell$ in the combined $4e + 2e2\mu + 4\mu$ final state, for $m_H = 125$ GeV. The $\pm 1\sigma$ and $\pm 2\sigma$ expected exclusion regions are indicated in green and yellow, respectively.

($\kappa \gg \epsilon$), $m_S > m_H/2$, $m_{Z_d} < m_H/2$ and $H \rightarrow Z_d Z^* \rightarrow 4\ell$ is negligible, the only relevant decay is $H \rightarrow Z_d Z_d$. Therefore the partial width $\Gamma(H \rightarrow Z_d Z_d)$ can be written as:

$$\Gamma(H \rightarrow Z_d Z_d) = \Gamma_{\text{SM}} \frac{\text{BR}(H \rightarrow Z_d Z_d)}{1 - \text{BR}(H \rightarrow Z_d Z_d)}. \quad (11)$$

The Higgs portal coupling parameter κ is obtained using Eq. (53) of Ref. [6] or Table 2 of Ref. [5]:

$$\kappa^2 = \frac{\Gamma_{\text{SM}}}{f(m_{Z_d})} \frac{\text{BR}(H \rightarrow Z_d Z_d)}{1 - \text{BR}(H \rightarrow Z_d Z_d)}, \quad (12)$$

where

$$f(m_{Z_d}) = \frac{v^2}{32\pi m_H} \times \sqrt{1 - \frac{4m_{Z_d}^2}{m_H^2}} \times \frac{(m_H^2 + 2m_{Z_d}^2)^2 - 8(m_H^2 - m_{Z_d}^2)m_{Z_d}^2}{(m_H^2 - m_S^2)^2}. \quad (13)$$

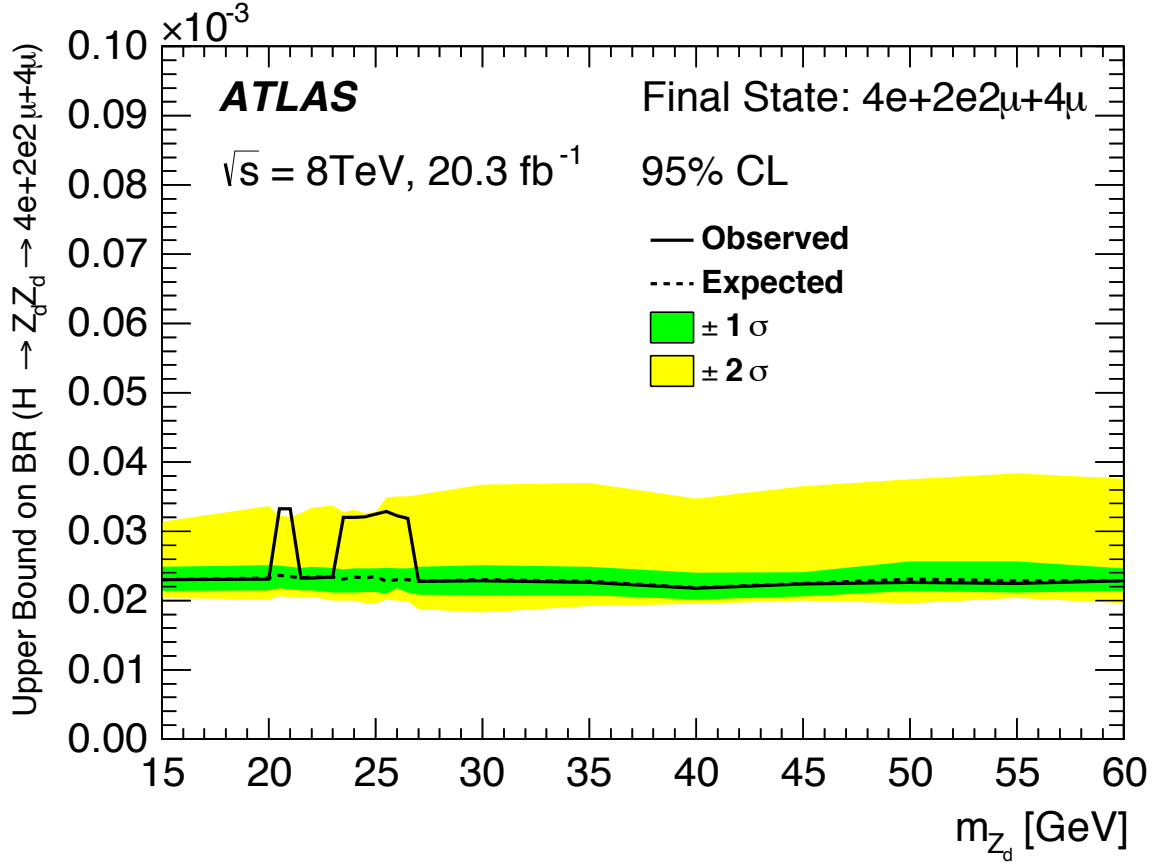


Figure 15: The 95% confidence level upper bound on the branching ratio of $H \rightarrow Z_d Z_d \rightarrow 4\ell$ as a function of m_{Z_d} , in the combined $4e + 2e2\mu + 4\mu$ final state, for $m_H = 125$ GeV. The $\pm 1\sigma$ and $\pm 2\sigma$ expected exclusion regions are indicated in green and yellow, respectively.

Figure 17 shows the upper bound on the effective Higgs mixing parameter as a function of m_{Z_d} : for $m_H/2 < m_S < 2m_H$, this would correspond to an upper bound on the Higgs portal coupling in the range $\kappa \sim (1-10) \times 10^{-4}$.

An interpretation for $H \rightarrow Z_d Z_d$ is not done in the Z - Z_d mass mixing scenario described in Refs. [7, 8] since in this model the rate of $H \rightarrow Z_d Z_d$ is highly suppressed relative to that of $H \rightarrow ZZ_d$.

7 Conclusions

Two searches for an exotic gauge boson Z_d that couples to the discovered SM Higgs boson at a mass around 125 GeV in four-lepton events are presented, using the ATLAS detector at the LHC.

The $H \rightarrow ZZ_d \rightarrow 4\ell$ analysis uses the events resulting from Higgs boson decays to four leptons to search for an exotic gauge boson Z_d , by examining the m_{34} mass distribution. The results obtained in this search cover the exotic gauge boson mass range of $15 < m_{Z_d} < 55$ GeV, and are based on proton-proton collisions data at $\sqrt{s} = 8$ TeV with an integrated luminosity of 20.7 fb^{-1} . Observed and expected exclusion limits on the branching ratio of $H \rightarrow ZZ_d \rightarrow 4\ell$ relative to $H \rightarrow 4\ell$ are estimated for the combination of all

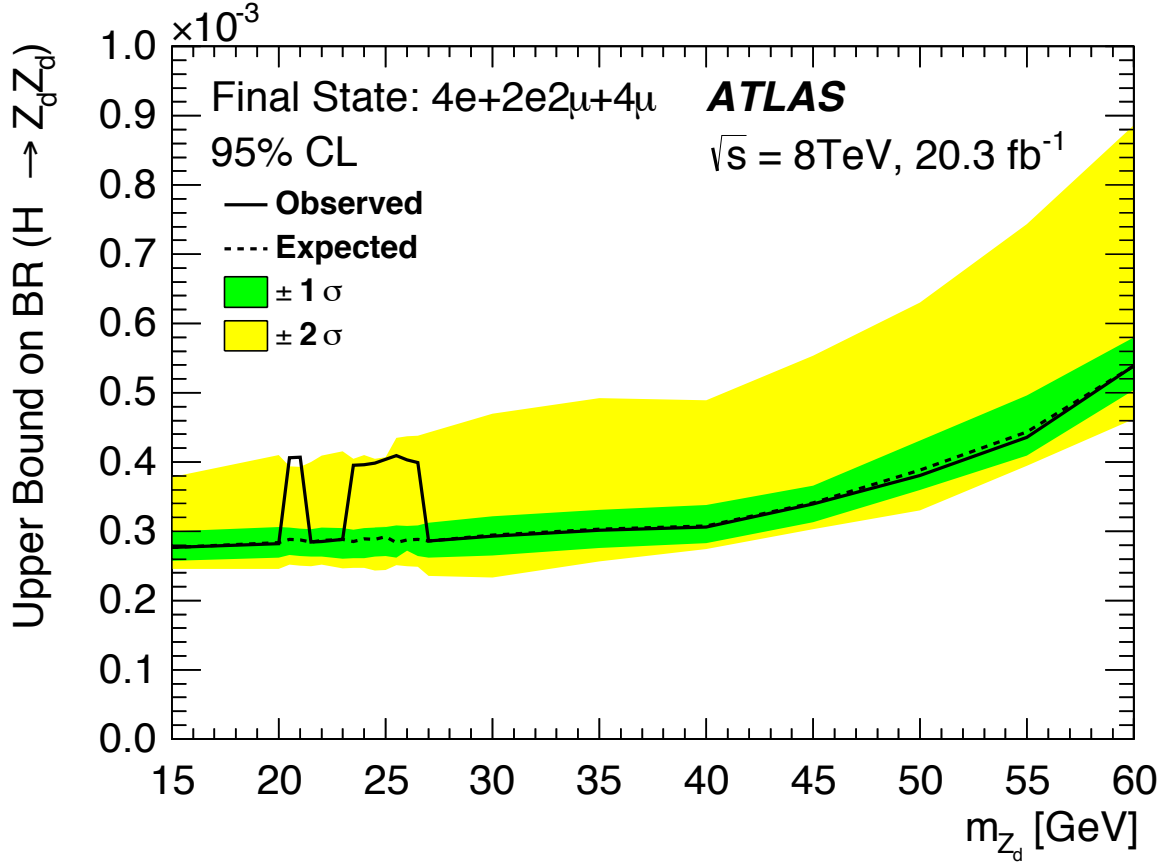


Figure 16: The 95% confidence level upper bound on the branching ratio of $H \rightarrow Z_d Z_d$ in the combined $4e + 2e2\mu + 4\mu$ final state, for $m_H = 125$ GeV. The $\pm 1\sigma$ and $\pm 2\sigma$ expected exclusion regions are indicated in green and yellow, respectively.

the final states. For relative branching ratios above 0.4 (observed) and 0.2 (expected), the entire mass range of $15 < m_{Z_d} < 55$ GeV is excluded at 95% CL. Upper bounds at 95% CL on the branching ratio of $H \rightarrow ZZ_d \rightarrow 4\ell$ are set in the range $(1-9) \times 10^{-5}$ for $15 < m_{Z_d} < 55$ GeV, assuming the SM branching ratio of $H \rightarrow ZZ^* \rightarrow 4\ell$.

The $H \rightarrow Z_d Z_d \rightarrow 4\ell$ search covers the exotic gauge boson mass range from 15 GeV up to the kinematic limit of $m_H/2$. An integrated luminosity of 20.3 fb^{-1} at 8 TeV is used in this search. One data event is observed to pass all the signal region selections in the $4e$ channel, and has dilepton invariant masses of 21.8 GeV and 28.1 GeV. This $4e$ event is consistent with a Z_d mass in the range $23.5 < m_{Z_d} < 26.5$ GeV. Another data event is observed to pass all the signal region selections in the 4μ channel, and has dilepton invariant masses of 23.2 GeV and 18.0 GeV. This 4μ event is consistent with a Z_d mass in the range $20.5 < m_{Z_d} < 21.0$ GeV. In the absence of a significant excess, upper bounds on the signal strength (and thus on the cross section times branching ratio) are set for the mass range of $15 < m_{Z_d} < 60$ GeV using the combined $4e, 2e2\mu, 4\mu$ final states.

Using a simplified model where the SM is extended with the addition of an exotic gauge boson and a dark Higgs boson, upper bounds on the gauge kinetic mixing parameter ϵ (when $\epsilon \gg \kappa$), are set in the range $(4-17) \times 10^{-2}$ at 95% CL, assuming the SM branching ratio of $H \rightarrow ZZ^* \rightarrow 4\ell$, for $15 < m_{Z_d} < 55$ GeV.

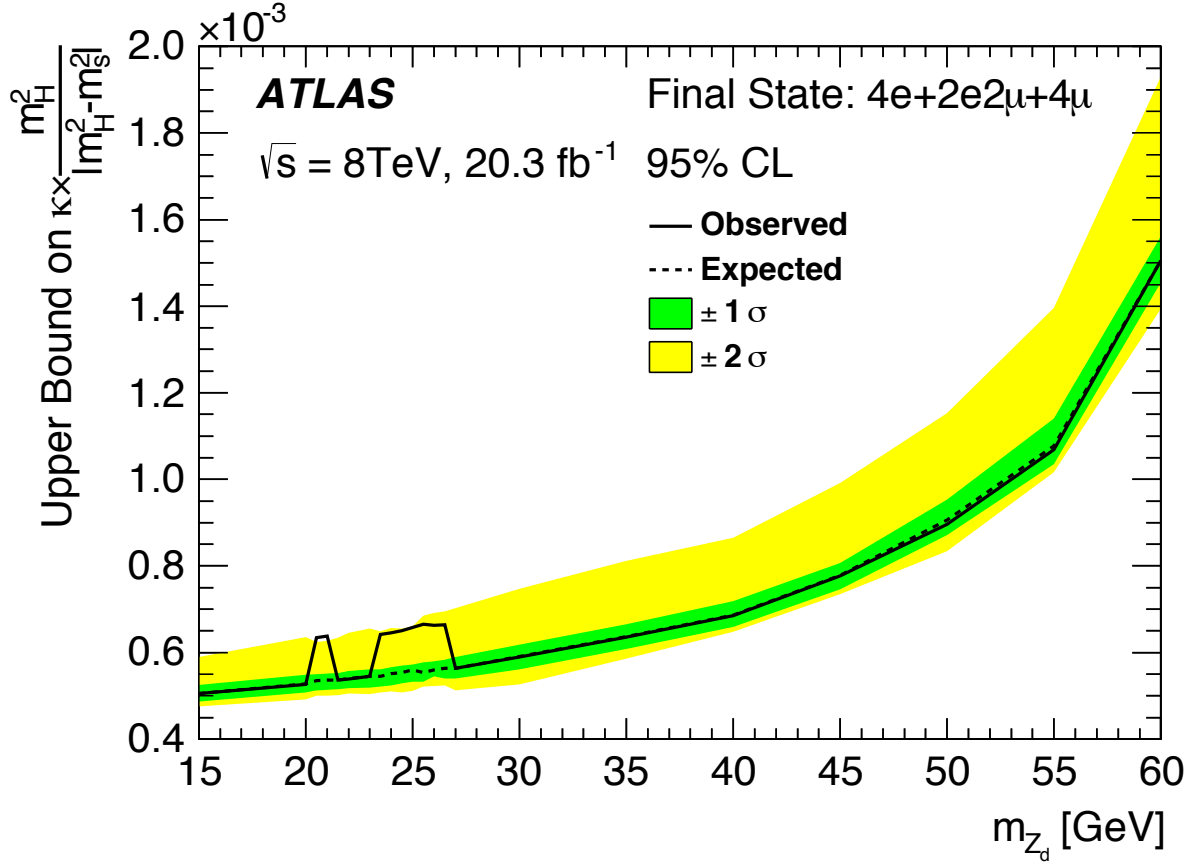


Figure 17: The 95% confidence level upper bound on the Higgs mixing parameter $\kappa \times m_H^2 / |m_H^2 - m_S^2|$ as a function of m_{Z_d} , in the combined $4e + 2e2\mu + 4\mu$ final state, for $m_H = 125$ GeV. The $\pm 1\sigma$ and $\pm 2\sigma$ expected exclusion regions are indicated in green and yellow, respectively.

Assuming the SM Higgs production cross section, upper bounds on the branching ratio of $H \rightarrow Z_d Z_d$, as well as on the Higgs portal coupling parameter κ are set in the range $(2-3) \times 10^{-5}$ and $(1-10) \times 10^{-4}$ respectively at 95% CL, for $15 < m_{Z_d} < 60$ GeV.

Upper bounds on the effective mass-mixing parameter $\delta^2 \times \text{BR}(Z_d \rightarrow \ell\ell)$, resulting from the $U(1)_d$ gauge symmetry, are also set using the branching ratio measurements in the $H \rightarrow ZZ_d \rightarrow 4\ell$ search, and are in the range $(1.5 - 8.7) \times 10^{-5}$ for $15 < m_{Z_d} < 35$ GeV.

Acknowledgments

We thank CERN for the very successful operation of the LHC, as well as the support staff from our institutions without whom ATLAS could not be operated efficiently.

We acknowledge the support of ANPCyT, Argentina; YerPhI, Armenia; ARC, Australia; BMWFW and FWF, Austria; ANAS, Azerbaijan; SSTC, Belarus; CNPq and FAPESP, Brazil; NSERC, NRC and CFI, Canada; CERN; CONICYT, Chile; CAS, MOST and NSFC, China; COLCIENCIAS, Colombia; MSMT CR, MPO CR and VSC CR, Czech Republic; DNRF, DNSRC and Lundbeck Foundation, Denmark;

EPLANET, ERC and NSRF, European Union; IN2P3-CNRS, CEA-DSM/IRFU, France; GNSF, Georgia; BMBF, DFG, HGF, MPG and AvH Foundation, Germany; GSRT and NSRF, Greece; ISF, MINERVA, GIF, I-CORE and Benozio Center, Israel; INFN, Italy; MEXT and JSPS, Japan; CNRST, Morocco; FOM and NWO, Netherlands; BRF and RCN, Norway; MNiSW and NCN, Poland; GRICES and FCT, Portugal; MNE/IFA, Romania; MES of Russia and ROSATOM, Russian Federation; JINR; MSTD, Serbia; MSSR, Slovakia; ARRS and MIZŠ, Slovenia; DST/NRF, South Africa; MINECO, Spain; SRC and Wallenberg Foundation, Sweden; SER, SNSF and Cantons of Bern and Geneva, Switzerland; NSC, Taiwan; TAEK, Turkey; STFC, the Royal Society and Leverhulme Trust, United Kingdom; DOE and NSF, United States of America.

The crucial computing support from all WLCG partners is acknowledged gratefully, in particular from CERN and the ATLAS Tier-1 facilities at TRIUMF (Canada), NDGF (Denmark, Norway, Sweden), CC-IN2P3 (France), KIT/GridKA (Germany), INFN-CNAF (Italy), NL-T1 (Netherlands), PIC (Spain), ASGC (Taiwan), RAL (UK) and BNL (USA) and in the Tier-2 facilities worldwide.

References

- [1] P. Fayet, *Light spin 1/2 or spin 0 dark matter particles*, *Phys.Rev. D* **70** (2004) 023514, arXiv:[hep-ph/0403226](#) [[hep-ph](#)].
- [2] D. P. Finkbeiner and N. Weiner, *Exciting Dark Matter and the INTEGRAL/SPI 511 keV signal*, *Phys.Rev. D* **76** (2007) 083519, arXiv:[astro-ph/0702587](#) [[astro-ph](#)].
- [3] N. Arkani-Hamed et al., *A Theory of Dark Matter*, *Phys.Rev. D* **79** (2009) 015014, arXiv:[0810.0713](#) [[hep-ph](#)].
- [4] E. Dudas et al., *Extra U(1) as natural source of a monochromatic gamma ray line*, *J. High Energy Phys.* **1210** (2012) 123, arXiv:[1205.1520](#) [[hep-ph](#)].
- [5] D. Curtin et al., *Illuminating Dark Photons with High-Energy Colliders*, *J. High Energy Phys.* **1502** (2015) 157, arXiv:[1412.0018](#) [[hep-ph](#)].
- [6] D. Curtin et al., *Exotic Decays of the 125 GeV Higgs Boson*, *Phys.Rev. D* **90** (2014) 075004, arXiv:[1312.4992](#) [[hep-ph](#)].
- [7] H. Davoudiasl et al., *Higgs Decays as a Window into the Dark Sector*, *Phys.Rev. D* **88.1** (2013) 015022, arXiv:[1304.4935](#) [[hep-ph](#)].
- [8] H. Davoudiasl, H.-S. Lee and W. J. Marciano, *'Dark' Z implications for Parity Violation, Rare Meson Decays, and Higgs Physics*, *Phys.Rev. D* **85** (2012) 115019, arXiv:[1203.2947](#) [[hep-ph](#)].
- [9] J. D. Wells, *How to Find a Hidden World at the Large Hadron Collider* (2008), arXiv:[0803.1243](#) [[hep-ph](#)].
- [10] S. Gopalakrishna, S. Jung and J. D. Wells, *Higgs boson decays to four fermions through an abelian hidden sector*, *Phys.Rev. D* **78** (2008) 055002, arXiv:[0801.3456](#) [[hep-ph](#)].
- [11] D. Clowe et al., *A direct empirical proof of the existence of dark matter*, *Astrophys.J.* **648** (2006) L109–L113, arXiv:[astro-ph/0608407](#) [[astro-ph](#)].
- [12] O. Adriani, et al. (PAMELA Collaboration), *An anomalous positron abundance in cosmic rays with energies 1.5–100 GeV*, *Nature* **458** (2009) 607–609, arXiv:[0810.4995](#) [[astro-ph](#)].
- [13] J. Chang et al. (ATIC Collaboration), *An excess of cosmic ray electrons at energies of 300–800 GeV*, *Nature News* **456** (2008) 362.
- [14] M. Aguilar et al. (AMS Collaboration), *First Result from the Alpha Magnetic Spectrometer on the International Space Station: Precision Measurement of the Positron Fraction in Primary Cosmic Rays of 0.5–350 GeV*, *Phys. Rev. Lett.* **110** (14 2013) 141102.
- [15] P. Galison and A. Manohar, *TWO Z's OR NOT TWO Z's?*, *Phys.Lett.* **B136** (1984) 279.
- [16] B. Holdom, *Two U(1)'s and Epsilon Charge Shifts*, *Phys.Lett.* **B166** (1986) 196.
- [17] K. R. Dienes, C. F. Kolda and J. March-Russell, *Kinetic mixing and the supersymmetric gauge hierarchy*, *Nucl.Phys.* **B492** (1997) 104–118, arXiv:[hep-ph/9610479](#) [[hep-ph](#)].

- [18] A. Hook, E. Izaguirre and J. G. Wacker, *Model Independent Bounds on Kinetic Mixing*, *Adv.High Energy Phys.* **2011** (2011) 859762, arXiv:1006.0973 [hep-ph].
- [19] M. Pospelov, *Secluded U(1) below the weak scale*, *Phys.Rev. D* **80** (2009) 095002, arXiv:0811.1030 [hep-ph].
- [20] I. Hoenig, G. Samach and D. Tucker-Smith, *Searching for dilepton resonances below the Z mass at the LHC*, *Phys.Rev. D* **90.7** (2014) 075016, arXiv:1408.1075 [hep-ph].
- [21] F. Englert and R. Brout, *Broken Symmetry and the Mass of Gauge Vector Mesons*, *Phys. Rev. Lett.* **13** (9 1964) 321–323, URL: <http://link.aps.org/doi/10.1103/PhysRevLett.13.321>.
- [22] P. W. Higgs, *Broken Symmetries and the Masses of Gauge Bosons*, *Phys. Rev. Lett.* **13** (16 1964) 508–509, URL: <http://link.aps.org/doi/10.1103/PhysRevLett.13.508>.
- [23] G. S. Guralnik, C. R. Hagen and T. W. B. Kibble, *Global Conservation Laws and Massless Particles*, *Phys. Rev. Lett.* **13** (20 1964) 585–587, URL: <http://link.aps.org/doi/10.1103/PhysRevLett.13.585>.
- [24] ATLAS Collaboration, *Observation of a new particle in the search for the Standard Model Higgs boson with the ATLAS detector at the LHC*, *Phys.Lett.* **B716** (2012) 1–29, arXiv:1207.7214 [hep-ex].
- [25] CMS Collaboration, *Observation of a new boson at a mass of 125 GeV with the CMS experiment at the LHC*, *Phys.Lett.* **B716** (2012) 30–61, arXiv:1207.7235 [hep-ex].
- [26] ATLAS Collaboration, *Measurements of the properties of the Higgs-like boson in the four lepton decay channel with the ATLAS detector using 25 fb⁻¹ of proton-proton collision data*, ATLAS-CONF-2013-013 (2013), URL: <https://cds.cern.ch/record/1523699>.
- [27] ATLAS Collaboration, *Measurements of Higgs boson production and couplings in diboson final states with the ATLAS detector at the LHC*, *Phys. Lett.* **B726** (2013) 88–119, arXiv:1307.1427 [hep-ex].
- [28] ATLAS Collaboration, *Improved luminosity determination in pp collisions at $\sqrt{s} = 7$ TeV using the ATLAS detector at the LHC*, *Eur.Phys.J.* **C73.8** (2013) 2518, arXiv:1302.4393 [hep-ex].
- [29] ATLAS Collaboration, *Search for long-lived neutral particles decaying into lepton jets in proton-proton collisions at $\sqrt{s} = 8$ TeV with the ATLAS detector*, *J. High Energy Phys.* **1411** (2014) 088, arXiv:1409.0746 [hep-ex].
- [30] ATLAS Collaboration, *Expected Performance of the ATLAS Experiment - Detector, Trigger and Physics* (2009), arXiv:0901.0512 [hep-ex].
- [31] ATLAS Collaboration, *Performance of the ATLAS Trigger System in 2010*, *Eur.Phys.J.* **C72** (2012) 1849, arXiv:1110.1530 [hep-ex].
- [32] J. Alwall et al., *MadGraph 5 : Going Beyond*, *J. High Energy Phys.* **1106** (2011) 128, arXiv:1106.0522 [hep-ph].
- [33] H.-L. Lai et al., *New parton distributions for collider physics*, *Phys.Rev. D* **82** (2010) 074024, arXiv:1007.2241 [hep-ph].

- [34] T. Sjostrand, S. Mrenna and P. Z. Skands, *PYTHIA 6.4 Physics and Manual*, *J. High Energy Phys.* **0605** (2006) 026, arXiv:[hep-ph/0603175](#) [[hep-ph](#)].
- [35] T. Sjostrand, S. Mrenna and P. Z. Skands, *A brief introduction to PYTHIA 8.1*, *Comput.Phys.Commun.* **178** (2008) 852–827, arXiv:[0710.3820](#) [[hep-ph](#)].
- [36] P. Golonka and Z. Was, *Next to Leading Logarithms and the PHOTOS Monte Carlo*, *Eur.Phys.J.* **C50** (2007) 53–62, arXiv:[hep-ph/0604232](#) [[hep-ph](#)].
- [37] Z. Was, P. Golonka and G. Nanava, *PHOTOS Monte Carlo for precision simulation of QED in decays: History and properties of the project*, *PoS ACAT* (2007) 071, arXiv:[0707.3044](#) [[hep-ph](#)].
- [38] N. Davidson, T. Przedzinski and Z. Was, *PHOTOS Interface in C++: Technical and Physics Documentation* (2010), arXiv:[1011.0937](#) [[hep-ph](#)].
- [39] ATLAS Collaboration, *Measurements of Higgs boson production and couplings in the four-lepton channel in pp collisions at center-of-mass energies of 7 and 8 TeV with the ATLAS detector*, *Phys. Rev. D* **91** (2015) 012006, arXiv:[1408.5191](#) [[hep-ex](#)].
- [40] LHC Higgs cross section working group et al., *Handbook of LHC Higgs cross sections: 1. Inclusive observables*, *CERN-2011-002* (2011), arXiv:[1101.0593](#) [[hep-ph](#)].
- [41] LHC Higgs cross section working group et al., *Handbook of LHC Higgs Cross Sections: 2. Differential distributions*, *CERN-2012-002* (2012), arXiv:[1201.3084](#) [[hep-ph](#)].
- [42] A. Djouadi, M. Spira and P. M. Zerwas, *Production of Higgs bosons in proton colliders: QCD corrections*, *Phys. Lett.* **B 264** (1991) 440.
- [43] S. Dawson, *Radiative corrections to Higgs boson production*, *Nucl. Phys.* **B 359** (1991) 283.
- [44] M. Spira et al., *Higgs boson production at the LHC*, *Nucl. Phys.* **B 453** (1995) 17, arXiv:[hep-ph/9504378](#).
- [45] R. V. Harlander and W. B. Kilgore, *Next-to-next-to-leading order Higgs production at hadron colliders*, *Phys. Rev. Lett.* **88** (2002) 201801, arXiv:[hep-ph/0201206](#).
- [46] C. Anastasiou and K. Melnikov, *Higgs boson production at hadron colliders in NNLO QCD*, *Nucl. Phys.* **B 646** (2002) 220, arXiv:[hep-ph/0207004](#).
- [47] V. Ravindran, J. Smith and W. L. van Neerven, *NNLO corrections to the total cross section for Higgs boson production in hadron hadron collisions*, *Nucl. Phys.* **B 665** (2003) 325, arXiv:[hep-ph/0302135](#).
- [48] S. Catani et al., *Soft-gluon resummation for Higgs boson production at hadron colliders*, *J. High Energy Phys.* **07** (2003) 028, arXiv:[hep-ph/0306211](#).
- [49] U. Aglietti et al., *Two-loop light fermion contribution to Higgs production and decays*, *Phys. Lett.* **B 595** (2004) 432, arXiv:[hep-ph/0404071](#).
- [50] S. Actis et al., *NLO electroweak corrections to Higgs Boson production at hadron colliders*, *Phys. Lett.* **B 670** (2008) 12, arXiv:[0809.1301](#) [[hep-ph](#)].

- [51] D. de Florian and M. Grazzini, *Higgs production at the LHC: updated cross sections at $\sqrt{s} = 8$ TeV*, *Phys.Lett.* **B718** (2012) 117, arXiv:1206.4133 [hep-ph].
- [52] C. Anastasiou et al., *Inclusive Higgs boson cross-section for the LHC at 8 TeV*, *J. High Energy Phys.* **1204** (2012) 004, arXiv:1202.3638 [hep-ph].
- [53] J. Baglio and A. Djouadi, *Higgs production at the LHC*, *J. High Energy Phys.* **1103** (2011) 055, arXiv:1012.0530 [hep-ph].
- [54] M. Ciccolini, A. Denner and S. Dittmaier, *Strong and electroweak corrections to the production of Higgs+2jets via weak interactions at the LHC*, *Phys. Rev. Lett.* **99** (2007) 161803, arXiv:0707.0381 [hep-ph].
- [55] M. Ciccolini, A. Denner and S. Dittmaier, *Electroweak and QCD corrections to Higgs production via vector-boson fusion at the LHC*, *Phys. Rev.* **D 77** (2008) 013002, arXiv:0710.4749 [hep-ph].
- [56] K. Arnold et al., *VBFNLO: A Parton level Monte Carlo for processes with electroweak bosons*, *Comput.Phys.Commun.* **180** (2009) 1661–1670, arXiv:0811.4559 [hep-ph].
- [57] P. Bolzoni et al., *Higgs production via vector-boson fusion at NNLO in QCD*, *Phys. Rev. Lett.* **105** (2010) 011801, arXiv:1003.4451 [hep-ph].
- [58] T. Han and S. Willenbrock, *QCD correction to the $p p \rightarrow W H$ and $Z H$ total cross- sections*, *Phys. Lett.* **B 273** (1991) 167.
- [59] O. Brein, A. Djouadi and R. Harlander, *NNLO QCD corrections to the Higgs-strahlung processes at hadron colliders*, *Phys. Lett.* **B 579** (2004) 149, arXiv:hep-ph/0307206.
- [60] M. L. Ciccolini, S. Dittmaier and M. Krämer, *Electroweak radiative corrections to associated WH and ZH production at hadron colliders*, *Phys. Rev.* **D 68** (2003) 073003, arXiv:hep-ph/0306234.
- [61] W. Beenakker et al., *Higgs radiation off top quarks at the Tevatron and the LHC*, *Phys. Rev. Lett.* **87** (2001) 201805, arXiv:hep-ph/0107081.
- [62] W. Beenakker et al., *NLO QCD corrections to $t\bar{t} H$ production in hadron collisions*, *Nucl. Phys.* **B 653** (2003) 151, arXiv:hep-ph/0211352.
- [63] S. Dawson et al., *Next-to-leading order QCD corrections to $pp \rightarrow t\bar{t}h$ at the CERN Large Hadron Collider*, *Phys. Rev.* **D 67** (2003) 071503, arXiv:hep-ph/0211438.
- [64] S. Dawson et al., *Associated Higgs production with top quarks at the Large Hadron Collider: NLO QCD corrections*, *Phys. Rev.* **D 68** (2003) 034022, arXiv:hep-ph/0305087.
- [65] T. Melia et al., *W+W-, WZ and ZZ production in the POWHEG BOX*, *J. High Energy Phys.* **1111** (2011) 078, arXiv:1107.5051 [hep-ph].
- [66] N. Kauer and G. Passarino, *Inadequacy of zero-width approximation for a light Higgs boson signal*, *J. High Energy Phys.* **1208** (2012) 116, arXiv:1206.4803 [hep-ph].
- [67] J. Butterworth, J. R. Forshaw and M. Seymour, *Multiparton interactions in photoproduction at HERA*, *Z.Phys.* **C72** (1996) 637–646, arXiv:hep-ph/9601371 [hep-ph].

- [68] M. L. Mangano et al., *ALPGEN, a generator for hard multiparton processes in hadronic collisions*, *J. High Energy Phys.* **0307** (2003) 001, arXiv:[hep-ph/0206293](#) [[hep-ph](#)].
- [69] M. L. Mangano et al., *Matching matrix elements and shower evolution for top-quark production in hadronic collisions*, *J. High Energy Phys.* **0701** (2007) 013, arXiv:[hep-ph/0611129](#) [[hep-ph](#)].
- [70] K. Melnikov and F. Petriello, *Electroweak gauge boson production at hadron colliders through $O(\alpha_s^2)$* , *Phys. Rev. D* **74** (2006) 114017, arXiv:[hep-ph/0609070](#).
- [71] C. Anastasiou et al., *High precision QCD at hadron colliders: electroweak gauge boson rapidity distributions at NNLO*, *Phys. Rev. D* **69** (2004) 094008, arXiv:[hep-ph/0312266](#) [[hep-ph](#)].
- [72] J. M. Campbell and R. Ellis, *MCFM for the Tevatron and the LHC*, *Nucl. Phys. Proc. Suppl.* **205-206** (2010) 10–15, arXiv:[1007.3492](#) [[hep-ph](#)].
- [73] J. M. Campbell and R. K. Ellis, *Radiative corrections to $Z b$ anti- b production*, *Phys. Rev. D* **62** (2000) 114012, arXiv:[hep-ph/0006304](#).
- [74] S. Frixione, P. Nason and B. R. Webber, *Matching NLO QCD and parton showers in heavy flavor production*, *J. High Energy Phys.* **0308** (2003) 007, arXiv:[hep-ph/0305252](#) [[hep-ph](#)].
- [75] G. Corcella et al., *HERWIG 6: An Event generator for hadron emission reactions with interfering gluons (including supersymmetric processes)*, *J. High Energy Phys.* **0101** (2001) 010, arXiv:[hep-ph/0011363](#) [[hep-ph](#)].
- [76] ATLAS Collaboration, *ATLAS tunes of PYTHIA 6 and PYTHIA 8 for MC11*, ATLAS-PHYS-PUB-2011-009 (2011), URL: <http://cdsweb.cern.ch/record/1363300>.
- [77] J. M. Campbell, R. K. Ellis and C. Williams, *Vector boson pair production at the LHC*, *J. High Energy Phys.* **1107** (2011) 018, arXiv:[1105.0020](#) [[hep-ph](#)].
- [78] T. Gleisberg et al., *Event generation with SHERPA 1.1*, *J. High Energy Phys.* **0902** (2009) 007, arXiv:[0811.4622](#) [[hep-ph](#)].
- [79] ATLAS Collaboration, *Observation and measurements of the production of prompt and non-prompt J/ψ mesons in association with a Z boson in pp collisions at $\sqrt{s} = 8$ TeV with the ATLAS detector* (2014), arXiv:[1412.6428](#) [[hep-ex](#)].
- [80] ATLAS Collaboration, *The ATLAS Simulation Infrastructure*, *Eur. Phys. J.* **C70** (2010) 823–874.
- [81] S. Agostinelli et al. (GEANT4 Collaboration), *GEANT4: A simulation toolkit*, *Nucl. Instrum. Meth.* **A506** (2003) 250–303.
- [82] ATLAS Collaboration, *The simulation principle and performance of the ATLAS fast calorimeter simulation FastCaloSim*, ATLAS-PHYS-PUB-2010-013 (2010), URL: <https://cds.cern.ch/record/1300517>.
- [83] ATLAS Collaboration, *Monitoring and data quality assessment of the ATLAS liquid argon calorimeter*, *JINST* **9** (2014) P07024, arXiv:[1405.3768](#) [[hep-ex](#)].

- [84] ATLAS Collaboration, *Electron performance measurements with the ATLAS detector using the 2010 LHC proton-proton collision data*, *Eur.Phys.J.* **C72** (2012) 1909, arXiv:1110.3174 [hep-ex].
- [85] ATLAS Collaboration, *Measurement of the $W \rightarrow \ell\nu$ and $Z/\gamma^* \rightarrow \ell\ell$ production cross sections in proton-proton collisions at $\sqrt{s} = 7$ TeV with the ATLAS detector*, *J. High Energy Phys.* **1012** (2010) 060, arXiv:1010.2130 [hep-ex].
- [86] K. Olive, et al. (Particle Data Group), *Review of Particle Physics*, *Chin.Phys.* **C38** (2014) 090001.
- [87] A. L. Read, *Linear interpolation of histograms*, *Nucl.Instrum.Meth.* **A425** (1999) 357–360.
- [88] A. L. Read, *Presentation of search results: The CL(s) technique*, *J.Phys.* **G28** (2002) 2693–2704.
- [89] R. D. Cousins and V. L. Highland, *Incorporating systematic uncertainties into an upper limit*, *Nucl.Instrum.Meth.* **A320** (1992) 331–335.
- [90] G. Cowan et al., *Asymptotic formulae for likelihood-based tests of new physics*, *Eur.Phys.J.* **C71** (2011) 1554, arXiv:1007.1727 [physics.data-an].
- [91] G. Cowan et al., *Erratum to: Asymptotic formulae for likelihood-based tests of new physics*, *Eur.Phys.J.* **C73.7**, 2501 (2013), ISSN: 1434-6044, URL: <http://dx.doi.org/10.1140/epjc/s10052-013-2501-z>.
- [92] C. Gumpert et al., *Software for statistical data analysis used in Higgs searches*, *J.Phys.Conf.Ser.* **490** (2014) 012229.
- [93] ATLAS Collaboration, *Search for the Standard Model Higgs boson in the decay channel $H \rightarrow ZZ(*) \rightarrow 4\ell$ with 4.8 fb^{-1} of pp collision data at $\sqrt{s} = 7$ TeV with ATLAS*, *Phys.Lett.* **B710** (2012) 383–402, arXiv:1202.1415 [hep-ex].
- [94] ATLAS and CMS Collaborations, *Combined Measurement of the Higgs Boson Mass in pp Collisions at $\sqrt{s} = 7$ and 8 TeV with the ATLAS and CMS Experiments*, *Phys. Rev. Lett.* **114** (2015) 191803, arXiv:1503.07589 [hep-ex].

The ATLAS Collaboration

G. Aad⁸⁵, B. Abbott¹¹³, J. Abdallah¹⁵¹, O. Abdinov¹¹, R. Aben¹⁰⁷, M. Abolins⁹⁰, O.S. AbouZeid¹⁵⁸, H. Abramowicz¹⁵³, H. Abreu¹⁵², R. Abreu³⁰, Y. Abulaiti^{146a,146b}, B.S. Acharya^{164a,164b,a}, L. Adamczyk^{38a}, D.L. Adams²⁵, J. Adelman¹⁰⁸, S. Adomeit¹⁰⁰, T. Adye¹³¹, A.A. Affolder⁷⁴, T. Agatonovic-Jovin¹³, J.A. Aguilar-Saavedra^{126a,126f}, S.P. Ahlen²², F. Ahmadov^{65,b}, G. Aielli^{133a,133b}, H. Akerstedt^{146a,146b}, T.P.A. Åkesson⁸¹, G. Akimoto¹⁵⁵, A.V. Akimov⁹⁶, G.L. Alberghi^{20a,20b}, J. Albert¹⁶⁹, S. Albrand⁵⁵, M.J. Alconada Verzini⁷¹, M. Aleksa³⁰, I.N. Aleksandrov⁶⁵, C. Alexa^{26a}, G. Alexander¹⁵³, T. Alexopoulos¹⁰, M. Alhroob¹¹³, G. Alimonti^{91a}, L. Alio⁸⁵, J. Alison³¹, S.P. Alkire³⁵, B.M.M. Allbrooke¹⁸, P.P. Allport⁷⁴, A. Aloisio^{104a,104b}, A. Alonso³⁶, F. Alonso⁷¹, C. Alpigiani⁷⁶, A. Altheimer³⁵, B. Alvarez Gonzalez³⁰, D. Álvarez Piqueras¹⁶⁷, M.G. Alviggi^{104a,104b}, B.T. Amadio¹⁵, K. Amako⁶⁶, Y. Amaral Coutinho^{24a}, C. Amelung²³, D. Amidei⁸⁹, S.P. Amor Dos Santos^{126a,126c}, A. Amorim^{126a,126b}, S. Amoroso⁴⁸, N. Amram¹⁵³, G. Amundsen²³, C. Anastopoulos¹³⁹, L.S. Ancu⁴⁹, N. Andari³⁰, T. Andeen³⁵, C.F. Anders^{58b}, G. Anders³⁰, J.K. Anders⁷⁴, K.J. Anderson³¹, A. Andreazza^{91a,91b}, V. Andrei^{58a}, S. Angelidakis⁹, I. Angelozzi¹⁰⁷, P. Anger⁴⁴, A. Angerami³⁵, F. Anghinolfi³⁰, A.V. Anisenkov^{109,c}, N. Anjos¹², A. Annovi^{124a,124b}, M. Antonelli⁴⁷, A. Antonov⁹⁸, J. Antos^{144b}, F. Anulli^{132a}, M. Aoki⁶⁶, L. Aperio Bella¹⁸, G. Arabidze⁹⁰, Y. Arai⁶⁶, J.P. Araque^{126a}, A.T.H. Arce⁴⁵, F.A. Arduh⁷¹, J-F. Arguin⁹⁵, S. Argyropoulos⁴², M. Arik^{19a}, A.J. Armbruster³⁰, O. Arnaez³⁰, V. Arnal⁸², H. Arnold⁴⁸, M. Arratia²⁸, O. Arslan²¹, A. Artamonov⁹⁷, G. Artoni²³, S. Asai¹⁵⁵, N. Asbah⁴², A. Ashkenazi¹⁵³, B. Åsman^{146a,146b}, L. Asquith¹⁴⁹, K. Assamagan²⁵, R. Astalos^{144a}, M. Atkinson¹⁶⁵, N.B. Atlay¹⁴¹, B. Auerbach⁶, K. Augsten¹²⁸, M. Aurousseau^{145b}, G. Avolio³⁰, B. Axen¹⁵, M.K. Ayoub¹¹⁷, G. Azuelos^{95,d}, M.A. Baak³⁰, A.E. Baas^{58a}, C. Bacci^{134a,134b}, H. Bachacou¹³⁶, K. Bachas¹⁵⁴, M. Backes³⁰, M. Backhaus³⁰, P. Bagiacchi^{132a,132b}, P. Bagnaia^{132a,132b}, Y. Bai^{33a}, T. Bain³⁵, J.T. Baines¹³¹, O.K. Baker¹⁷⁶, P. Balek¹²⁹, T. Balestri¹⁴⁸, F. Balli⁸⁴, E. Banas³⁹, Sw. Banerjee¹⁷³, A.A.E. Bannoura¹⁷⁵, H.S. Bansil¹⁸, L. Barak³⁰, E.L. Barberio⁸⁸, D. Barberis^{50a,50b}, M. Barbero⁸⁵, T. Barillari¹⁰¹, M. Barisonzi^{164a,164b}, T. Barklow¹⁴³, N. Barlow²⁸, S.L. Barnes⁸⁴, B.M. Barnett¹³¹, R.M. Barnett¹⁵, Z. Barnovska⁵, A. Baroncelli^{134a}, G. Barone⁴⁹, A.J. Barr¹²⁰, F. Barreiro⁸², J. Barreiro Guimarães da Costa⁵⁷, R. Bartoldus¹⁴³, A.E. Barton⁷², P. Bartos^{144a}, A. Basalae¹²³, A. Bassalat¹¹⁷, A. Basye¹⁶⁵, R.L. Bates⁵³, S.J. Batista¹⁵⁸, J.R. Batley²⁸, M. Battaglia¹³⁷, M. Bauce^{132a,132b}, F. Bauer¹³⁶, H.S. Bawa^{143,e}, J.B. Beacham¹¹¹, M.D. Beattie⁷², T. Beau⁸⁰, P.H. Beauchemin¹⁶¹, R. Beccherle^{124a,124b}, P. Bechtel²¹, H.P. Beck^{17,f}, K. Becker¹²⁰, M. Becker⁸³, S. Becker¹⁰⁰, M. Beckingham¹⁷⁰, C. Becot¹¹⁷, A.J. Beddall^{19c}, A. Beddall^{19c}, V.A. Bednyakov⁶⁵, C.P. Bee¹⁴⁸, L.J. Beamster¹⁰⁷, T.A. Beermann¹⁷⁵, M. Beger²⁵, J.K. Behr¹²⁰, C. Belanger-Champagne⁸⁷, W.H. Bell⁴⁹, G. Bella¹⁵³, L. Bellagamba^{20a}, A. Bellerive²⁹, M. Bellomo⁸⁶, K. Belotskiy⁹⁸, O. Beltramello³⁰, O. Benary¹⁵³, D. Bencheikroun^{135a}, M. Bender¹⁰⁰, K. Bendtz^{146a,146b}, N. Benekos¹⁰, Y. Benhammou¹⁵³, E. Benhar Noccioli⁴⁹, J.A. Benitez Garcia^{159b}, D.P. Benjamin⁴⁵, J.R. Bensinger²³, S. Bentvelsen¹⁰⁷, L. Beresford¹²⁰, M. Beretta⁴⁷, D. Berge¹⁰⁷, E. Bergeaas Kuutmann¹⁶⁶, N. Berger⁵, F. Berghaus¹⁶⁹, J. Beringer¹⁵, C. Bernard²², N.R. Bernard⁸⁶, C. Bernius¹¹⁰, F.U. Bernlochner²¹, T. Berry⁷⁷, P. Berta¹²⁹, C. Bertella⁸³, G. Bertoli^{146a,146b}, F. Bertolucci^{124a,124b}, C. Bertsche¹¹³, D. Bertsche¹¹³, M.I. Besana^{91a}, G.J. Besjes¹⁰⁶, O. Bessidskaia Bylund^{146a,146b}, M. Bessner⁴², N. Besson¹³⁶, C. Betancourt⁴⁸, S. Bethke¹⁰¹, A.J. Bevan⁷⁶, W. Bhimji⁴⁶, R.M. Bianchi¹²⁵, L. Bianchini²³, M. Bianco³⁰, O. Biebel¹⁰⁰, S.P. Bieniek⁷⁸, M. Biglietti^{134a}, J. Bilbao De Mendizabal⁴⁹, H. Bilokon⁴⁷, M. Bindi⁵⁴, S. Binet¹¹⁷, A. Bingul^{19c}, C. Bini^{132a,132b}, C.W. Black¹⁵⁰, J.E. Black¹⁴³, K.M. Black²², D. Blackburn¹³⁸, R.E. Blair⁶, J.-B. Blanchard¹³⁶, J.E. Blanco⁷⁷, T. Blazek^{144a}, I. Bloch⁴², C. Blocker²³, W. Blum^{83,*}, U. Blumenschein⁵⁴, G.J. Bobbink¹⁰⁷, V.S. Bobrovnikov^{109,c}, S.S. Bocchetta⁸¹, A. Bocci⁴⁵, C. Bock¹⁰⁰, M. Boehler⁴⁸, J.A. Bogaerts³⁰, A.G. Bogdanchikov¹⁰⁹,

C. Bohm^{146a}, V. Boisvert⁷⁷, T. Bold^{38a}, V. Boldea^{26a}, A.S. Boldyrev⁹⁹, M. Bomben⁸⁰, M. Bona⁷⁶, M. Boonekamp¹³⁶, A. Borisov¹³⁰, G. Borissov⁷², S. Borroni⁴², J. Bortfeldt¹⁰⁰, V. Bortolotto^{60a,60b,60c}, K. Bos¹⁰⁷, D. Boscherini^{20a}, M. Bosman¹², J. Boudreau¹²⁵, J. Bouffard², E.V. Bouhova-Thacker⁷², D. Boumediene³⁴, C. Bourdarios¹¹⁷, N. Bousson¹¹⁴, A. Boveia³⁰, J. Boyd³⁰, I.R. Boyko⁶⁵, I. Bozic¹³, J. Bracinik¹⁸, A. Brandt⁸, G. Brandt⁵⁴, O. Brandt^{58a}, U. Bratzler¹⁵⁶, B. Brau⁸⁶, J.E. Brau¹¹⁶, H.M. Braun^{175,*}, S.F. Brazzale^{164a,164c}, K. Brendlinger¹²², A.J. Brennan⁸⁸, L. Brenner¹⁰⁷, R. Brenner¹⁶⁶, S. Bressler¹⁷², K. Bristow^{145c}, T.M. Bristow⁴⁶, D. Britton⁵³, D. Britzger⁴², F.M. Brochu²⁸, I. Brock²¹, R. Brock⁹⁰, J. Bronner¹⁰¹, G. Brooijmans³⁵, T. Brooks⁷⁷, W.K. Brooks^{32b}, J. Brosamer¹⁵, E. Brost¹¹⁶, J. Brown⁵⁵, P.A. Bruckman de Renstrom³⁹, D. Bruncko^{144b}, R. Bruneliere⁴⁸, A. Bruni^{20a}, G. Bruni^{20a}, M. Bruschi^{20a}, L. Bryngemark⁸¹, T. Buanes¹⁴, Q. Buat¹⁴², P. Buchholz¹⁴¹, A.G. Buckley⁵³, S.I. Buda^{26a}, I.A. Budagov⁶⁵, F. Buehrer⁴⁸, L. Bugge¹¹⁹, M.K. Bugge¹¹⁹, O. Bulekov⁹⁸, D. Bullock⁸, H. Burckhart³⁰, S. Burdin⁷⁴, B. Burghgrave¹⁰⁸, S. Burke¹³¹, I. Burmeister⁴³, E. Busato³⁴, D. Büscher⁴⁸, V. Büscher⁸³, P. Bussey⁵³, J.M. Butler²², A.I. Butt³, C.M. Buttar⁵³, J.M. Butterworth⁷⁸, P. Butti¹⁰⁷, W. Buttinger²⁵, A. Buzatu⁵³, A.R. Buzykaev^{109,c}, S. Cabrera Urbán¹⁶⁷, D. Caforio¹²⁸, V.M. Cairo^{37a,37b}, O. Cakir^{4a}, P. Calafiura¹⁵, A. Calandri¹³⁶, G. Calderini⁸⁰, P. Calfayan¹⁰⁰, L.P. Caloba^{24a}, D. Calvet³⁴, S. Calvet³⁴, R. Camacho Toro³¹, S. Camarda⁴², P. Camarri^{133a,133b}, D. Cameron¹¹⁹, L.M. Caminada¹⁵, R. Caminal Armadans¹², S. Campana³⁰, M. Campanelli⁷⁸, A. Campoverde¹⁴⁸, V. Canale^{104a,104b}, A. Canepa^{159a}, M. Cano Bret⁷⁶, J. Cantero⁸², R. Cantrill^{126a}, T. Cao⁴⁰, M.D.M. Capeans Garrido³⁰, I. Caprini^{26a}, M. Caprini^{26a}, M. Capua^{37a,37b}, R. Caputo⁸³, R. Cardarelli^{133a}, T. Carli³⁰, G. Carlino^{104a}, L. Carminati^{91a,91b}, S. Caron¹⁰⁶, E. Carquin^{32a}, G.D. Carrillo-Montoya⁸, J.R. Carter²⁸, J. Carvalho^{126a,126c}, D. Casadei⁷⁸, M.P. Casado¹², M. Casolino¹², E. Castaneda-Miranda^{145b}, A. Castelli¹⁰⁷, V. Castillo Gimenez¹⁶⁷, N.F. Castro^{126a,g}, P. Catastini⁵⁷, A. Catinaccio³⁰, J.R. Catmore¹¹⁹, A. Cattai³⁰, J. Caudron⁸³, V. Cavaliere¹⁶⁵, D. Cavalli^{91a}, M. Cavalli-Sforza¹², V. Cavasinni^{124a,124b}, F. Ceradini^{134a,134b}, B.C. Cerio⁴⁵, K. Cerny¹²⁹, A.S. Cerqueira^{24b}, A. Cerri¹⁴⁹, L. Cerrito⁷⁶, F. Cerutti¹⁵, M. Cerv³⁰, A. Cervelli¹⁷, S.A. Cetin^{19b}, A. Chafaq^{135a}, D. Chakraborty¹⁰⁸, I. Chalupkova¹²⁹, P. Chang¹⁶⁵, B. Chapleau⁸⁷, J.D. Chapman²⁸, D.G. Charlton¹⁸, C.C. Chau¹⁵⁸, C.A. Chavez Barajas¹⁴⁹, S. Cheatham¹⁵², A. Chegwidden⁹⁰, S. Chekanov⁶, S.V. Chekulaev^{159a}, G.A. Chelkov^{65,h}, M.A. Chelstowska⁸⁹, C. Chen⁶⁴, H. Chen²⁵, K. Chen¹⁴⁸, L. Chen^{33d,i}, S. Chen^{33c}, X. Chen^{33f}, Y. Chen⁶⁷, H.C. Cheng⁸⁹, Y. Cheng³¹, A. Cheplakov⁶⁵, E. Cheremushkina¹³⁰, R. Cherkaoui El Moursli^{135e}, V. Chernyatin^{25,*}, E. Cheu⁷, L. Chevalier¹³⁶, V. Chiarella⁴⁷, J.T. Childers⁶, G. Chiodini^{73a}, A.S. Chisholm¹⁸, R.T. Chislett⁷⁸, A. Chitan^{26a}, M.V. Chizhov⁶⁵, K. Choi⁶¹, S. Chouridou⁹, B.K.B. Chow¹⁰⁰, V. Christodoulou⁷⁸, D. Chromek-Burckhart³⁰, M.L. Chu¹⁵¹, J. Chudoba¹²⁷, A.J. Chuinard⁸⁷, J.J. Chwastowski³⁹, L. Chytka¹¹⁵, G. Ciapetti^{132a,132b}, A.K. Ciftci^{4a}, D. Cincă⁵³, V. Cindro⁷⁵, I.A. Cioara²¹, A. Ciocio¹⁵, Z.H. Citron¹⁷², M. Ciubancan^{26a}, A. Clark⁴⁹, B.L. Clark⁵⁷, P.J. Clark⁴⁶, R.N. Clarke¹⁵, W. Cleland¹²⁵, C. Clement^{146a,146b}, Y. Coadou⁸⁵, M. Cobal^{164a,164c}, A. Coccaro¹³⁸, J. Cochran⁶⁴, L. Coffey²³, J.G. Cogan¹⁴³, B. Cole³⁵, S. Cole¹⁰⁸, A.P. Colijn¹⁰⁷, J. Collot⁵⁵, T. Colombo^{58c}, G. Compostella¹⁰¹, P. Conde Muiño^{126a,126b}, E. Coniavitis⁴⁸, S.H. Connell^{145b}, I.A. Connelly⁷⁷, S.M. Consonni^{91a,91b}, V. Consorti⁴⁸, S. Constantinescu^{26a}, C. Conta^{121a,121b}, G. Conti³⁰, F. Conventi^{104a,j}, M. Cooke¹⁵, B.D. Cooper⁷⁸, A.M. Cooper-Sarkar¹²⁰, T. Cornelissen¹⁷⁵, M. Corradi^{20a}, F. Corriveau^{87,k}, A. Corso-Radu¹⁶³, A. Cortes-Gonzalez¹², G. Cortiana¹⁰¹, G. Costa^{91a}, M.J. Costa¹⁶⁷, D. Costanzo¹³⁹, D. Côté⁸, G. Cottin²⁸, G. Cowan⁷⁷, B.E. Cox⁸⁴, K. Cranmer¹¹⁰, G. Cree²⁹, S. Crépe-Renaudin⁵⁵, F. Crescioli⁸⁰, W.A. Cribbs^{146a,146b}, M. Crispin Ortuzar¹²⁰, M. Cristinziani²¹, V. Croft¹⁰⁶, G. Crosetti^{37a,37b}, T. Cuhadar Donszelmann¹³⁹, J. Cummings¹⁷⁶, M. Curatolo⁴⁷, C. Cuthbert¹⁵⁰, H. Czirr¹⁴¹, P. Czodrowski³, S. D'Auria⁵³, M. D'Onofrio⁷⁴, M.J. Da Cunha Sargedas De Sousa^{126a,126b}, C. Da Via⁸⁴, W. Dabrowski^{38a}, A. Dafinca¹²⁰, T. Dai⁸⁹, O. Dale¹⁴, F. Dallaire⁹⁵, C. Dallapiccola⁸⁶, M. Dam³⁶, J.R. Dandoy³¹, N.P. Dang⁴⁸, A.C. Daniells¹⁸, M. Danninger¹⁶⁸, M. Dano Hoffmann¹³⁶, V. Dao⁴⁸, G. Darbo^{50a},

S. Darmora⁸, J. Dassoulas³, A. Dattagupta⁶¹, W. Davey²¹, C. David¹⁶⁹, T. Davidek¹²⁹, E. Davies^{120,l},
 M. Davies¹⁵³, P. Davison⁷⁸, Y. Davygora^{58a}, E. Dawe⁸⁸, I. Dawson¹³⁹, R.K. Daya-Ishmukhametova⁸⁶,
 K. De⁸, R. de Asmundis^{104a}, S. De Castro^{20a,20b}, S. De Cecco⁸⁰, N. De Groot¹⁰⁶, P. de Jong¹⁰⁷,
 H. De la Torre⁸², F. De Lorenzi⁶⁴, L. De Nooij¹⁰⁷, D. De Pedis^{132a}, A. De Salvo^{132a}, U. De Sanctis¹⁴⁹,
 A. De Santo¹⁴⁹, J.B. De Vivie De Regie¹¹⁷, W.J. Dearnaley⁷², R. Debbe²⁵, C. Debenedetti¹³⁷,
 D.V. Dedovich⁶⁵, I. Deigaard¹⁰⁷, J. Del Peso⁸², T. Del Prete^{124a,124b}, D. Delgove¹¹⁷, F. Deliot¹³⁶,
 C.M. Delitzsch⁴⁹, M. Deliyergiyev⁷⁵, A. Dell'Acqua³⁰, L. Dell'Asta²², M. Dell'Orso^{124a,124b},
 M. Della Pietra^{104a,j}, D. della Volpe⁴⁹, M. Delmastro⁵, P.A. Delsart⁵⁵, C. Deluca¹⁰⁷, D.A. DeMarco¹⁵⁸,
 S. Demers¹⁷⁶, M. Demichev⁶⁵, A. Demilly⁸⁰, S.P. Denisov¹³⁰, D. Derendarz³⁹, J.E. Derkaoui^{135d},
 F. Derue⁸⁰, P. Dervan⁷⁴, K. Desch²¹, C. Deterre⁴², P.O. Deviveiros³⁰, A. Dewhurst¹³¹, S. Dhaliwal²³,
 A. Di Ciaccio^{133a,133b}, L. Di Ciaccio⁵, A. Di Domenico^{132a,132b}, C. Di Donato^{104a,104b},
 A. Di Girolamo³⁰, B. Di Girolamo³⁰, A. Di Mattia¹⁵², B. Di Micco^{134a,134b}, R. Di Nardo⁴⁷,
 A. Di Simone⁴⁸, R. Di Sipio¹⁵⁸, D. Di Valentino²⁹, C. Diaconu⁸⁵, M. Diamond¹⁵⁸, F.A. Dias⁴⁶,
 M.A. Diaz^{32a}, E.B. Diehl⁸⁹, J. Dietrich¹⁶, S. Diglio⁸⁵, A. Dimitrievska¹³, J. Dingfelder²¹, P. Dita^{26a},
 S. Dita^{26a}, F. Dittus³⁰, F. Djama⁸⁵, T. Djobava^{51b}, J.I. Djuvslund^{58a}, M.A.B. do Vale^{24c}, D. Dobos³⁰,
 M. Dobre^{26a}, C. Doglioni⁴⁹, T. Dohmae¹⁵⁵, J. Dolejsi¹²⁹, Z. Dolezal¹²⁹, B.A. Dolgoshein^{98,*},
 M. Donadelli^{24d}, S. Donati^{124a,124b}, P. Dondero^{121a,121b}, J. Donini³⁴, J. Dopke¹³¹, A. Doria^{104a},
 M.T. Dova⁷¹, A.T. Doyle⁵³, E. Drechsler⁵⁴, M. Dris¹⁰, E. Dubreuil³⁴, E. Duchovni¹⁷², G. Duckeck¹⁰⁰,
 O.A. Ducu^{26a,85}, D. Duda¹⁷⁵, A. Dudarev³⁰, L. Duflot¹¹⁷, L. Duguid⁷⁷, M. Dührssen³⁰, M. Dunford^{58a},
 H. Duran Yildiz^{4a}, M. Düren⁵², A. Durglishvili^{51b}, D. Duschinger⁴⁴, M. Dyndal^{38a}, C. Eckardt⁴²,
 K.M. Ecker¹⁰¹, R.C. Edgar⁸⁹, W. Edson², N.C. Edwards⁴⁶, W. Ehrenfeld²¹, T. Eifert³⁰, G. Eigen¹⁴,
 K. Einsweiler¹⁵, T. Ekelof¹⁶⁶, M. El Kacimi^{135c}, M. Ellert¹⁶⁶, S. Elles⁵, F. Ellinghaus⁸³, A.A. Elliot¹⁶⁹,
 N. Ellis³⁰, J. Elmsheuser¹⁰⁰, M. Elsing³⁰, D. Emeliyanov¹³¹, Y. Enari¹⁵⁵, O.C. Endner⁸³, M. Endo¹¹⁸,
 J. Erdmann⁴³, A. Ereditato¹⁷, G. Ernis¹⁷⁵, J. Ernst², M. Ernst²⁵, S. Errede¹⁶⁵, E. Ertel⁸³, M. Escalier¹¹⁷,
 H. Esch⁴³, C. Escobar¹²⁵, B. Esposito⁴⁷, A.I. Etienne¹³⁶, E. Etzion¹⁵³, H. Evans⁶¹, A. Ezhilov¹²³,
 L. Fabbri^{20a,20b}, G. Facini³¹, R.M. Fakhruddinov¹³⁰, S. Falciano^{132a}, R.J. Falla⁷⁸, J. Faltova¹²⁹,
 Y. Fang^{33a}, M. Fanti^{91a,91b}, A. Farbin⁸, A. Farilla^{134a}, T. Farooque¹², S. Farrell¹⁵, S.M. Farrington¹⁷⁰,
 P. Farthouat³⁰, F. Fassi^{135e}, P. Fassnacht³⁰, D. Fassouliotis⁹, M. Fauci Giannelli⁷⁷, A. Favareto^{50a,50b},
 L. Fayard¹¹⁷, P. Federic^{144a}, O.L. Fedin^{123,m}, W. Fedorko¹⁶⁸, S. Feigl³⁰, L. Felgioni⁸⁵, C. Feng^{33d},
 E.J. Feng⁶, H. Feng⁸⁹, A.B. Fenyuk¹³⁰, P. Fernandez Martinez¹⁶⁷, S. Fernandez Perez³⁰, J. Ferrando⁵³,
 A. Ferrari¹⁶⁶, P. Ferrari¹⁰⁷, R. Ferrari^{121a}, D.E. Ferreira de Lima⁵³, A. Ferrer¹⁶⁷, D. Ferrere⁴⁹,
 C. Ferretti⁸⁹, A. Ferretto Parodi^{50a,50b}, M. Fiascaris³¹, F. Fiedler⁸³, A. Filipčić⁷⁵, M. Filipuzzi⁴²,
 F. Filthaut¹⁰⁶, M. Fincke-Keeler¹⁶⁹, K.D. Finelli¹⁵⁰, M.C.N. Fiolhais^{126a,126c}, L. Fiorini¹⁶⁷, A. Firan⁴⁰,
 A. Fischer², C. Fischer¹², J. Fischer¹⁷⁵, W.C. Fisher⁹⁰, E.A. Fitzgerald²³, M. Flechl⁴⁸, I. Fleck¹⁴¹,
 P. Fleischmann⁸⁹, S. Fleischmann¹⁷⁵, G.T. Fletcher¹³⁹, G. Fletcher⁷⁶, T. Flick¹⁷⁵, A. Floderus⁸¹,
 L.R. Flores Castillo^{60a}, M.J. Flowerdew¹⁰¹, A. Formica¹³⁶, A. Forti⁸⁴, D. Fournier¹¹⁷, H. Fox⁷²,
 S. Fracchia¹², P. Francavilla⁸⁰, M. Franchini^{20a,20b}, D. Francis³⁰, L. Franconi¹¹⁹, M. Franklin⁵⁷,
 M. Fraternali^{121a,121b}, D. Freeborn⁷⁸, S.T. French²⁸, F. Friedrich⁴⁴, D. Froidevaux³⁰, J.A. Frost¹²⁰,
 C. Fukunaga¹⁵⁶, E. Fullana Torregrosa⁸³, B.G. Fulsom¹⁴³, J. Fuster¹⁶⁷, C. Gabaldon⁵⁵, O. Gabizon¹⁷⁵,
 A. Gabrielli^{20a,20b}, A. Gabrielli^{132a,132b}, S. Gadatsch¹⁰⁷, S. Gadomski⁴⁹, G. Gagliardi^{50a,50b}, P. Gagnon⁶¹,
 C. Galea¹⁰⁶, B. Galhardo^{126a,126c}, E.J. Gallas¹²⁰, B.J. Gallop¹³¹, P. Gallus¹²⁸, G. Galster³⁶, K.K. Gan¹¹¹,
 J. Gao^{33b,85}, Y. Gao⁴⁶, Y.S. Gao^{143,e}, F.M. Garay Walls⁴⁶, F. Garbersson¹⁷⁶, C. García¹⁶⁷,
 J.E. García Navarro¹⁶⁷, M. Garcia-Sciveres¹⁵, R.W. Gardner³¹, N. Garelli¹⁴³, V. Garonne¹¹⁹, C. Gatti⁴⁷,
 A. Gaudiello^{50a,50b}, G. Gaudio^{121a}, B. Gaur¹⁴¹, L. Gauthier⁹⁵, P. Gauzzi^{132a,132b}, I.L. Gavrilenko⁹⁶,
 C. Gay¹⁶⁸, G. Gaycken²¹, E.N. Gazis¹⁰, P. Ge^{33d}, Z. Gece¹⁶⁸, C.N.P. Gee¹³¹, D.A.A. Geerts¹⁰⁷,
 Ch. Geich-Gimbel²¹, M.P. Geisler^{58a}, C. Gemme^{50a}, M.H. Genest⁵⁵, S. Gentile^{132a,132b}, M. George⁵⁴,
 S. George⁷⁷, D. Gerbaudo¹⁶³, A. Gershon¹⁵³, H. Ghazlane^{135b}, B. Giacobbe^{20a}, S. Giagu^{132a,132b},

V. Giangiobbe¹², P. Giannetti^{124a,124b}, B. Gibbard²⁵, S.M. Gibson⁷⁷, M. Gilchriese¹⁵, T.P.S. Gillam²⁸, D. Gillberg³⁰, G. Gilles³⁴, D.M. Gingrich^{3,d}, N. Giokaris⁹, M.P. Giordani^{164a,164c}, F.M. Giorgi^{20a}, F.M. Giorgi¹⁶, P.F. Giraud¹³⁶, P. Giromini⁴⁷, D. Giugni^{91a}, C. Giuliani⁴⁸, M. Giulini^{58b}, B.K. Gjelsten¹¹⁹, S. Gkaitatzis¹⁵⁴, I. Gkialas¹⁵⁴, E.L. Gkoukousis¹¹⁷, L.K. Gladilin⁹⁹, C. Glasman⁸², J. Glatzer³⁰, P.C.F. Glaysher⁴⁶, A. Glazov⁴², M. Goblirsch-Kolb¹⁰¹, J.R. Goddard⁷⁶, J. Godlewski³⁹, S. Goldfarb⁸⁹, T. Golling⁴⁹, D. Golubkov¹³⁰, A. Gomes^{126a,126b,126d}, R. Gonçalo^{126a}, J. Goncalves Pinto Firmino Da Costa¹³⁶, L. Gonella²¹, S. González de la Hoz¹⁶⁷, G. Gonzalez Parra¹², S. Gonzalez-Sevilla⁴⁹, L. Goossens³⁰, P.A. Gorbounov⁹⁷, H.A. Gordon²⁵, I. Gorelov¹⁰⁵, B. Gorini³⁰, E. Gorini^{73a,73b}, A. Gorišek⁷⁵, E. Gornicki³⁹, A.T. Goshaw⁴⁵, C. Gössling⁴³, M.I. Gostkin⁶⁵, D. Goujdami^{135c}, A.G. Goussiou¹³⁸, N. Govender^{145b}, H.M.X. Grabas¹³⁷, L. Graber⁵⁴, I. Grabowska-Bold^{38a}, P. Grafström^{20a,20b}, K.-J. Grahn⁴², J. Gramling⁴⁹, E. Gramstad¹¹⁹, S. Grancagnolo¹⁶, V. Grassi¹⁴⁸, V. Gratchev¹²³, H.M. Gray³⁰, E. Graziani^{134a}, Z.D. Greenwood^{79,n}, K. Gregersen⁷⁸, I.M. Gregor⁴², P. Grenier¹⁴³, J. Griffiths⁸, A.A. Grillo¹³⁷, K. Grimm⁷², S. Grinstein^{12,o}, Ph. Gris³⁴, J.-F. Grivaz¹¹⁷, J.P. Grohs⁴⁴, A. Grohsjean⁴², E. Gross¹⁷², J. Grosse-Knetter⁵⁴, G.C. Grossi⁷⁹, Z.J. Grout¹⁴⁹, L. Guan^{33b}, J. Guenther¹²⁸, F. Guescini⁴⁹, D. Guest¹⁷⁶, O. Gueta¹⁵³, E. Guido^{50a,50b}, T. Guillemin¹¹⁷, S. Guindon², U. Gul⁵³, C. Gumpert⁴⁴, J. Guo^{33e}, S. Gupta¹²⁰, P. Gutierrez¹¹³, N.G. Gutierrez Ortiz⁵³, C. Gutsche⁴⁴, C. Guyot¹³⁶, C. Gwenlan¹²⁰, C.B. Gwilliam⁷⁴, A. Haas¹¹⁰, C. Haber¹⁵, H.K. Hadavand⁸, N. Haddad^{135e}, P. Haefner²¹, S. Hageböck²¹, Z. Hajduk³⁹, H. Hakobyan¹⁷⁷, M. Haleem⁴², J. Haley¹¹⁴, D. Hall¹²⁰, G. Halladjian⁹⁰, G.D. Hallowell⁸⁵, K. Hamacher¹⁷⁵, P. Hamal¹¹⁵, K. Hamano¹⁶⁹, M. Hamer⁵⁴, A. Hamilton^{145a}, G.N. Hamity^{145c}, P.G. Hamnett⁴², L. Han^{33b}, K. Hanagaki¹¹⁸, K. Hanawa¹⁵⁵, M. Hance¹⁵, P. Hanke^{58a}, R. Hanna¹³⁶, J.B. Hansen³⁶, J.D. Hansen³⁶, M.C. Hansen²¹, P.H. Hansen³⁶, K. Hara¹⁶⁰, A.S. Hard¹⁷³, T. Harenberg¹⁷⁵, F. Hariri¹¹⁷, S. Harkusha⁹², R.D. Harrington⁴⁶, P.F. Harrison¹⁷⁰, F. Hartjes¹⁰⁷, M. Hasegawa⁶⁷, S. Hasegawa¹⁰³, Y. Hasegawa¹⁴⁰, A. Hasib¹¹³, S. Hassani¹³⁶, S. Haug¹⁷, R. Hauser⁹⁰, L. Hauswald⁴⁴, M. Havranek¹²⁷, C.M. Hawkes¹⁸, R.J. Hawkins³⁰, A.D. Hawkins⁸¹, T. Hayashi¹⁶⁰, D. Hayden⁹⁰, C.P. Hays¹²⁰, J.M. Hays⁷⁶, H.S. Hayward⁷⁴, S.J. Haywood¹³¹, S.J. Head¹⁸, T. Heck⁸³, V. Hedberg⁸¹, L. Heelan⁸, S. Heim¹²², T. Heim¹⁷⁵, B. Heinemann¹⁵, L. Heinrich¹¹⁰, J. Hejbal¹²⁷, L. Helary²², S. Hellman^{146a,146b}, D. Hellmich²¹, C. Helsen³⁰, J. Henderson¹²⁰, R.C.W. Henderson⁷², Y. Heng¹⁷³, C. Hengler⁴², A. Henrichs¹⁷⁶, A.M. Henriques Correia³⁰, S. Henrot-Versille¹¹⁷, G.H. Herbert¹⁶, Y. Hernández Jiménez¹⁶⁷, R. Herrberg-Schubert¹⁶, G. Herten⁴⁸, R. Hertenberger¹⁰⁰, L. Hervas³⁰, G.G. Hesketh⁷⁸, N.P. Hessey¹⁰⁷, J.W. Hetherly⁴⁰, R. Hickling⁷⁶, E. Higón-Rodríguez¹⁶⁷, E. Hill¹⁶⁹, J.C. Hill²⁸, K.H. Hiller⁴², S.J. Hillier¹⁸, I. Hinchliffe¹⁵, E. Hines¹²², R.R. Hinman¹⁵, M. Hirose¹⁵⁷, D. Hirschbuehl¹⁷⁵, J. Hobbs¹⁴⁸, N. Hod¹⁰⁷, M.C. Hodgkinson¹³⁹, P. Hodgson¹³⁹, A. Hoecker³⁰, M.R. Hoferkamp¹⁰⁵, F. Hoenig¹⁰⁰, M. Hohlfeld⁸³, D. Hohn²¹, T.R. Holmes¹⁵, M. Homann⁴³, T.M. Hong¹²⁵, L. Hooft van Huysduynen¹¹⁰, W.H. Hopkins¹¹⁶, Y. Horii¹⁰³, A.J. Horton¹⁴², J.-Y. Hostachy⁵⁵, S. Hou¹⁵¹, A. Hoummada^{135a}, J. Howard¹²⁰, J. Howarth⁴², M. Hrabovsky¹¹⁵, I. Hristova¹⁶, J. Hrivnac¹¹⁷, T. Hryn'ova⁵, A. Hrynevich⁹³, C. Hsu^{145c}, P.J. Hsu^{151,p}, S.-C. Hsu¹³⁸, D. Hu³⁵, Q. Hu^{33b}, X. Hu⁸⁹, Y. Huang⁴², Z. Hubacek³⁰, F. Hubaut⁸⁵, F. Huegging²¹, T.B. Huffman¹²⁰, E.W. Hughes³⁵, G. Hughes⁷², M. Huhtinen³⁰, T.A. Hülsing⁸³, N. Huseynov^{65,b}, J. Huston⁹⁰, J. Huth⁵⁷, G. Iacobucci⁴⁹, G. Iakovidis²⁵, I. Ibragimov¹⁴¹, L. Iconomidou-Fayard¹¹⁷, E. Ideal¹⁷⁶, Z. Idrissi^{135e}, P. Iengo³⁰, O. Igonkina¹⁰⁷, T. Iizawa¹⁷¹, Y. Ikegami⁶⁶, K. Ikematsu¹⁴¹, M. Ikeno⁶⁶, Y. Ilchenko^{31,q}, D. Iliadis¹⁵⁴, N. Ilic¹⁴³, Y. Inamaru⁶⁷, T. Ince¹⁰¹, P. Ioannou⁹, M. Iodice^{134a}, K. Iordanidou³⁵, V. Ippolito⁵⁷, A. Irlles Quiles¹⁶⁷, C. Isaksson¹⁶⁶, M. Ishino⁶⁸, M. Ishitsuka¹⁵⁷, R. Ishmukhametov¹¹¹, C. Issever¹²⁰, S. Istin^{19a}, J.M. Iturbe Ponce⁸⁴, R. Iuppa^{133a,133b}, J. Ivarsson⁸¹, W. Iwanski³⁹, H. Iwasaki⁶⁶, J.M. Izen⁴¹, V. Izzo^{104a}, S. Jabbar³, B. Jackson¹²², M. Jackson⁷⁴, P. Jackson¹, M.R. Jaekel³⁰, V. Jain², K. Jakobs⁴⁸, S. Jakobsen³⁰, T. Jakoubek¹²⁷, J. Jakubek¹²⁸, D.O. Jamin¹⁵¹, D.K. Jana⁷⁹, E. Jansen⁷⁸, R.W. Jansky⁶², J. Janssen²¹, M. Janus¹⁷⁰, G. Jarlskog⁸¹,

N. Javadov^{65,b}, T. Javůrek⁴⁸, L. Jeanty¹⁵, J. Jejelava^{51a,r}, G.-Y. Jeng¹⁵⁰, D. Jennens⁸⁸, P. Jenni^{48,s},
 J. Jentzsch⁴³, C. Jeske¹⁷⁰, S. Jézéquel⁵, H. Ji¹⁷³, J. Jia¹⁴⁸, Y. Jiang^{33b}, S. Jiggins⁷⁸, J. Jimenez Pena¹⁶⁷,
 S. Jin^{33a}, A. Jinaru^{26a}, O. Jinnouchi¹⁵⁷, M.D. Joergensen³⁶, P. Johansson¹³⁹, K.A. Johns⁷,
 K. Jon-And^{146a,146b}, G. Jones¹⁷⁰, R.W.L. Jones⁷², T.J. Jones⁷⁴, J. Jongmanns^{58a}, P.M. Jorge^{126a,126b},
 K.D. Joshi⁸⁴, J. Jovicevic^{159a}, X. Ju¹⁷³, C.A. Jung⁴³, P. Jussel⁶², A. Juste Rozas^{12,o}, M. Kaci¹⁶⁷,
 A. Kaczmarzka³⁹, M. Kado¹¹⁷, H. Kagan¹¹¹, M. Kagan¹⁴³, S.J. Kahn⁸⁵, E. Kajomovitz⁴⁵,
 C.W. Kalderon¹²⁰, S. Kama⁴⁰, A. Kamenshchikov¹³⁰, N. Kanaya¹⁵⁵, M. Kaneda³⁰, S. Kaneti²⁸,
 V.A. Kantserov⁹⁸, J. Kanzaki⁶⁶, B. Kaplan¹¹⁰, A. Kapliy³¹, D. Kar⁵³, K. Karakostas¹⁰, A. Karamaoun³,
 N. Karastathis^{10,107}, M.J. Kareem⁵⁴, M. Karnevskiy⁸³, S.N. Karpov⁶⁵, Z.M. Karpova⁶⁵, K. Karthik¹¹⁰,
 V. Kartvelishvili⁷², A.N. Karyukhin¹³⁰, L. Kashif¹⁷³, R.D. Kass¹¹¹, A. Kastanas¹⁴, Y. Kataoka¹⁵⁵,
 A. Katre⁴⁹, J. Katzy⁴², K. Kawagoe⁷⁰, T. Kawamoto¹⁵⁵, G. Kawamura⁵⁴, S. Kazama¹⁵⁵,
 V.F. Kazanin^{109,c}, M.Y. Kazarinov⁶⁵, R. Keeler¹⁶⁹, R. Kehoe⁴⁰, J.S. Keller⁴², J.J. Kempster⁷⁷,
 H. Keoshkerian⁸⁴, O. Kepka¹²⁷, B.P. Kerševan⁷⁵, S. Kersten¹⁷⁵, R.A. Keyes⁸⁷, F. Khalil-zada¹¹,
 H. Khandanyan^{146a,146b}, A. Khanov¹¹⁴, A.G. Kharlamov^{109,c}, T.J. Khoo²⁸, V. Khovanskiy⁹⁷,
 E. Khramov⁶⁵, J. Khubua^{51b,t}, H.Y. Kim⁸, H. Kim^{146a,146b}, S.H. Kim¹⁶⁰, Y. Kim³¹, N. Kimura¹⁵⁴,
 O.M. Kind¹⁶, B.T. King⁷⁴, M. King¹⁶⁷, R.S.B. King¹²⁰, S.B. King¹⁶⁸, J. Kirk¹³¹, A.E. Kiryunin¹⁰¹,
 T. Kishimoto⁶⁷, D. Kisielewska^{38a}, F. Kiss⁴⁸, K. Kiuchi¹⁶⁰, O. Kivernyk¹³⁶, E. Kladiva^{144b},
 M.H. Klein³⁵, M. Klein⁷⁴, U. Klein⁷⁴, K. Kleinknecht⁸³, P. Klimek^{146a,146b}, A. Klimentov²⁵,
 R. Klingenberg⁴³, J.A. Klinger⁸⁴, T. Klioutchnikova³⁰, E.-E. Kluge^{58a}, P. Kluit¹⁰⁷, S. Kluth¹⁰¹,
 E. Kneringer⁶², E.B.F.G. Knoop⁸⁵, A. Knue⁵³, A. Kobayashi¹⁵⁵, D. Kobayashi¹⁵⁷, T. Kobayashi¹⁵⁵,
 M. Kobel⁴⁴, M. Kocian¹⁴³, P. Kodys¹²⁹, T. Koffas²⁹, E. Koffeman¹⁰⁷, L.A. Kogan¹²⁰, S. Kohlmann¹⁷⁵,
 Z. Kohout¹²⁸, T. Kohriki⁶⁶, T. Koi¹⁴³, H. Kolanoski¹⁶, I. Koletsou⁵, A.A. Komar^{96,*}, Y. Komori¹⁵⁵,
 T. Kondo⁶⁶, N. Kondrashova⁴², K. Köneke⁴⁸, A.C. König¹⁰⁶, S. König⁸³, T. Kono^{66,u}, R. Konoplich^{110,v},
 N. Konstantinidis⁷⁸, R. Kopeliansky¹⁵², S. Koperny^{38a}, L. Köpke⁸³, A.K. Kopp⁴⁸, K. Korcyl³⁹,
 K. Kordas¹⁵⁴, A. Korn⁷⁸, A.A. Korol^{109,c}, I. Korolkov¹², E.V. Korolkova¹³⁹, O. Kortner¹⁰¹, S. Kortner¹⁰¹,
 T. Kosek¹²⁹, V.V. Kostyukhin²¹, V.M. Kotov⁶⁵, A. Kotwal⁴⁵, A. Kourkoumeli-Charalampidi¹⁵⁴,
 C. Kourkoumelis⁹, V. Kouskoura²⁵, A. Koutsman^{159a}, R. Kowalewski¹⁶⁹, T.Z. Kowalski^{38a},
 W. Kozanecki¹³⁶, A.S. Kozhin¹³⁰, V.A. Kramarenko⁹⁹, G. Kramberger⁷⁵, D. Krasnopevtsev⁹⁸,
 M.W. Krasny⁸⁰, A. Krasznahorkay³⁰, J.K. Kraus²¹, A. Kravchenko²⁵, S. Kreiss¹¹⁰, M. Kretz^{58c},
 J. Kretzschmar⁷⁴, K. Kreutzfeldt⁵², P. Krieger¹⁵⁸, K. Krizka³¹, K. Kroeninger⁴³, H. Kroha¹⁰¹, J. Kroll¹²²,
 J. Kroseberg²¹, J. Krstic¹³, U. Kruchonak⁶⁵, H. Krüger²¹, N. Krumnack⁶⁴, Z.V. Krumshiteyn⁶⁵,
 A. Kruse¹⁷³, M.C. Kruse⁴⁵, M. Kruskal²², T. Kubota⁸⁸, H. Kucuk⁷⁸, S. Kuday^{4c}, S. Kuehn⁴⁸,
 A. Kugel^{58c}, F. Kuger¹⁷⁴, A. Kuhl¹³⁷, T. Kuhl⁴², V. Kukhtin⁶⁵, Y. Kulchitsky⁹², S. Kuleshov^{32b},
 M. Kuna^{132a,132b}, T. Kunigo⁶⁸, A. Kupco¹²⁷, H. Kurashige⁶⁷, Y.A. Kurochkin⁹², R. Kurumida⁶⁷,
 V. Kus¹²⁷, E.S. Kuwertz¹⁶⁹, M. Kuze¹⁵⁷, J. Kvita¹¹⁵, T. Kwan¹⁶⁹, D. Kyriazopoulos¹³⁹, A. La Rosa⁴⁹,
 J.L. La Rosa Navarro^{24d}, L. La Rotonda^{37a,37b}, C. Lacasta¹⁶⁷, F. Lacava^{132a,132b}, J. Lacey²⁹, H. Lacker¹⁶,
 D. Lacour⁸⁰, V.R. Lacuesta¹⁶⁷, E. Ladygin⁶⁵, R. Lafaye⁵, B. Laforge⁸⁰, T. Lagouri¹⁷⁶, S. Lai⁴⁸,
 L. Lambourne⁷⁸, S. Lammers⁶¹, C.L. Lampen⁷, W. Lampl⁷, E. Lançon¹³⁶, U. Landgraf⁴⁸,
 M.P.J. Landon⁷⁶, V.S. Lang^{58a}, J.C. Lange¹², A.J. Lankford¹⁶³, F. Lanni²⁵, K. Lantzsch³⁰, S. Laplace⁸⁰,
 C. Lapoire³⁰, J.F. Laporte¹³⁶, T. Lari^{91a}, F. Lasagni Manghi^{20a,20b}, M. Lassnig³⁰, P. Laurelli⁴⁷,
 W. Lavrijsen¹⁵, A.T. Law¹³⁷, P. Laycock⁷⁴, O. Le Dortz⁸⁰, E. Le Guirriec⁸⁵, E. Le Menedeu¹²,
 M. LeBlanc¹⁶⁹, T. LeCompte⁶, F. Ledroit-Guillon⁵⁵, C.A. Lee^{145b}, S.C. Lee¹⁵¹, L. Lee¹, G. Lefebvre⁸⁰,
 M. Lefebvre¹⁶⁹, F. Legger¹⁰⁰, C. Leggett¹⁵, A. Lehan⁷⁴, G. Lehmann Miotto³⁰, X. Lei⁷, W.A. Leight²⁹,
 A. Leisos^{154,w}, A.G. Leister¹⁷⁶, M.A.L. Leite^{24d}, R. Leitner¹²⁹, D. Lellouch¹⁷², B. Lemmer⁵⁴,
 K.J.C. Leney⁷⁸, T. Lenz²¹, B. Lenzi³⁰, R. Leone⁷, S. Leone^{124a,124b}, C. Leonidopoulos⁴⁶, S. Leontsinis¹⁰,
 C. Leroy⁹⁵, C.G. Lester²⁸, M. Levchenko¹²³, J. Levêque⁵, D. Levin⁸⁹, L.J. Levinson¹⁷², M. Levy¹⁸,
 A. Lewis¹²⁰, A.M. Leyko²¹, M. Leyton⁴¹, B. Li^{33b,x}, H. Li¹⁴⁸, H.L. Li³¹, L. Li⁴⁵, L. Li^{33e}, S. Li⁴⁵,

Y. Li^{33c,y}, Z. Liang¹³⁷, H. Liao³⁴, B. Liberti^{133a}, A. Liblong¹⁵⁸, P. Lichard³⁰, K. Lie¹⁶⁵, J. Liebal²¹,
 W. Liebig¹⁴, C. Limbach²¹, A. Limosani¹⁵⁰, S.C. Lin^{151,z}, T.H. Lin⁸³, F. Linde¹⁰⁷, B.E. Lindquist¹⁴⁸,
 J.T. Linnemann⁹⁰, E. Lipeles¹²², A. Lipniacka¹⁴, M. Lisovyi^{58b}, T.M. Liss¹⁶⁵, D. Lissauer²⁵,
 A. Lister¹⁶⁸, A.M. Litke¹³⁷, B. Liu^{151,aa}, D. Liu¹⁵¹, J. Liu⁸⁵, J.B. Liu^{33b}, K. Liu⁸⁵, L. Liu¹⁶⁵, M. Liu⁴⁵,
 M. Liu^{33b}, Y. Liu^{33b}, M. Livan^{121a,121b}, A. Lleres⁵⁵, J. Llorente Merino⁸², S.L. Lloyd⁷⁶, F. Lo Sterzo¹⁵¹,
 E. Lobodzinska⁴², P. Loch⁷, W.S. Lockman¹³⁷, F.K. Loebinger⁸⁴, A.E. Loevschall-Jensen³⁶,
 A. Loginov¹⁷⁶, T. Lohse¹⁶, K. Lohwasser⁴², M. Lokajicek¹²⁷, B.A. Long²², J.D. Long⁸⁹, R.E. Long⁷²,
 K.A. Looper¹¹¹, L. Lopes^{126a}, D. Lopez Mateos⁵⁷, B. Lopez Paredes¹³⁹, I. Lopez Paz¹², J. Lorenz¹⁰⁰,
 N. Lorenzo Martinez⁶¹, M. Losada¹⁶², P. Loscutoff¹⁵, P.J. Lösel¹⁰⁰, X. Lou^{33a}, A. Lounis¹¹⁷, J. Love⁶,
 P.A. Love⁷², N. Lu⁸⁹, H.J. Lubatti¹³⁸, C. Luci^{132a,132b}, A. Lucotte⁵⁵, F. Luehring⁶¹, W. Lukas⁶²,
 L. Luminari^{132a}, O. Lundberg^{146a,146b}, B. Lund-Jensen¹⁴⁷, D. Lynn²⁵, R. Lysak¹²⁷, E. Lytken⁸¹, H. Ma²⁵,
 L.L. Ma^{33d}, G. Maccarrone⁴⁷, A. Macchiolo¹⁰¹, C.M. Macdonald¹³⁹, J. Machado Miguens^{122,126b},
 D. Macina³⁰, D. Madaffari⁸⁵, R. Madar³⁴, H.J. Maddocks⁷², W.F. Mader⁴⁴, A. Madsen¹⁶⁶, S. Maeland¹⁴,
 T. Maeno²⁵, A. Maevskiy⁹⁹, E. Magradze⁵⁴, K. Mahboubi⁴⁸, J. Mahlstedt¹⁰⁷, C. Maiani¹³⁶,
 C. Maidantchik^{24a}, A.A. Maier¹⁰¹, T. Maier¹⁰⁰, A. Maio^{126a,126b,126d}, S. Majewski¹¹⁶, Y. Makida⁶⁶,
 N. Makovec¹¹⁷, B. Malaescu⁸⁰, Pa. Malecki³⁹, V.P. Maleev¹²³, F. Malek⁵⁵, U. Mallik⁶³, D. Malon⁶,
 C. Malone¹⁴³, S. Maltezos¹⁰, V.M. Malyshev¹⁰⁹, S. Malyukov³⁰, J. Mamuzic⁴², G. Mancini⁴⁷,
 B. Mandelli³⁰, L. Mandelli^{91a}, I. Mandić⁷⁵, R. Mandrysch⁶³, J. Maneira^{126a,126b}, A. Manfredini¹⁰¹,
 L. Manhaes de Andrade Filho^{24b}, J. Manjarres Ramos^{159b}, A. Mann¹⁰⁰, P.M. Manning¹³⁷,
 A. Manousakis-Katsikakis⁹, B. Mansoulie¹³⁶, R. Mantifel⁸⁷, M. Mantoani⁵⁴, L. Mapelli³⁰, L. March^{145c},
 G. Marchiori⁸⁰, M. Marcisovsky¹²⁷, C.P. Marino¹⁶⁹, M. Marjanovic¹³, F. Marroquim^{24a}, S.P. Marsden⁸⁴,
 Z. Marshall¹⁵, L.F. Marti¹⁷, S. Marti-Garcia¹⁶⁷, B. Martin⁹⁰, T.A. Martin¹⁷⁰, V.J. Martin⁴⁶,
 B. Martin dit Latour¹⁴, M. Martinez^{12,o}, S. Martin-Haugh¹³¹, V.S. Martoiu^{26a}, A.C. Martyniuk⁷⁸,
 M. Marx¹³⁸, F. Marzano^{132a}, A. Marzin³⁰, L. Masetti⁸³, T. Mashimo¹⁵⁵, R. Mashinistov⁹⁶, J. Masik⁸⁴,
 A.L. Maslennikov^{109,c}, I. Massa^{20a,20b}, L. Massa^{20a,20b}, N. Massol⁵, P. Mastrandrea¹⁴⁸,
 A. Mastroberardino^{37a,37b}, T. Masubuchi¹⁵⁵, P. Mättig¹⁷⁵, J. Mattmann⁸³, J. Maurer^{26a}, S.J. Maxfield⁷⁴,
 D.A. Maximov^{109,c}, R. Mazini¹⁵¹, S.M. Mazza^{91a,91b}, L. Mazzaferro^{133a,133b}, G. Mc Goldrick¹⁵⁸,
 S.P. Mc Kee⁸⁹, A. McCarn⁸⁹, R.L. McCarthy¹⁴⁸, T.G. McCarthy²⁹, N.A. McCubbin¹³¹,
 K.W. McFarlane^{56,*}, J.A. Mcfayden⁷⁸, G. Mchedlidze⁵⁴, S.J. McMahon¹³¹, R.A. McPherson^{169,k},
 M. Medinnis⁴², S. Meehan^{145a}, S. Mehlhase¹⁰⁰, A. Mehta⁷⁴, K. Meier^{58a}, C. Meineck¹⁰⁰, B. Meirose⁴¹,
 B.R. Mellado Garcia^{145c}, F. Meloni¹⁷, A. Mengarelli^{20a,20b}, S. Menke¹⁰¹, E. Meoni¹⁶¹, K.M. Mercurio⁵⁷,
 S. Mergelmeyer²¹, P. Mermod⁴⁹, L. Merola^{104a,104b}, C. Meroni^{91a}, F.S. Merritt³¹, A. Messina^{132a,132b},
 J. Metcalfe²⁵, A.S. Mete¹⁶³, C. Meyer⁸³, C. Meyer¹²², J-P. Meyer¹³⁶, J. Meyer¹⁰⁷, R.P. Middleton¹³¹,
 S. Miglioranzi^{164a,164c}, L. Mijović²¹, G. Mikenberg¹⁷², M. Mikestikova¹²⁷, M. Mikuž⁷⁵, M. Milesi⁸⁸,
 A. Milic³⁰, D.W. Miller³¹, C. Mills⁴⁶, A. Milov¹⁷², D.A. Milstead^{146a,146b}, A.A. Minaenko¹³⁰,
 Y. Minami¹⁵⁵, I.A. Minashvili⁶⁵, A.I. Mincer¹¹⁰, B. Mindur^{38a}, M. Mineev⁶⁵, Y. Ming¹⁷³, L.M. Mir¹²,
 T. Mitani¹⁷¹, J. Mitrevski¹⁰⁰, V.A. Mitsou¹⁶⁷, A. Miucci⁴⁹, P.S. Miyagawa¹³⁹, J.U. Mjörnmark⁸¹,
 T. Moa^{146a,146b}, K. Mochizuki⁸⁵, S. Mohapatra³⁵, W. Mohr⁴⁸, S. Molander^{146a,146b}, R. Moles-Valls¹⁶⁷,
 K. Mönig⁴², C. Monini⁵⁵, J. Monk³⁶, E. Monnier⁸⁵, J. Montejo Berlingen¹², F. Monticelli⁷¹,
 S. Monzani^{132a,132b}, R.W. Moore³, N. Morange¹¹⁷, D. Moreno¹⁶², M. Moreno Llácer⁵⁴, P. Morettini^{50a},
 M. Morgenstern⁴⁴, M. Morii⁵⁷, M. Morinaga¹⁵⁵, V. Morisbak¹¹⁹, S. Moritz⁸³, A.K. Morley¹⁴⁷,
 G. Mornacchi³⁰, J.D. Morris⁷⁶, S.S. Mortensen³⁶, A. Morton⁵³, L. Morvaj¹⁰³, M. Mosidze^{51b},
 J. Moss¹¹¹, K. Motohashi¹⁵⁷, R. Mount¹⁴³, E. Mountricha²⁵, S.V. Mouraviev^{96,*}, E.J.W. Moyse⁸⁶,
 S. Muanza⁸⁵, R.D. Mudd¹⁸, F. Mueller¹⁰¹, J. Mueller¹²⁵, K. Mueller²¹, R.S.P. Mueller¹⁰⁰, T. Mueller²⁸,
 D. Muenstermann⁴⁹, P. Mullen⁵³, Y. Munwes¹⁵³, J.A. Murillo Quijada¹⁸, W.J. Murray^{170,131},
 H. Musheghyan⁵⁴, E. Musto¹⁵², A.G. Myagkov^{130,ab}, M. Myska¹²⁸, O. Nackenhorst⁵⁴, J. Nadal⁵⁴,
 K. Nagai¹²⁰, R. Nagai¹⁵⁷, Y. Nagai⁸⁵, K. Nagano⁶⁶, A. Nagarkar¹¹¹, Y. Nagasaka⁵⁹, K. Nagata¹⁶⁰,

M. Nagel¹⁰¹, E. Nagy⁸⁵, A.M. Nairz³⁰, Y. Nakahama³⁰, K. Nakamura⁶⁶, T. Nakamura¹⁵⁵, I. Nakano¹¹²,
H. Namasivayam⁴¹, R.F. Naranjo Garcia⁴², R. Narayan³¹, T. Naumann⁴², G. Navarro¹⁶², R. Nayyar⁷,
H.A. Neal⁸⁹, P.Yu. Nechaeva⁹⁶, T.J. Neep⁸⁴, P.D. Nef¹⁴³, A. Negri^{121a,121b}, M. Negrini^{20a},
S. Nektarijevic¹⁰⁶, C. Nellist¹¹⁷, A. Nelson¹⁶³, S. Nemecek¹²⁷, P. Nemethy¹¹⁰, A.A. Nepomuceno^{24a},
M. Nessi^{30,ac}, M.S. Neubauer¹⁶⁵, M. Neumann¹⁷⁵, R.M. Neves¹¹⁰, P. Nevski²⁵, P.R. Newman¹⁸,
D.H. Nguyen⁶, R.B. Nickerson¹²⁰, R. Nicolaidou¹³⁶, B. Nicquevert³⁰, J. Nielsen¹³⁷, N. Nikiforou³⁵,
A. Nikiforov¹⁶, V. Nikolaenko^{130,ab}, I. Nikolic-Audit⁸⁰, K. Nikolopoulos¹⁸, J.K. Nilsen¹¹⁹, P. Nilsson²⁵,
Y. Ninomiya¹⁵⁵, A. Nisati^{132a}, R. Nisius¹⁰¹, T. Nobe¹⁵⁷, M. Nomachi¹¹⁸, I. Nomidis²⁹, T. Nooney⁷⁶,
S. Norberg¹¹³, M. Nordberg³⁰, O. Novgorodova⁴⁴, S. Nowak¹⁰¹, M. Nozaki⁶⁶, L. Nozka¹¹⁵, K. Ntekas¹⁰,
G. Nunes Hanninger⁸⁸, T. Nunnemann¹⁰⁰, E. Nurse⁷⁸, F. Nuti⁸⁸, B.J. O'Brien⁴⁶, F. O'grady⁷,
D.C. O'Neil¹⁴², V. O'Shea⁵³, F.G. Oakham^{29,d}, H. Oberlack¹⁰¹, T. Obermann²¹, J. Ocariz⁸⁰, A. Ochi⁶⁷,
I. Ochoa⁷⁸, J.P. Ochoa-Ricoux^{32a}, S. Oda⁷⁰, S. Odaka⁶⁶, H. Ogren⁶¹, A. Oh⁸⁴, S.H. Oh⁴⁵, C.C. Ohm¹⁵,
H. Ohman¹⁶⁶, H. Oide³⁰, W. Okamura¹¹⁸, H. Okawa¹⁶⁰, Y. Okumura³¹, T. Okuyama¹⁵⁵, A. Olariu^{26a},
S.A. Olivares Pino⁴⁶, D. Oliveira Damazio²⁵, E. Oliver Garcia¹⁶⁷, A. Olszewski³⁹, J. Olszowska³⁹,
A. Onofre^{126a,126e}, P.U.E. Onyisi^{31,q}, C.J. Oram^{159a}, M.J. Oreglia³¹, Y. Oren¹⁵³, D. Orestano^{134a,134b},
N. Orlando¹⁵⁴, C. Oropeza Barrera⁵³, R.S. Orr¹⁵⁸, B. Osculati^{50a,50b}, R. Ospanov⁸⁴,
G. Otero y Garzon²⁷, H. Otono⁷⁰, M. Ouchrif^{135d}, E.A. Ouellette¹⁶⁹, F. Ould-Saada¹¹⁹, A. Ouraou¹³⁶,
K.P. Oussoren¹⁰⁷, Q. Ouyang^{33a}, A. Ovcharova¹⁵, M. Owen⁵³, R.E. Owen¹⁸, V.E. Ozcan^{19a}, N. Ozturk⁸,
K. Pachal¹⁴², A. Pacheco Pages¹², C. Padilla Aranda¹², M. Pagáčová⁴⁸, S. Pagan Griso¹⁵, E. Paganis¹³⁹,
C. Pahl¹⁰¹, F. Paige²⁵, P. Pais⁸⁶, K. Pajchel¹¹⁹, G. Palacino^{159b}, S. Palestini³⁰, M. Palka^{38b}, D. Pallin³⁴,
A. Palma^{126a,126b}, Y.B. Pan¹⁷³, E. Panagiotopoulou¹⁰, C.E. Pandini⁸⁰, J.G. Panduro Vazquez⁷⁷,
P. Pani^{146a,146b}, S. Panitkin²⁵, D. Pantea^{26a}, L. Paolozzi⁴⁹, Th.D. Papadopoulou¹⁰, K. Papageorgiou¹⁵⁴,
A. Paramonov⁶, D. Paredes Hernandez¹⁵⁴, M.A. Parker²⁸, K.A. Parker¹³⁹, F. Parodi^{50a,50b},
J.A. Parsons³⁵, U. Parzefall⁴⁸, E. Pasqualucci^{132a}, S. Passaggio^{50a}, F. Pastore^{134a,134b,*}, Fr. Pastore⁷⁷,
G. Pásztor²⁹, S. Pataraja¹⁷⁵, N.D. Patel¹⁵⁰, J.R. Pater⁸⁴, T. Pauly³⁰, J. Pearce¹⁶⁹, B. Pearson¹¹³,
L.E. Pedersen³⁶, M. Pedersen¹¹⁹, S. Pedraza Lopez¹⁶⁷, R. Pedro^{126a,126b}, S.V. Peleganchuk^{109,c},
D. Pelikan¹⁶⁶, H. Peng^{33b}, B. Penning³¹, J. Penwell⁶¹, D.V. Perepelitsa²⁵, E. Perez Codina^{159a},
M.T. Pérez García-Estañ¹⁶⁷, L. Perini^{91a,91b}, H. Pernegger³⁰, S. Perrella^{104a,104b}, R. Peschke⁴²,
V.D. Peshekhonov⁶⁵, K. Peters³⁰, R.F.Y. Peters⁸⁴, B.A. Petersen³⁰, T.C. Petersen³⁶, E. Petit⁴²,
A. Petridis^{146a,146b}, C. Petridou¹⁵⁴, E. Petrolo^{132a}, F. Petrucci^{134a,134b}, N.E. Pettersson¹⁵⁷, R. Pezoa^{32b},
P.W. Phillips¹³¹, G. Piacquadio¹⁴³, E. Pianori¹⁷⁰, A. Picazio⁴⁹, E. Piccaro⁷⁶, M. Piccinini^{20a,20b},
M.A. Pickering¹²⁰, R. Piegaia²⁷, D.T. Pignotti¹¹¹, J.E. Pilcher³¹, A.D. Pilkington⁸⁴, J. Pina^{126a,126b,126d},
M. Pinamonti^{164a,164c,ad}, J.L. Pinfold³, A. Pingel³⁶, B. Pinto^{126a}, S. Pires⁸⁰, M. Pitt¹⁷², C. Pizio^{91a,91b},
L. Plazak^{144a}, M.-A. Pleier²⁵, V. Pleskot¹²⁹, E. Plotnikova⁶⁵, P. Plucinski^{146a,146b}, D. Pluth⁶⁴,
R. Poettgen⁸³, L. Poggioli¹¹⁷, D. Pohl²¹, G. Polesello^{121a}, A. Policicchio^{37a,37b}, R. Polifka¹⁵⁸,
A. Polini^{20a}, C.S. Pollard⁵³, V. Polychronakos²⁵, K. Pommès³⁰, L. Pontecorvo^{132a}, B.G. Pope⁹⁰,
G.A. Popeneciu^{26b}, D.S. Popovic¹³, A. Poppleton³⁰, S. Pospisil¹²⁸, K. Potamianos¹⁵, I.N. Potrap⁶⁵,
C.J. Potter¹⁴⁹, C.T. Potter¹¹⁶, G. Poulard³⁰, J. Poveda³⁰, V. Pozdnyakov⁶⁵, P. Pralavorio⁸⁵, A. Pranko¹⁵,
S. Prasad³⁰, S. Prell⁶⁴, D. Price⁸⁴, L.E. Price⁶, M. Primavera^{73a}, S. Prince⁸⁷, M. Proissl⁴⁶,
K. Prokofiev^{60c}, F. Prokoshin^{32b}, E. Protopapadaki¹³⁶, S. Protopopescu²⁵, J. Proudfoot⁶,
M. Przybycien^{38a}, E. Ptacek¹¹⁶, D. Puddu^{134a,134b}, E. Pueschel⁸⁶, D. Puldon¹⁴⁸, M. Purohit^{25,ae},
P. Puzo¹¹⁷, J. Qian⁸⁹, G. Qin⁵³, Y. Qin⁸⁴, A. Quadt⁵⁴, D.R. Quarrie¹⁵, W.B. Quayle^{164a,164b},
M. Queitsch-Maitland⁸⁴, D. Quilty⁵³, S. Raddum¹¹⁹, V. Radeka²⁵, V. Radescu⁴², S.K. Radhakrishnan¹⁴⁸,
P. Radloff¹¹⁶, P. Rados⁸⁸, F. Ragusa^{91a,91b}, G. Rahal¹⁷⁸, S. Rajagopalan²⁵, M. Rammensee³⁰,
C. Rangel-Smith¹⁶⁶, F. Rauscher¹⁰⁰, S. Rave⁸³, T. Ravenscroft⁵³, M. Raymond³⁰, A.L. Read¹¹⁹,
N.P. Readioff⁷⁴, D.M. Rebuffi^{121a,121b}, A. Redelbach¹⁷⁴, G. Redlinger²⁵, R. Reece¹³⁷, K. Reeves⁴¹,
L. Rehnisch¹⁶, H. Reisin²⁷, M. Relich¹⁶³, C. Rembser³⁰, H. Ren^{33a}, A. Renaud¹¹⁷, M. Rescigno^{132a},

S. Resconi^{91a}, O.L. Rezanova^{109,c}, P. Reznicek¹²⁹, R. Rezvani⁹⁵, R. Richter¹⁰¹, S. Richter⁷⁸,
 E. Richter-Was^{38b}, O. Ricken²¹, M. Ridel⁸⁰, P. Rieck¹⁶, C.J. Riegel¹⁷⁵, J. Rieger⁵⁴, M. Rijssenbeek¹⁴⁸,
 A. Rimoldi^{121a,121b}, L. Rinaldi^{20a}, B. Ristic⁴⁹, E. Ritsch⁶², I. Riu¹², F. Rizatdinova¹¹⁴, E. Rizvi⁷⁶,
 S.H. Robertson^{87,k}, A. Robichaud-Veronneau⁸⁷, D. Robinson²⁸, J.E.M. Robinson⁸⁴, A. Robson⁵³,
 C. Roda^{124a,124b}, S. Roe³⁰, O. Røhne¹¹⁹, S. Rolli¹⁶¹, A. Romaniouk⁹⁸, M. Romano^{20a,20b},
 S.M. Romano Saez³⁴, E. Romero Adam¹⁶⁷, N. Rompotis¹³⁸, M. Ronzani⁴⁸, L. Roos⁸⁰, E. Ros¹⁶⁷,
 S. Rosati^{132a}, K. Rosbach⁴⁸, P. Rose¹³⁷, P.L. Rosendahl¹⁴, O. Rosenthal¹⁴¹, V. Rossetti^{146a,146b},
 E. Rossi^{104a,104b}, L.P. Rossi^{50a}, R. Rosten¹³⁸, M. Rotaru^{26a}, I. Roth¹⁷², J. Rothberg¹³⁸, D. Rousseau¹¹⁷,
 C.R. Royon¹³⁶, A. Rozanov⁸⁵, Y. Rozen¹⁵², X. Ruan^{145c}, F. Rubbo¹⁴³, I. Rubinskiy⁴², V.I. Rud⁹⁹,
 C. Rudolph⁴⁴, M.S. Rudolph¹⁵⁸, F. Rühr⁴⁸, A. Ruiz-Martinez³⁰, Z. Rurikova⁴⁸, N.A. Rusakovich⁶⁵,
 A. Ruschke¹⁰⁰, H.L. Russell¹³⁸, J.P. Rutherford⁷, N. Ruthmann⁴⁸, Y.F. Ryabov¹²³, M. Rybar¹²⁹,
 G. Rybkin¹¹⁷, N.C. Ryder¹²⁰, A.F. Saavedra¹⁵⁰, G. Sabato¹⁰⁷, S. Sacerdoti²⁷, A. Saddique³,
 H.F.W. Sadrozinski¹³⁷, R. Sadykov⁶⁵, F. Safai Tehrani^{132a}, M. Saimpert¹³⁶, H. Sakamoto¹⁵⁵,
 Y. Sakurai¹⁷¹, G. Salamanna^{134a,134b}, A. Salamon^{133a}, M. Saleem¹¹³, D. Salek¹⁰⁷,
 P.H. Sales De Bruin¹³⁸, D. Salihagic¹⁰¹, A. Salnikov¹⁴³, J. Salt¹⁶⁷, D. Salvatore^{37a,37b}, F. Salvatore¹⁴⁹,
 A. Salvucci¹⁰⁶, A. Salzburger³⁰, D. Sampsonidis¹⁵⁴, A. Sanchez^{104a,104b}, J. Sánchez¹⁶⁷,
 V. Sanchez Martinez¹⁶⁷, H. Sandaker¹⁴, R.L. Sandbach⁷⁶, H.G. Sander⁸³, M.P. Sanders¹⁰⁰,
 M. Sandhoff¹⁷⁵, C. Sandoval¹⁶², R. Sandstroem¹⁰¹, D.P.C. Sankey¹³¹, M. Sannino^{50a,50b}, A. Sansoni⁴⁷,
 C. Santoni³⁴, R. Santonico^{133a,133b}, H. Santos^{126a}, I. Santoyo Castillo¹⁴⁹, K. Sapp¹²⁵, A. Saponov⁶⁵,
 J.G. Saraiva^{126a,126d}, B. Sarrazin²¹, O. Sasaki⁶⁶, Y. Sasaki¹⁵⁵, K. Sato¹⁶⁰, G. Sauvage^{5,*}, E. Sauvan⁵,
 G. Savage⁷⁷, P. Savard^{158,d}, C. Sawyer¹²⁰, L. Sawyer^{79,n}, J. Saxon³¹, C. Sbarra^{20a}, A. Sbrizzi^{20a,20b},
 T. Scanlon⁷⁸, D.A. Scannicchio¹⁶³, M. Scarcella¹⁵⁰, V. Scarfone^{37a,37b}, J. Schaarschmidt¹⁷²,
 P. Schacht¹⁰¹, D. Schaefer³⁰, R. Schaefer⁴², J. Schaeffer⁸³, S. Schaepe²¹, S. Schaezel^{58b}, U. Schäfer⁸³,
 A.C. Schaffer¹¹⁷, D. Schaile¹⁰⁰, R.D. Schamberger¹⁴⁸, V. Scharf^{58a}, V.A. Schegelsky¹²³, D. Scheirich¹²⁹,
 M. Schernau¹⁶³, C. Schiavi^{50a,50b}, C. Schillo⁴⁸, M. Schioppa^{37a,37b}, S. Schlenker³⁰, E. Schmidt⁴⁸,
 K. Schmieden³⁰, C. Schmitt⁸³, S. Schmitt^{58b}, S. Schmitt⁴², B. Schneider^{159a}, Y.J. Schnellbach⁷⁴,
 U. Schnoor⁴⁴, L. Schoeffel¹³⁶, A. Schoening^{58b}, B.D. Schoenrock⁹⁰, E. Schopf²¹,
 A.L.S. Schorlemmer⁵⁴, M. Schott⁸³, D. Schouten^{159a}, J. Schovancova⁸, S. Schramm¹⁵⁸, M. Schreyer¹⁷⁴,
 C. Schroeder⁸³, N. Schuh⁸³, M.J. Schultens²¹, H.-C. Schultz-Coulon^{58a}, H. Schulz¹⁶, M. Schumacher⁴⁸,
 B.A. Schumm¹³⁷, Ph. Schune¹³⁶, C. Schwanenberger⁸⁴, A. Schwartzman¹⁴³, T.A. Schwarz⁸⁹,
 Ph. Schwegler¹⁰¹, Ph. Schwemling¹³⁶, R. Schwiendorst⁹⁰, J. Schwindling¹³⁶, T. Schwindt²¹,
 M. Schwoerer⁵, F.G. Sciacca¹⁷, E. Scifo¹¹⁷, G. Sciolla²³, F. Scuri^{124a,124b}, F. Scutti²¹, J. Searcy⁸⁹,
 G. Sedov⁴², E. Sedykh¹²³, P. Seema²¹, S.C. Seidel¹⁰⁵, A. Seiden¹³⁷, F. Seifert¹²⁸, J.M. Seixas^{24a},
 G. Sekhniaidze^{104a}, K. Sekhon⁸⁹, S.J. Sekula⁴⁰, K.E. Selbach⁴⁶, D.M. Seliverstov^{123,*},
 N. Semprini-Cesari^{20a,20b}, C. Serfon³⁰, L. Serin¹¹⁷, L. Serkin^{164a,164b}, T. Serre⁸⁵, M. Sessa^{134a,134b},
 R. Seuster^{159a}, H. Severini¹¹³, T. Sfiligoi⁷⁵, F. Sforza¹⁰¹, A. Sfyrla³⁰, E. Shabalina⁵⁴, M. Shamim¹¹⁶,
 L.Y. Shan^{33a}, R. Shang¹⁶⁵, J.T. Shank²², M. Shapiro¹⁵, P.B. Shatalov⁹⁷, K. Shaw^{164a,164b}, S.M. Shaw⁸⁴,
 A. Shcherbakova^{146a,146b}, C.Y. Shehu¹⁴⁹, P. Sherwood⁷⁸, L. Shi^{151,af}, S. Shimizu⁶⁷, C.O. Shimmin¹⁶³,
 M. Shimojima¹⁰², M. Shiyakova⁶⁵, A. Shmeleva⁹⁶, D. Shoaleh Saadi⁹⁵, M.J. Shochet³¹, S. Shojai^{91a,91b},
 S. Shrestha¹¹¹, E. Shulga⁹⁸, M.A. Shupe⁷, S. Shushkevich⁴², P. Sicho¹²⁷, O. Sidiropoulou¹⁷⁴,
 D. Sidorov¹¹⁴, A. Sidoti^{20a,20b}, F. Siegert⁴⁴, Dj. Sijacki¹³, J. Silva^{126a,126d}, Y. Silver¹⁵³,
 S.B. Silverstein^{146a}, V. Simak¹²⁸, O. Simard⁵, Lj. Simic¹³, S. Simion¹¹⁷, E. Simioni⁸³, B. Simmons⁷⁸,
 D. Simon³⁴, R. Simoniello^{91a,91b}, P. Sinervo¹⁵⁸, N.B. Sinev¹¹⁶, G. Siragusa¹⁷⁴, A.N. Sisakyan^{65,*},
 S.Yu. Sivoklov⁹⁹, J. Sjölin^{146a,146b}, T.B. Sjursen¹⁴, M.B. Skinner⁷², H.P. Skottowe⁵⁷, P. Skubic¹¹³,
 M. Slater¹⁸, T. Slavicek¹²⁸, M. Slawinska¹⁰⁷, K. Sliwa¹⁶¹, V. Smakhtin¹⁷², B.H. Smart⁴⁶, L. Smestad¹⁴,
 S.Yu. Smirnov⁹⁸, Y. Smirnov⁹⁸, L.N. Smirnova^{99,ag}, O. Smirnova⁸¹, M.N.K. Smith³⁵, R.W. Smith³⁵,
 M. Smizanska⁷², K. Smolek¹²⁸, A.A. Snesev⁹⁶, G. Snidero⁷⁶, S. Snyder²⁵, R. Sobie^{169,k}, F. Socher⁴⁴,

A. Soffer¹⁵³, D.A. Soh^{151,af}, C.A. Solans³⁰, M. Solar¹²⁸, J. Solc¹²⁸, E. Yu. Soldatov⁹⁸, U. Soldevila¹⁶⁷,
 A.A. Solodkov¹³⁰, A. Soloshenko⁶⁵, O.V. Solovyanov¹³⁰, V. Solovyev¹²³, P. Sommer⁴⁸, H.Y. Song^{33b},
 N. Soni¹, A. Sood¹⁵, A. Sopczak¹²⁸, B. Sopko¹²⁸, V. Sopko¹²⁸, V. Sorin¹², D. Sosa^{58b}, M. Sosebee⁸,
 C.L. Sotiropoulou^{124a,124b}, R. Soualah^{164a,164c}, P. Soueid⁹⁵, A.M. Soukharev^{109,c}, D. South⁴²,
 B.C. Sowden⁷⁷, S. Spagnolo^{73a,73b}, M. Spalla^{124a,124b}, F. Spanò⁷⁷, W.R. Spearman⁵⁷, F. Spettel¹⁰¹,
 R. Spighi^{20a}, G. Spigo³⁰, L.A. Spiller⁸⁸, M. Spousta¹²⁹, T. Spreitzer¹⁵⁸, R.D. St. Denis^{53,*}, S. Staerz⁴⁴,
 J. Stahlman¹²², R. Stamen^{58a}, S. Stamm¹⁶, E. Stanecka³⁹, C. Stanescu^{134a}, M. Stanescu-Bellu⁴²,
 M.M. Stanitzki⁴², S. Stapnes¹¹⁹, E.A. Starchenko¹³⁰, J. Stark⁵⁵, P. Staroba¹²⁷, P. Starovoitov⁴²,
 R. Staszewski³⁹, P. Stavina^{144a,*}, P. Steinberg²⁵, B. Stelzer¹⁴², H.J. Stelzer³⁰, O. Stelzer-Chilton^{159a},
 H. Stenzel⁵², S. Stern¹⁰¹, G.A. Stewart⁵³, J.A. Stillings²¹, M.C. Stockton⁸⁷, M. Stoebe⁸⁷, G. Stoicea^{26a},
 P. Stolte⁵⁴, S. Stonjek¹⁰¹, A.R. Stradling⁸, A. Straessner⁴⁴, M.E. Stramaglia¹⁷, J. Strandberg¹⁴⁷,
 S. Strandberg^{146a,146b}, A. Strandlie¹¹⁹, E. Strauss¹⁴³, M. Strauss¹¹³, P. Strizenc^{144b}, R. Ströhmer¹⁷⁴,
 D.M. Strom¹¹⁶, R. Stroynowski⁴⁰, A. Strubig¹⁰⁶, S.A. Stucci¹⁷, B. Stugu¹⁴, N.A. Styles⁴², D. Su¹⁴³,
 J. Su¹²⁵, R. Subramaniam⁷⁹, A. Succurro¹², Y. Sugaya¹¹⁸, C. Suhr¹⁰⁸, M. Suk¹²⁸, V.V. Sulin⁹⁶,
 S. Sultansoy^{4d}, T. Sumida⁶⁸, S. Sun⁵⁷, X. Sun^{33a}, J.E. Sundermann⁴⁸, K. Suruliz¹⁴⁹, G. Susinno^{37a,37b},
 M.R. Sutton¹⁴⁹, S. Suzuki⁶⁶, Y. Suzuki⁶⁶, M. Svatos¹²⁷, S. Swedish¹⁶⁸, M. Swiatlowski¹⁴³, I. Sykora^{144a},
 T. Sykora¹²⁹, D. Ta⁹⁰, C. Taccini^{134a,134b}, K. Tackmann⁴², J. Taenzer¹⁵⁸, A. Taffard¹⁶³, R. Tafirout^{159a},
 N. Taiblum¹⁵³, H. Takai²⁵, R. Takashima⁶⁹, H. Takeda⁶⁷, T. Takeshita¹⁴⁰, Y. Takubo⁶⁶, M. Talby⁸⁵,
 A.A. Talyshev^{109,c}, J.Y.C. Tam¹⁷⁴, K.G. Tan⁸⁸, J. Tanaka¹⁵⁵, R. Tanaka¹¹⁷, S. Tanaka⁶⁶,
 B.B. Tannenwald¹¹¹, N. Tannoury²¹, S. Tapprogge⁸³, S. Tarem¹⁵², F. Tarrade²⁹, G.F. Tartarelli^{91a},
 P. Tas¹²⁹, M. Tasevsky¹²⁷, T. Tashiro⁶⁸, E. Tassi^{37a,37b}, A. Tavares Delgado^{126a,126b}, Y. Tayalati^{135d},
 F.E. Taylor⁹⁴, G.N. Taylor⁸⁸, W. Taylor^{159b}, F.A. Teischinger³⁰, M. Teixeira Dias Castanheira⁷⁶,
 P. Teixeira-Dias⁷⁷, K.K. Temming⁴⁸, H. Ten Kate³⁰, P.K. Teng¹⁵¹, J.J. Teoh¹¹⁸, F. Tepel¹⁷⁵, S. Terada⁶⁶,
 K. Terashi¹⁵⁵, J. Terron⁸², S. Terzo¹⁰¹, M. Testa⁴⁷, R.J. Teuscher^{158,k}, J. Therhaag²¹,
 T. Thevenaux-Pelzer³⁴, J.P. Thomas¹⁸, J. Thomas-Wilsker⁷⁷, E.N. Thompson³⁵, P.D. Thompson¹⁸,
 R.J. Thompson⁸⁴, A.S. Thompson⁵³, L.A. Thomsen¹⁷⁶, E. Thomson¹²², M. Thomson²⁸, R.P. Thun^{89,*},
 M.J. Tibbetts¹⁵, R.E. Ticse Torres⁸⁵, V.O. Tikhomirov^{96,ah}, Yu.A. Tikhonov^{109,c}, S. Timoshenko⁹⁸,
 E. Tiouchichine⁸⁵, P. Tipton¹⁷⁶, S. Tisserant⁸⁵, T. Todorov^{5,*}, S. Todorova-Nova¹²⁹, J. Tojo⁷⁰,
 S. Tokár^{144a}, K. Tokushuku⁶⁶, K. Tollefson⁹⁰, E. Tolley⁵⁷, L. Tomlinson⁸⁴, M. Tomoto¹⁰³,
 L. Tompkins^{143,ai}, K. Toms¹⁰⁵, E. Torrence¹¹⁶, H. Torres¹⁴², E. Torró Pastor¹⁶⁷, J. Toth^{85,aj},
 F. Touchard⁸⁵, D.R. Tovey¹³⁹, T. Trefzger¹⁷⁴, L. Tremblet³⁰, A. Tricoli³⁰, I.M. Trigger^{159a},
 S. Trincaz-Duvoid⁸⁰, M.F. Tripiana¹², W. Trischuk¹⁵⁸, B. Trocmé⁵⁵, C. Troncon^{91a},
 M. Trottier-McDonald¹⁵, M. Trovatelli^{134a,134b}, P. True⁹⁰, L. Truong^{164a,164c}, M. Trzebinski³⁹,
 A. Trzupek³⁹, C. Tsarouchas³⁰, J.C-L. Tseng¹²⁰, P.V. Tsiarehka⁹², D. Tsionou¹⁵⁴, G. Tsipolitis¹⁰,
 N. Tsirintanis⁹, S. Tsiskaridze¹², V. Tsiskaridze⁴⁸, E.G. Tskhadadze^{51a}, I.I. Tsukerman⁹⁷, V. Tsulaia¹⁵,
 S. Tsuno⁶⁶, D. Tsybychev¹⁴⁸, A. Tudorache^{26a}, V. Tudorache^{26a}, A.N. Tuna¹²², S.A. Tuppiti^{20a,20b},
 S. Turchikhin^{99,ag}, D. Turecek¹²⁸, R. Turra^{91a,91b}, A.J. Turvey⁴⁰, P.M. Tuts³⁵, A. Tykhonov⁴⁹,
 M. Tylmad^{146a,146b}, M. Tyndel¹³¹, I. Ueda¹⁵⁵, R. Ueno²⁹, M. Ughetto^{146a,146b}, M. Uglan¹⁴,
 M. Uhlenbrock²¹, F. Ukegawa¹⁶⁰, G. Unal³⁰, A. Undrus²⁵, G. Unel¹⁶³, F.C. Ungaro⁴⁸, Y. Unno⁶⁶,
 C. Unverdorben¹⁰⁰, J. Urban^{144b}, P. Urquijo⁸⁸, P. Urrejola⁸³, G. Usai⁸, A. Usanova⁶², L. Vacavant⁸⁵,
 V. Vacek¹²⁸, B. Vachon⁸⁷, C. Valderanis⁸³, N. Valencic¹⁰⁷, S. Valentini^{20a,20b}, A. Valero¹⁶⁷,
 L. Valery¹², S. Valkar¹²⁹, E. Valladolid Gallego¹⁶⁷, S. Vallecorsa⁴⁹, J.A. Valls Ferrer¹⁶⁷,
 W. Van Den Wollenberg¹⁰⁷, P.C. Van Der Deijl¹⁰⁷, R. van der Geer¹⁰⁷, H. van der Graaf¹⁰⁷,
 R. Van Der Leeuw¹⁰⁷, N. van Eldik¹⁵², P. van Gemmeren⁶, J. Van Nieuwkoop¹⁴², I. van Vulpen¹⁰⁷,
 M.C. van Woerden³⁰, M. Vanadia^{132a,132b}, W. Vandelli³⁰, R. Vanguri¹²², A. Vaniachine⁶, F. Vannucci⁸⁰,
 G. Vardanyan¹⁷⁷, R. Vari^{132a}, E.W. Varnes⁷, T. Varol⁴⁰, D. Varouchas⁸⁰, A. Vartapetian⁸, K.E. Varvell¹⁵⁰,
 F. Vazeille³⁴, T. Vazquez Schroeder⁸⁷, J. Veatch⁷, L.M. Veloce¹⁵⁸, F. Veloso^{126a,126c}, T. Velz²¹,

S. Veneziano^{132a}, A. Ventura^{73a,73b}, D. Ventura⁸⁶, M. Venturi¹⁶⁹, N. Venturi¹⁵⁸, A. Venturini²³, V. Vercesi^{121a}, M. Verducci^{132a,132b}, W. Verkerke¹⁰⁷, J.C. Vermeulen¹⁰⁷, A. Vest⁴⁴, M.C. Vetterli^{142,d}, O. Viazlo⁸¹, I. Vichou¹⁶⁵, T. Vickey¹³⁹, O.E. Vickey Boeriu¹³⁹, G.H.A. Viehhauser¹²⁰, S. Viel¹⁵, R. Vigne³⁰, M. Villa^{20a,20b}, M. Villaplana Perez^{91a,91b}, E. Vilucchi⁴⁷, M.G. Vinciter²⁹, V.B. Vinogradov⁶⁵, I. Vivarelli¹⁴⁹, F. Vives Vaque³, S. Vlachos¹⁰, D. Vladioiu¹⁰⁰, M. Vlasak¹²⁸, M. Vogel^{32a}, P. Vokac¹²⁸, G. Volpi^{124a,124b}, M. Volpi⁸⁸, H. von der Schmitt¹⁰¹, H. von Radziewski⁴⁸, E. von Toerne²¹, V. Vorobel¹²⁹, K. Vorobev⁹⁸, M. Vos¹⁶⁷, R. Voss³⁰, J.H. Vossebeld⁷⁴, N. Vranjes¹³, M. Vranjes Milosavljevic¹³, V. Vrba¹²⁷, M. Vreeswijk¹⁰⁷, R. Vuillermet³⁰, I. Vukotic³¹, Z. Vykydal¹²⁸, P. Wagner²¹, W. Wagner¹⁷⁵, H. Wahlberg⁷¹, S. Wahrmund⁴⁴, J. Wakabayashi¹⁰³, J. Walder⁷², R. Walker¹⁰⁰, W. Walkowiak¹⁴¹, C. Wang^{33c}, F. Wang¹⁷³, H. Wang¹⁵, H. Wang⁴⁰, J. Wang⁴², J. Wang^{33a}, K. Wang⁸⁷, R. Wang⁶, S.M. Wang¹⁵¹, T. Wang²¹, X. Wang¹⁷⁶, C. Wanotayaroj¹¹⁶, A. Warburton⁸⁷, C.P. Ward²⁸, D.R. Wardrope⁷⁸, M. Warsinsky⁴⁸, A. Washbrook⁴⁶, C. Wasicki⁴², P.M. Watkins¹⁸, A.T. Watson¹⁸, I.J. Watson¹⁵⁰, M.F. Watson¹⁸, G. Watts¹³⁸, S. Watts⁸⁴, B.M. Waugh⁷⁸, S. Webb⁸⁴, M.S. Weber¹⁷, S.W. Weber¹⁷⁴, J.S. Webster³¹, A.R. Weidberg¹²⁰, B. Weinert⁶¹, J. Weingarten⁵⁴, C. Weiser⁴⁸, H. Weits¹⁰⁷, P.S. Wells³⁰, T. Wenaus²⁵, T. Wengler³⁰, S. Wenig³⁰, N. Wermes²¹, M. Werner⁴⁸, P. Werner³⁰, M. Wessels^{58a}, J. Wetter¹⁶¹, K. Whalen²⁹, A.M. Wharton⁷², A. White⁸, M.J. White¹, R. White^{32b}, S. White^{124a,124b}, D. Whiteson¹⁶³, F.J. Wickens¹³¹, W. Wiedenmann¹⁷³, M. Wielers¹³¹, P. Wienemann²¹, C. Wiglesworth³⁶, L.A.M. Wiik-Fuchs²¹, A. Wildauer¹⁰¹, H.G. Wilkens³⁰, H.H. Williams¹²², S. Williams¹⁰⁷, C. Willis⁹⁰, S. Willocq⁸⁶, A. Wilson⁸⁹, J.A. Wilson¹⁸, I. Wingerter-Seez⁵, F. Winklmeier¹¹⁶, B.T. Winter²¹, M. Wittgen¹⁴³, J. Wittkowski¹⁰⁰, S.J. Wollstadt⁸³, M.W. Wolter³⁹, H. Wolters^{126a,126c}, B.K. Wosiek³⁹, J. Wotschack³⁰, M.J. Woudstra⁸⁴, K.W. Wozniak³⁹, M. Wu⁵⁵, M. Wu³¹, S.L. Wu¹⁷³, X. Wu⁴⁹, Y. Wu⁸⁹, T.R. Wyatt⁸⁴, B.M. Wynne⁴⁶, S. Xella³⁶, D. Xu^{33a}, L. Xu^{33b,ak}, B. Yabsley¹⁵⁰, S. Yacoub^{145b,al}, R. Yakabe⁶⁷, M. Yamada⁶⁶, Y. Yamaguchi¹¹⁸, A. Yamamoto⁶⁶, S. Yamamoto¹⁵⁵, T. Yamanaka¹⁵⁵, K. Yamauchi¹⁰³, Y. Yamazaki⁶⁷, Z. Yan²², H. Yang^{33e}, H. Yang¹⁷³, Y. Yang¹⁵¹, L. Yao^{33a}, W-M. Yao¹⁵, Y. Yasu⁶⁶, E. Yatsenko⁵, K.H. Yau Wong²¹, J. Ye⁴⁰, S. Ye²⁵, I. Yeletsikh⁶⁵, A.L. Yen⁵⁷, E. Yildirim⁴², K. Yorita¹⁷¹, R. Yoshida⁶, K. Yoshihara¹²², C. Young¹⁴³, C.J.S. Young³⁰, S. Youssef²², D.R. Yu¹⁵, J. Yu⁸, J.M. Yu⁸⁹, J. Yu¹¹⁴, L. Yuan⁶⁷, A. Yurkewicz¹⁰⁸, I. Yusuff^{28,am}, B. Zabinski³⁹, R. Zaidan⁶³, A.M. Zaitsev^{130,ab}, J. Zalieckas¹⁴, A. Zaman¹⁴⁸, S. Zambito⁵⁷, L. Zanello^{132a,132b}, D. Zanzi⁸⁸, C. Zeitnitz¹⁷⁵, M. Zeman¹²⁸, A. Zemla^{38a}, K. Zengel²³, O. Zenin¹³⁰, T. Ženiš^{144a}, D. Zerwas¹¹⁷, D. Zhang⁸⁹, F. Zhang¹⁷³, J. Zhang⁶, L. Zhang⁴⁸, R. Zhang^{33b}, X. Zhang^{33d}, Z. Zhang¹¹⁷, X. Zhao⁴⁰, Y. Zhao^{33d,117}, Z. Zhao^{33b}, A. Zhemchugov⁶⁵, J. Zhong¹²⁰, B. Zhou⁸⁹, C. Zhou⁴⁵, L. Zhou³⁵, L. Zhou⁴⁰, N. Zhou¹⁶³, C.G. Zhu^{33d}, H. Zhu^{33a}, J. Zhu⁸⁹, Y. Zhu^{33b}, X. Zhuang^{33a}, K. Zhukov⁹⁶, A. Zibell¹⁷⁴, D. Zieminska⁶¹, N.I. Zimine⁶⁵, C. Zimmermann⁸³, S. Zimmermann⁴⁸, Z. Zinonos⁵⁴, M. Zinser⁸³, M. Ziolkowski¹⁴¹, L. Živković¹³, G. Zobernig¹⁷³, A. Zoccoli^{20a,20b}, M. zur Nedden¹⁶, G. Zurzolo^{104a,104b}, L. Zwalinski³⁰.

¹ Department of Physics, University of Adelaide, Adelaide, Australia

² Physics Department, SUNY Albany, Albany NY, United States of America

³ Department of Physics, University of Alberta, Edmonton AB, Canada

⁴ (a) Department of Physics, Ankara University, Ankara; (c) Istanbul Aydin University, Istanbul; (d)

Division of Physics, TOBB University of Economics and Technology, Ankara, Turkey

⁵ LAPP, CNRS/IN2P3 and Université Savoie Mont Blanc, Annecy-le-Vieux, France

⁶ High Energy Physics Division, Argonne National Laboratory, Argonne IL, United States of America

⁷ Department of Physics, University of Arizona, Tucson AZ, United States of America

⁸ Department of Physics, The University of Texas at Arlington, Arlington TX, United States of America

⁹ Physics Department, University of Athens, Athens, Greece

¹⁰ Physics Department, National Technical University of Athens, Zografou, Greece

- ¹¹ Institute of Physics, Azerbaijan Academy of Sciences, Baku, Azerbaijan
- ¹² Institut de Física d'Altes Energies and Departament de Física de la Universitat Autònoma de Barcelona, Barcelona, Spain
- ¹³ Institute of Physics, University of Belgrade, Belgrade, Serbia
- ¹⁴ Department for Physics and Technology, University of Bergen, Bergen, Norway
- ¹⁵ Physics Division, Lawrence Berkeley National Laboratory and University of California, Berkeley CA, United States of America
- ¹⁶ Department of Physics, Humboldt University, Berlin, Germany
- ¹⁷ Albert Einstein Center for Fundamental Physics and Laboratory for High Energy Physics, University of Bern, Bern, Switzerland
- ¹⁸ School of Physics and Astronomy, University of Birmingham, Birmingham, United Kingdom
- ¹⁹ ^(a) Department of Physics, Bogazici University, Istanbul; ^(b) Department of Physics, Dogus University, Istanbul; ^(c) Department of Physics Engineering, Gaziantep University, Gaziantep, Turkey
- ²⁰ ^(a) INFN Sezione di Bologna; ^(b) Dipartimento di Fisica e Astronomia, Università di Bologna, Bologna, Italy
- ²¹ Physikalisches Institut, University of Bonn, Bonn, Germany
- ²² Department of Physics, Boston University, Boston MA, United States of America
- ²³ Department of Physics, Brandeis University, Waltham MA, United States of America
- ²⁴ ^(a) Universidade Federal do Rio De Janeiro COPPE/EE/IF, Rio de Janeiro; ^(b) Electrical Circuits Department, Federal University of Juiz de Fora (UFJF), Juiz de Fora; ^(c) Federal University of Sao Joao del Rei (UFSJ), Sao Joao del Rei; ^(d) Instituto de Fisica, Universidade de Sao Paulo, Sao Paulo, Brazil
- ²⁵ Physics Department, Brookhaven National Laboratory, Upton NY, United States of America
- ²⁶ ^(a) National Institute of Physics and Nuclear Engineering, Bucharest; ^(b) National Institute for Research and Development of Isotopic and Molecular Technologies, Physics Department, Cluj Napoca; ^(c) University Politehnica Bucharest, Bucharest; ^(d) West University in Timisoara, Timisoara, Romania
- ²⁷ Departamento de Física, Universidad de Buenos Aires, Buenos Aires, Argentina
- ²⁸ Cavendish Laboratory, University of Cambridge, Cambridge, United Kingdom
- ²⁹ Department of Physics, Carleton University, Ottawa ON, Canada
- ³⁰ CERN, Geneva, Switzerland
- ³¹ Enrico Fermi Institute, University of Chicago, Chicago IL, United States of America
- ³² ^(a) Departamento de Física, Pontificia Universidad Católica de Chile, Santiago; ^(b) Departamento de Física, Universidad Técnica Federico Santa María, Valparaíso, Chile
- ³³ ^(a) Institute of High Energy Physics, Chinese Academy of Sciences, Beijing; ^(b) Department of Modern Physics, University of Science and Technology of China, Anhui; ^(c) Department of Physics, Nanjing University, Jiangsu; ^(d) School of Physics, Shandong University, Shandong; ^(e) Department of Physics and Astronomy, Shanghai Key Laboratory for Particle Physics and Cosmology, Shanghai Jiao Tong University, Shanghai; ^(f) Physics Department, Tsinghua University, Beijing 100084, China
- ³⁴ Laboratoire de Physique Corpusculaire, Clermont Université and Université Blaise Pascal and CNRS/IN2P3, Clermont-Ferrand, France
- ³⁵ Nevis Laboratory, Columbia University, Irvington NY, United States of America
- ³⁶ Niels Bohr Institute, University of Copenhagen, Kobenhavn, Denmark
- ³⁷ ^(a) INFN Gruppo Collegato di Cosenza, Laboratori Nazionali di Frascati; ^(b) Dipartimento di Fisica, Università della Calabria, Rende, Italy
- ³⁸ ^(a) AGH University of Science and Technology, Faculty of Physics and Applied Computer Science, Krakow; ^(b) Marian Smoluchowski Institute of Physics, Jagiellonian University, Krakow, Poland
- ³⁹ Institute of Nuclear Physics Polish Academy of Sciences, Krakow, Poland
- ⁴⁰ Physics Department, Southern Methodist University, Dallas TX, United States of America

41 Physics Department, University of Texas at Dallas, Richardson TX, United States of America
42 DESY, Hamburg and Zeuthen, Germany
43 Institut für Experimentelle Physik IV, Technische Universität Dortmund, Dortmund, Germany
44 Institut für Kern- und Teilchenphysik, Technische Universität Dresden, Dresden, Germany
45 Department of Physics, Duke University, Durham NC, United States of America
46 SUPA - School of Physics and Astronomy, University of Edinburgh, Edinburgh, United Kingdom
47 INFN Laboratori Nazionali di Frascati, Frascati, Italy
48 Fakultät für Mathematik und Physik, Albert-Ludwigs-Universität, Freiburg, Germany
49 Section de Physique, Université de Genève, Geneva, Switzerland
50 ^(a) INFN Sezione di Genova; ^(b) Dipartimento di Fisica, Università di Genova, Genova, Italy
51 ^(a) E. Andronikashvili Institute of Physics, Iv. Javakhishvili Tbilisi State University, Tbilisi; ^(b) High Energy Physics Institute, Tbilisi State University, Tbilisi, Georgia
52 II Physikalisches Institut, Justus-Liebig-Universität Giessen, Giessen, Germany
53 SUPA - School of Physics and Astronomy, University of Glasgow, Glasgow, United Kingdom
54 II Physikalisches Institut, Georg-August-Universität, Göttingen, Germany
55 Laboratoire de Physique Subatomique et de Cosmologie, Université Grenoble-Alpes, CNRS/IN2P3, Grenoble, France
56 Department of Physics, Hampton University, Hampton VA, United States of America
57 Laboratory for Particle Physics and Cosmology, Harvard University, Cambridge MA, United States of America
58 ^(a) Kirchhoff-Institut für Physik, Ruprecht-Karls-Universität Heidelberg, Heidelberg; ^(b) Physikalisches Institut, Ruprecht-Karls-Universität Heidelberg, Heidelberg; ^(c) ZITI Institut für technische Informatik, Ruprecht-Karls-Universität Heidelberg, Mannheim, Germany
59 Faculty of Applied Information Science, Hiroshima Institute of Technology, Hiroshima, Japan
60 ^(a) Department of Physics, The Chinese University of Hong Kong, Shatin, N.T., Hong Kong; ^(b) Department of Physics, The University of Hong Kong, Hong Kong; ^(c) Department of Physics, The Hong Kong University of Science and Technology, Clear Water Bay, Kowloon, Hong Kong, China
61 Department of Physics, Indiana University, Bloomington IN, United States of America
62 Institut für Astro- und Teilchenphysik, Leopold-Franzens-Universität, Innsbruck, Austria
63 University of Iowa, Iowa City IA, United States of America
64 Department of Physics and Astronomy, Iowa State University, Ames IA, United States of America
65 Joint Institute for Nuclear Research, JINR Dubna, Dubna, Russia
66 KEK, High Energy Accelerator Research Organization, Tsukuba, Japan
67 Graduate School of Science, Kobe University, Kobe, Japan
68 Faculty of Science, Kyoto University, Kyoto, Japan
69 Kyoto University of Education, Kyoto, Japan
70 Department of Physics, Kyushu University, Fukuoka, Japan
71 Instituto de Física La Plata, Universidad Nacional de La Plata and CONICET, La Plata, Argentina
72 Physics Department, Lancaster University, Lancaster, United Kingdom
73 ^(a) INFN Sezione di Lecce; ^(b) Dipartimento di Matematica e Fisica, Università del Salento, Lecce, Italy
74 Oliver Lodge Laboratory, University of Liverpool, Liverpool, United Kingdom
75 Department of Physics, Jožef Stefan Institute and University of Ljubljana, Ljubljana, Slovenia
76 School of Physics and Astronomy, Queen Mary University of London, London, United Kingdom
77 Department of Physics, Royal Holloway University of London, Surrey, United Kingdom
78 Department of Physics and Astronomy, University College London, London, United Kingdom
79 Louisiana Tech University, Ruston LA, United States of America

- ⁸⁰ Laboratoire de Physique Nucléaire et de Hautes Energies, UPMC and Université Paris-Diderot and CNRS/IN2P3, Paris, France
- ⁸¹ Fysiska institutionen, Lunds universitet, Lund, Sweden
- ⁸² Departamento de Física Teórica C-15, Universidad Autónoma de Madrid, Madrid, Spain
- ⁸³ Institut für Physik, Universität Mainz, Mainz, Germany
- ⁸⁴ School of Physics and Astronomy, University of Manchester, Manchester, United Kingdom
- ⁸⁵ CPPM, Aix-Marseille Université and CNRS/IN2P3, Marseille, France
- ⁸⁶ Department of Physics, University of Massachusetts, Amherst MA, United States of America
- ⁸⁷ Department of Physics, McGill University, Montreal QC, Canada
- ⁸⁸ School of Physics, University of Melbourne, Victoria, Australia
- ⁸⁹ Department of Physics, The University of Michigan, Ann Arbor MI, United States of America
- ⁹⁰ Department of Physics and Astronomy, Michigan State University, East Lansing MI, United States of America
- ⁹¹ ^(a) INFN Sezione di Milano; ^(b) Dipartimento di Fisica, Università di Milano, Milano, Italy
- ⁹² B.I. Stepanov Institute of Physics, National Academy of Sciences of Belarus, Minsk, Republic of Belarus
- ⁹³ National Scientific and Educational Centre for Particle and High Energy Physics, Minsk, Republic of Belarus
- ⁹⁴ Department of Physics, Massachusetts Institute of Technology, Cambridge MA, United States of America
- ⁹⁵ Group of Particle Physics, University of Montreal, Montreal QC, Canada
- ⁹⁶ P.N. Lebedev Institute of Physics, Academy of Sciences, Moscow, Russia
- ⁹⁷ Institute for Theoretical and Experimental Physics (ITEP), Moscow, Russia
- ⁹⁸ National Research Nuclear University MEPhI, Moscow, Russia
- ⁹⁹ D.V. Skobeltsyn Institute of Nuclear Physics, M.V. Lomonosov Moscow State University, Moscow, Russia
- ¹⁰⁰ Fakultät für Physik, Ludwig-Maximilians-Universität München, München, Germany
- ¹⁰¹ Max-Planck-Institut für Physik (Werner-Heisenberg-Institut), München, Germany
- ¹⁰² Nagasaki Institute of Applied Science, Nagasaki, Japan
- ¹⁰³ Graduate School of Science and Kobayashi-Maskawa Institute, Nagoya University, Nagoya, Japan
- ¹⁰⁴ ^(a) INFN Sezione di Napoli; ^(b) Dipartimento di Fisica, Università di Napoli, Napoli, Italy
- ¹⁰⁵ Department of Physics and Astronomy, University of New Mexico, Albuquerque NM, United States of America
- ¹⁰⁶ Institute for Mathematics, Astrophysics and Particle Physics, Radboud University Nijmegen/Nikhef, Nijmegen, Netherlands
- ¹⁰⁷ Nikhef National Institute for Subatomic Physics and University of Amsterdam, Amsterdam, Netherlands
- ¹⁰⁸ Department of Physics, Northern Illinois University, DeKalb IL, United States of America
- ¹⁰⁹ Budker Institute of Nuclear Physics, SB RAS, Novosibirsk, Russia
- ¹¹⁰ Department of Physics, New York University, New York NY, United States of America
- ¹¹¹ Ohio State University, Columbus OH, United States of America
- ¹¹² Faculty of Science, Okayama University, Okayama, Japan
- ¹¹³ Homer L. Dodge Department of Physics and Astronomy, University of Oklahoma, Norman OK, United States of America
- ¹¹⁴ Department of Physics, Oklahoma State University, Stillwater OK, United States of America
- ¹¹⁵ Palacký University, RCPTM, Olomouc, Czech Republic
- ¹¹⁶ Center for High Energy Physics, University of Oregon, Eugene OR, United States of America

- 117 LAL, Université Paris-Sud and CNRS/IN2P3, Orsay, France
- 118 Graduate School of Science, Osaka University, Osaka, Japan
- 119 Department of Physics, University of Oslo, Oslo, Norway
- 120 Department of Physics, Oxford University, Oxford, United Kingdom
- 121 ^(a) INFN Sezione di Pavia; ^(b) Dipartimento di Fisica, Università di Pavia, Pavia, Italy
- 122 Department of Physics, University of Pennsylvania, Philadelphia PA, United States of America
- 123 National Research Centre "Kurchatov Institute" B.P.Konstantinov Petersburg Nuclear Physics Institute, St. Petersburg, Russia
- 124 ^(a) INFN Sezione di Pisa; ^(b) Dipartimento di Fisica E. Fermi, Università di Pisa, Pisa, Italy
- 125 Department of Physics and Astronomy, University of Pittsburgh, Pittsburgh PA, United States of America
- 126 ^(a) Laboratório de Instrumentação e Física Experimental de Partículas - LIP, Lisboa; ^(b) Faculdade de Ciências, Universidade de Lisboa, Lisboa; ^(c) Department of Physics, University of Coimbra, Coimbra; ^(d) Centro de Física Nuclear da Universidade de Lisboa, Lisboa; ^(e) Departamento de Física, Universidade do Minho, Braga; ^(f) Departamento de Física Teórica y del Cosmos and CAFPE, Universidad de Granada, Granada (Spain); ^(g) Dep Física and CEFITEC of Faculdade de Ciências e Tecnologia, Universidade Nova de Lisboa, Caparica, Portugal
- 127 Institute of Physics, Academy of Sciences of the Czech Republic, Praha, Czech Republic
- 128 Czech Technical University in Prague, Praha, Czech Republic
- 129 Faculty of Mathematics and Physics, Charles University in Prague, Praha, Czech Republic
- 130 State Research Center Institute for High Energy Physics, Protvino, Russia
- 131 Particle Physics Department, Rutherford Appleton Laboratory, Didcot, United Kingdom
- 132 ^(a) INFN Sezione di Roma; ^(b) Dipartimento di Fisica, Sapienza Università di Roma, Roma, Italy
- 133 ^(a) INFN Sezione di Roma Tor Vergata; ^(b) Dipartimento di Fisica, Università di Roma Tor Vergata, Roma, Italy
- 134 ^(a) INFN Sezione di Roma Tre; ^(b) Dipartimento di Matematica e Fisica, Università Roma Tre, Roma, Italy
- 135 ^(a) Faculté des Sciences Ain Chock, Réseau Universitaire de Physique des Hautes Energies - Université Hassan II, Casablanca; ^(b) Centre National de l'Énergie des Sciences Techniques Nucleaires, Rabat; ^(c) Faculté des Sciences Semlalia, Université Cadi Ayyad, LPHEA-Marrakech; ^(d) Faculté des Sciences, Université Mohamed Premier and LPTPM, Oujda; ^(e) Faculté des sciences, Université Mohammed V-Agdal, Rabat, Morocco
- 136 DSM/IRFU (Institut de Recherches sur les Lois Fondamentales de l'Univers), CEA Saclay (Commissariat à l'Énergie Atomique et aux Énergies Alternatives), Gif-sur-Yvette, France
- 137 Santa Cruz Institute for Particle Physics, University of California Santa Cruz, Santa Cruz CA, United States of America
- 138 Department of Physics, University of Washington, Seattle WA, United States of America
- 139 Department of Physics and Astronomy, University of Sheffield, Sheffield, United Kingdom
- 140 Department of Physics, Shinshu University, Nagano, Japan
- 141 Fachbereich Physik, Universität Siegen, Siegen, Germany
- 142 Department of Physics, Simon Fraser University, Burnaby BC, Canada
- 143 SLAC National Accelerator Laboratory, Stanford CA, United States of America
- 144 ^(a) Faculty of Mathematics, Physics & Informatics, Comenius University, Bratislava; ^(b) Department of Subnuclear Physics, Institute of Experimental Physics of the Slovak Academy of Sciences, Kosice, Slovak Republic
- 145 ^(a) Department of Physics, University of Cape Town, Cape Town; ^(b) Department of Physics, University of Johannesburg, Johannesburg; ^(c) School of Physics, University of the Witwatersrand,

Johannesburg, South Africa

¹⁴⁶ ^(a) Department of Physics, Stockholm University; ^(b) The Oskar Klein Centre, Stockholm, Sweden

¹⁴⁷ Physics Department, Royal Institute of Technology, Stockholm, Sweden

¹⁴⁸ Departments of Physics & Astronomy and Chemistry, Stony Brook University, Stony Brook NY, United States of America

¹⁴⁹ Department of Physics and Astronomy, University of Sussex, Brighton, United Kingdom

¹⁵⁰ School of Physics, University of Sydney, Sydney, Australia

¹⁵¹ Institute of Physics, Academia Sinica, Taipei, Taiwan

¹⁵² Department of Physics, Technion: Israel Institute of Technology, Haifa, Israel

¹⁵³ Raymond and Beverly Sackler School of Physics and Astronomy, Tel Aviv University, Tel Aviv, Israel

¹⁵⁴ Department of Physics, Aristotle University of Thessaloniki, Thessaloniki, Greece

¹⁵⁵ International Center for Elementary Particle Physics and Department of Physics, The University of Tokyo, Tokyo, Japan

¹⁵⁶ Graduate School of Science and Technology, Tokyo Metropolitan University, Tokyo, Japan

¹⁵⁷ Department of Physics, Tokyo Institute of Technology, Tokyo, Japan

¹⁵⁸ Department of Physics, University of Toronto, Toronto ON, Canada

¹⁵⁹ ^(a) TRIUMF, Vancouver BC; ^(b) Department of Physics and Astronomy, York University, Toronto ON, Canada

¹⁶⁰ Faculty of Pure and Applied Sciences, University of Tsukuba, Tsukuba, Japan

¹⁶¹ Department of Physics and Astronomy, Tufts University, Medford MA, United States of America

¹⁶² Centro de Investigaciones, Universidad Antonio Narino, Bogota, Colombia

¹⁶³ Department of Physics and Astronomy, University of California Irvine, Irvine CA, United States of America

¹⁶⁴ ^(a) INFN Gruppo Collegato di Udine, Sezione di Trieste, Udine; ^(b) ICTP, Trieste; ^(c) Dipartimento di Chimica, Fisica e Ambiente, Università di Udine, Udine, Italy

¹⁶⁵ Department of Physics, University of Illinois, Urbana IL, United States of America

¹⁶⁶ Department of Physics and Astronomy, University of Uppsala, Uppsala, Sweden

¹⁶⁷ Instituto de Física Corpuscular (IFIC) and Departamento de Física Atómica, Molecular y Nuclear and Departamento de Ingeniería Electrónica and Instituto de Microelectrónica de Barcelona (IMB-CNM), University of Valencia and CSIC, Valencia, Spain

¹⁶⁸ Department of Physics, University of British Columbia, Vancouver BC, Canada

¹⁶⁹ Department of Physics and Astronomy, University of Victoria, Victoria BC, Canada

¹⁷⁰ Department of Physics, University of Warwick, Coventry, United Kingdom

¹⁷¹ Waseda University, Tokyo, Japan

¹⁷² Department of Particle Physics, The Weizmann Institute of Science, Rehovot, Israel

¹⁷³ Department of Physics, University of Wisconsin, Madison WI, United States of America

¹⁷⁴ Fakultät für Physik und Astronomie, Julius-Maximilians-Universität, Würzburg, Germany

¹⁷⁵ Fachbereich C Physik, Bergische Universität Wuppertal, Wuppertal, Germany

¹⁷⁶ Department of Physics, Yale University, New Haven CT, United States of America

¹⁷⁷ Yerevan Physics Institute, Yerevan, Armenia

¹⁷⁸ Centre de Calcul de l'Institut National de Physique Nucléaire et de Physique des Particules (IN2P3), Villeurbanne, France

^a Also at Department of Physics, King's College London, London, United Kingdom

^b Also at Institute of Physics, Azerbaijan Academy of Sciences, Baku, Azerbaijan

^c Also at Novosibirsk State University, Novosibirsk, Russia

^d Also at TRIUMF, Vancouver BC, Canada

- e* Also at Department of Physics, California State University, Fresno CA, United States of America
- f* Also at Department of Physics, University of Fribourg, Fribourg, Switzerland
- g* Also at Departamento de Fisica e Astronomia, Faculdade de Ciencias, Universidade do Porto, Portugal
- h* Also at Tomsk State University, Tomsk, Russia
- i* Also at CPPM, Aix-Marseille Université and CNRS/IN2P3, Marseille, France
- j* Also at Università di Napoli Parthenope, Napoli, Italy
- k* Also at Institute of Particle Physics (IPP), Canada
- l* Also at Particle Physics Department, Rutherford Appleton Laboratory, Didcot, United Kingdom
- m* Also at Department of Physics, St. Petersburg State Polytechnical University, St. Petersburg, Russia
- n* Also at Louisiana Tech University, Ruston LA, United States of America
- o* Also at Institucio Catalana de Recerca i Estudis Avancats, ICREA, Barcelona, Spain
- p* Also at Department of Physics, National Tsing Hua University, Taiwan
- q* Also at Department of Physics, The University of Texas at Austin, Austin TX, United States of America
- r* Also at Institute of Theoretical Physics, Ilia State University, Tbilisi, Georgia
- s* Also at CERN, Geneva, Switzerland
- t* Also at Georgian Technical University (GTU), Tbilisi, Georgia
- u* Also at O Chadai Academic Production, Ochanomizu University, Tokyo, Japan
- v* Also at Manhattan College, New York NY, United States of America
- w* Also at Hellenic Open University, Patras, Greece
- x* Also at Institute of Physics, Academia Sinica, Taipei, Taiwan
- y* Also at LAL, Université Paris-Sud and CNRS/IN2P3, Orsay, France
- z* Also at Academia Sinica Grid Computing, Institute of Physics, Academia Sinica, Taipei, Taiwan
- aa* Also at School of Physics, Shandong University, Shandong, China
- ab* Also at Moscow Institute of Physics and Technology State University, Dolgoprudny, Russia
- ac* Also at Section de Physique, Université de Genève, Geneva, Switzerland
- ad* Also at International School for Advanced Studies (SISSA), Trieste, Italy
- ae* Also at Department of Physics and Astronomy, University of South Carolina, Columbia SC, United States of America
- af* Also at School of Physics and Engineering, Sun Yat-sen University, Guangzhou, China
- ag* Also at Faculty of Physics, M.V.Lomonosov Moscow State University, Moscow, Russia
- ah* Also at National Research Nuclear University MEPhI, Moscow, Russia
- ai* Also at Department of Physics, Stanford University, Stanford CA, United States of America
- aj* Also at Institute for Particle and Nuclear Physics, Wigner Research Centre for Physics, Budapest, Hungary
- ak* Also at Department of Physics, The University of Michigan, Ann Arbor MI, United States of America
- al* Also at Discipline of Physics, University of KwaZulu-Natal, Durban, South Africa
- am* Also at University of Malaya, Department of Physics, Kuala Lumpur, Malaysia
- * Deceased